DISCRETE AND CONTINUOUS MODELS AND APPLIED COMPUTATIONAL SCIENCE

Volume 30 Number 1 (2022)

Founded in 1993
Founder: PEOPLES' FRIENDSHIP UNIVERSITY OF RUSSIA

DOI: 10.22363/2658-4670-2022-30-1

Edition registered by the Federal Service for Supervision of Communications, Information Technology and Mass Media
Registration Certificate: ПИ № ФС 77-76317, 19.07.2019

ISSN 2658-7149 (online); 2658-4670 (print)
4 issues per year.
Language: English.

Publisher: Peoples' Friendship University of Russia (RUDN University).
Indexed by Ulrich's Periodicals Directory (http://www.ulrichsweb.com), Directory of Open Access Journals (DOAJ) (https://doaj.org/), Russian Index of Science Citation (https://elibrary.ru), EBSCOhost (https://www.ebsco.com), CyberLeninka (https://cyberleninka.ru).

Aim and Scope

Discrete and Continuous Models and Applied Computational Science arose in 2019 as a continuation of RUDN Journal of Mathematics, Information Sciences and Physics. RUDN Journal of Mathematics, Information Sciences and Physics arose in 2006 as a merger and continuation of the series "Physics", "Mathematics", "Applied Mathematics and Computer Science", "Applied Mathematics and Computer Mathematics".

Discussed issues affecting modern problems of physics, mathematics, queuing theory, the Teletraffic theory, computer science, software and databases development.

It's an international journal regarding both the editorial board and contributing authors as well as research and topics of publications. Its authors are leading researchers possessing PhD and PhDr degrees, and PhD and MA students from Russia and abroad. Articles are indexed in the Russian and foreign databases. Each paper is reviewed by at least two reviewers, the composition of which includes PhDs, are well known in their circles. Author's part of the magazine includes both young scientists, graduate students and talented students, who publish their works, and famous giants of world science.

The Journal is published in accordance with the policies of COPE (Committee on Publication Ethics). The editors are open to thematic issue initiatives with guest editors. Further information regarding notes for contributors, subscription, and back volumes is available at http://journals.rudn.ru/miph.

E-mail: miphj@rudn.ru, dcm@sci.pfu.edu.ru.

EDITORIAL BOARD

Computer Design: *A. V. Korolkova, D. S. Kulyabov*

Address of editorial board:
Ordzhonikidze St., 3, Moscow, Russia, 115419
Tel. +7 (495) 955-07-16, e-mail: publishing@rudn.ru
Editorial office:
Tel. +7 (495) 952-02-50, miphj@rudn.ru, dcm@sci.pfu.edu.ru
site: http://journals.rudn.ru/miph

Paper size 70×100/16. Offset paper. Offset printing. Typeface "Computer Modern".
Conventional printed sheet 7.10. Printing run 500 copies. Open price. The order 2.
PEOPLES' FRIENDSHIP UNIVERSITY OF RUSSIA
6 Miklukho-Maklaya St., 117198 Moscow, Russia
Printed at RUDN Publishing House:
3 Ordzhonikidze St., 115419 Moscow, Russia,
Ph. +7 (495) 952-04-41; e-mail: publishing@rudn.ru

Discrete & Continuous Models
& Applied Computational Science
ISSN 2658-7149 (online), 2658-4670 (print)
2022, 30 (1) 4
http://journals.rudn.ru/miph

Contents

Discrete & Continuous Models
& Applied Computational Science
ISSN 2658-7149 (online), 2658-4670 (print)

2022, 30 (1) 5–20
http://journals.rudn.ru/miph

Research article

UDC 519.872:519.217
PACS 07.05.Tp, 02.60.Pn, 02.70.Bf
DOI: 10.22363/2658-4670-2022-30-1-5-20

Performance analysis of queueing system model under priority scheduling algorithms within 5G networks slicing framework

Kpangny Yves Berenger Adou, Ekaterina V. Markova, Elena A. Zhbankova

Peoples' Friendship University of Russia (RUDN University)
6, Miklukho-Maklaya St., Moscow, 117198, Russian Federation

(received: December 30, 2021; revised: January 21, 2022; accepted: February 18, 2022)

Abstract. A new era is opening for the world of information and communication technologies with the 5G networks' release. Indeed 5G networks appear in modern wireless systems as solutions to "traditional" networks' inflexibility and lack of radio resources problems. Using these networks the operators can expand their services' range at will and, therefore, manage daily operations by monitoring 'key performance indicators' (KPIs) — helping meet the quality of service (QoS) requirements much easily. To meet the QoS requirements 5G networks can be implemented alongside priority scheduling algorithms. This paper considers the operation of a wireless network slicing model under two scheduling algorithms. A comparative analysis of main performance measures is provided.

Key words and phrases: 5G networks, slicing, QoS, KPIs, priority scheduling, retrial queueing, iteration method

1. Introduction

The advent of new generation 5G networks with their flagship slicing technology have highly influenced the telecommunications sector in the best way. Network operators have now the latitude to manage their assets and therefore, are able to propose new types of services to customers [1]–[3]. Businesses and enterprises can now access network connectivity that fits their specific needs [4]–[6]. 3GPP defines slicing as a technology that offers on shared infrastructures the advantageous option to build fully dedicated logical networks, known as 'network slices', with very diverse quality of service (QoS) capabilities and requirements [7], [8]. Normally, meeting QoS requirements and extending capabilities are difficult tasks for network operators who can be helped by monitoring the 'key performance indicators' (KPIs) [9]–[12]. Essentially, monitoring the KPIs can allow network operators to significantly

reduce service interruptions or even prevent them in the best cases [13], [14]. Since the first release of slicing technology few years ago, the vast majority of researchers, scientists and organizations in the telecommunications industry is focused on developing methods and techniques to flexibly and efficiently share available radio resources within its framework [15]–[19]. In modern wireless networks, one of the possible solutions to meet the QoS requirements is the implementation of priority scheduling algorithms [20]–[23]. Models implementing such algorithms within slicing framework could be described using the mathematical apparatus of retrial queueing theory [24]–[26], where retrial queues, also known as 'orbits', can be used to address service's interruptions problem.

In this paper we consider one of the possible models for implementing slicing with priority scheduling algorithms. More precisely, we provide a comparative analysis of model's performance measures under preemptive and non-preemptive scheduling algorithms. For that we use the mathematical apparatus of queueing theory and describe the model as a retrial queueing system coupled with a buffer [27]–[29].

The paper is organized as follows. Section 2 provides the system's general description and proposes a mathematical model for its construction. Section 3 suggests formulas to compute the stationary probability distributions under preemptive and non-preemptive scheduling algorithms respectively. Section 4 proposes formulas to calculate the main performance measures under each priority scheduling algorithm. Section 5 provides a numerical example of system's model operation. Section 6 concludes the paper.

2. Mathematical model

Let us consider a single server retrial queueing system [25] coupled with a buffer. We assume two types of requests arrival in system according to Poisson process with rates λ_1 and λ_2 respectively. The average service times are exponentially distributed with means μ_1 and μ_2.

Let us assume that *first* type requests have access to server and buffer, while *second* type requests — to server and orbit. Let us consider two types of priority scheduling algorithms — preemptive and non-preemptive scheduling [20], [21], [29], [30].

The radio admission control (RAC) mechanism for *first* type requests is organized differently depending on the priority scheduling algorithm.

Preemptive scheduling. The RAC mechanism for *first* type requests is organized in such a way that:

1) when server is "vacant" or "occupied" by one *second* type request, the *first* type request immediately obtains service, i.e. the *second* type request occupying server at such moments automatically joins the orbit;
2) otherwise, the *first* type request awaits server's non-utilization in buffer with first-come, first-served (FCFS) service discipline [24]–[26].

Non-preemptive scheduling. The RAC mechanism for *first* type requests is organized in such a way that:

1) when server is "vacant", the request immediately obtains service;

2) otherwise, the request awaits server's non-utilization in buffer with `FCFS` service discipline.

Whether `preemptive` or `non-preemptive scheduling` algorithm, awaiting in buffer *first* type requests are always given priority when it comes to service once server is "vacant".

The `RAC` mechanism for *second* type requests is organized in such a way that:

1) when server is "vacant", the request immediately obtains service;
2) otherwise, the request either *leaves* the system with probability π or *joins* the orbit with probability $1 - \pi$.

A *second* type request that joined the orbit becomes a "retrial" *second* type request. A retrial *second* type request, as the name stipulates, *retries* to obtain service after some amount of time. The number of retrials is unlimited and time interval between two consecutive ones is exponentially distributed with rate σ^{-1}. Note that, as the "primary" *second* type request, the retrial *second* type request either *leaves* the system with probability π or *returns* to the orbit with probability $1 - \pi$ after an *unsuccessful* attempt to occupy server.

The scheme model of considered single server retrial queueing system coupled with a buffer is given in figure 1.

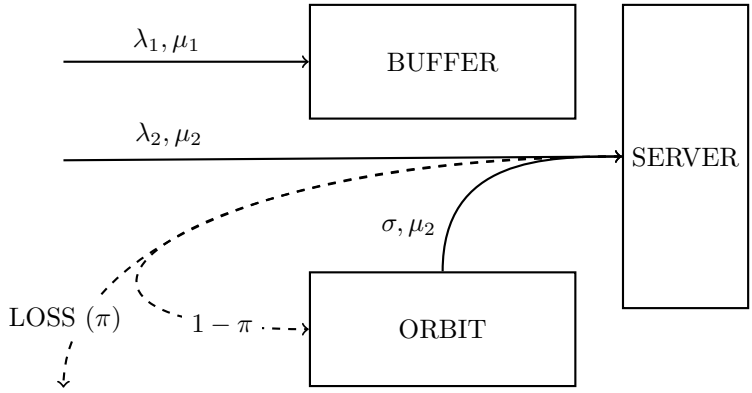

Figure 1. Scheme model of considered single server retrial queueing system coupled with an unlimited buffer

We describe system behavior using a three-dimensional vector $\mathbf{n} := (i, j, k)$ over "infinite" state spaces $\mathcal{X}$ and $\mathcal{Y}$ under `preemptive` and `non-preemptive scheduling` algorithms respectively:

$$\mathcal{X} = \left\{\mathbf{n} \in \mathbb{N}^3 : (i = 0 \wedge k \in \{0, 2\}) \vee k = 1\right\}, \tag{1a}$$

$$\mathcal{Y} = \left\{\mathbf{n} \in \mathbb{N}^3 : (i = 0 \wedge k = 0) \vee k \in \{1, 2\}\right\}, \tag{1b}$$

where $\mathbb{N}^3$ represents the state space of all three-dimensional vectors with natural elements; i — the current number of *first* type requests in buffer; j — the current number of *second* type requests in orbit; and k — the current *state* of server (i.e., value "0" means server is "vacant"; value "1" — server is

"occupied" by one *first* type request; and value "2" — server is "occupied" by one *second* type request).

The corresponding state transition diagrams are shown in figures 2, 3. The transition diagrams from random state are clarified in figures 4, 5.

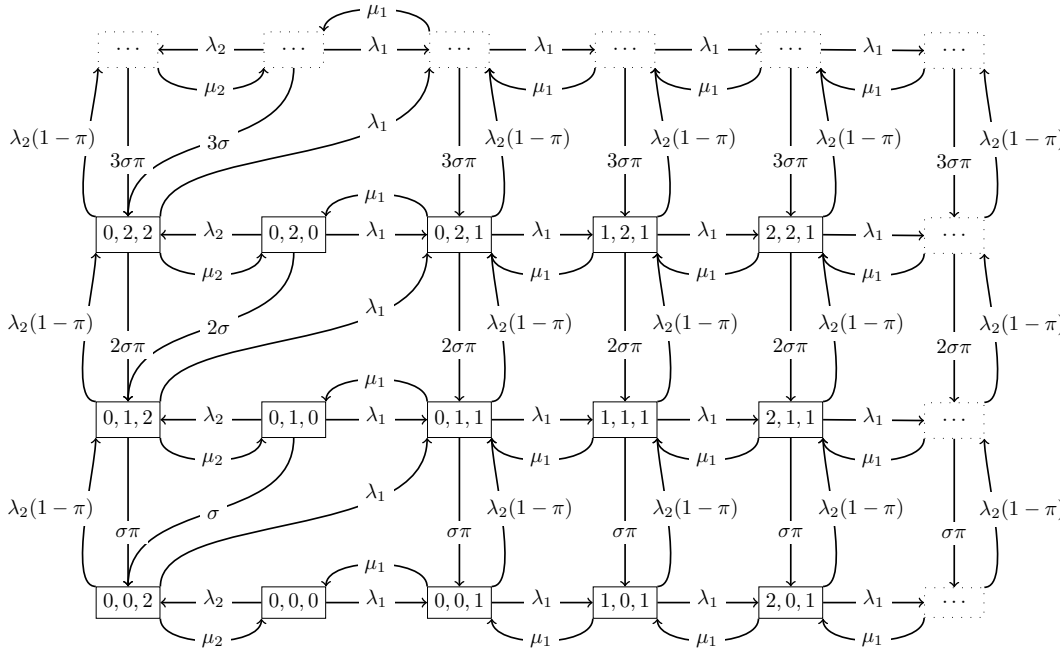

Figure 2. State transition diagram of considered single server retrial queueing system coupled with a buffer under `preemptive scheduling` algorithm

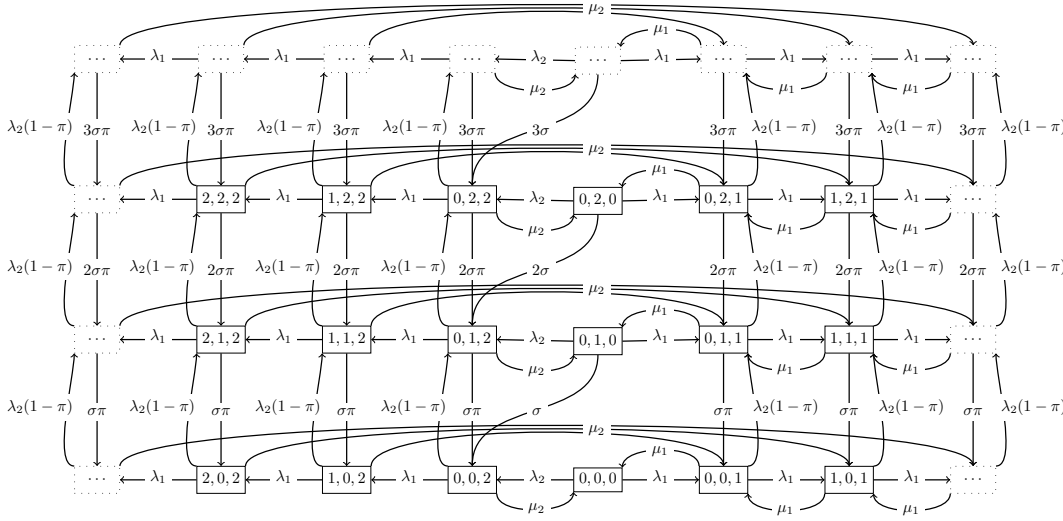

Figure 3. State transition diagram of considered single server retrial queueing system coupled with a buffer under `non-preemptive scheduling` algorithm

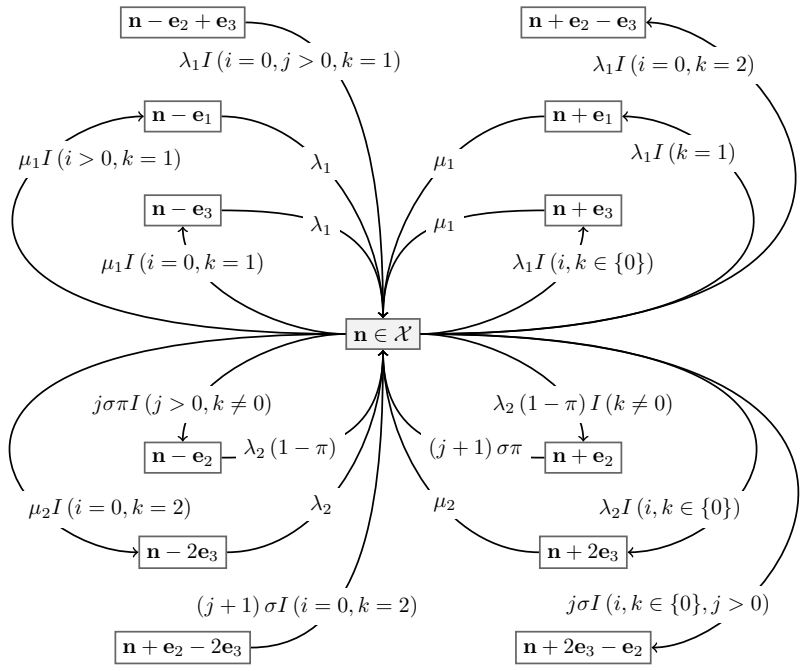

Figure 4. Transition diagram from random state for considered single server retrial queueing system coupled with a buffer under `preemptive scheduling` algorithm

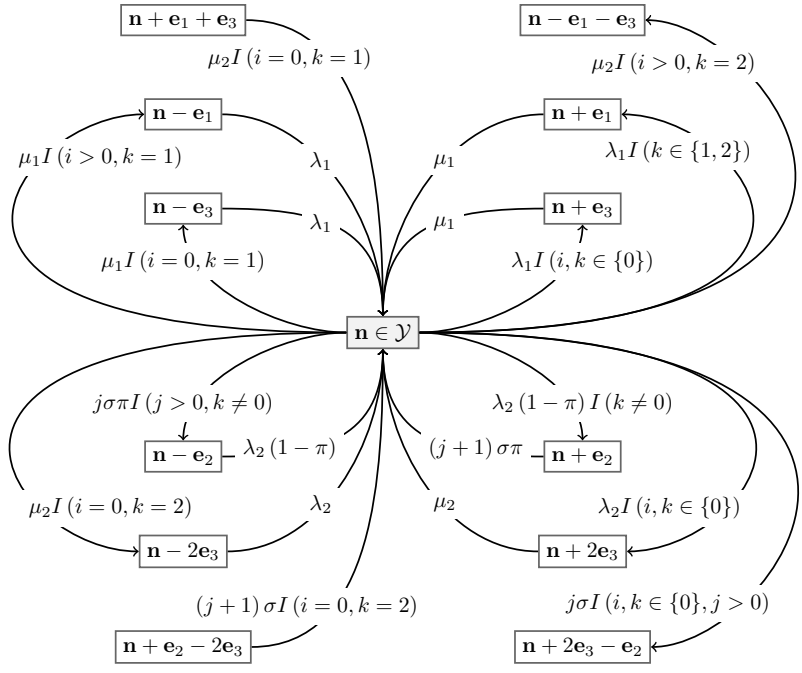

Figure 5. Transition diagram from random state for considered single server retrial queueing system coupled with a buffer under `non-preemptive scheduling` algorithm

According to investigated `priority scheduling` algorithms and considering the transition diagrams from random state (i.e., figures 4, 5) one can obtain the equilibrium equations systems given below that describe the discussed Markov processes $X(t)$ and $Y(t)$, where $t > 0$:

$$\begin{aligned}
&\big[\lambda_1 + \lambda_2 I\left(i, k \in \{0\}\right) + \lambda_2 \left(1-\pi\right) I\left(k \neq 0\right) + \mu_k I\left(k \neq 0\right) + \\
&+ j\sigma I\left(i, k \in \{0\}\right) + j\sigma\pi I\left(k \neq 0\right)\big] P(\mathbf{n}) = \lambda_1 I\left(i = 0, k = 1\right) P(\mathbf{n} - \mathbf{e}_3) + \\
&+ \lambda_1 I\left(i > 0, k = 1\right) P(\mathbf{n} - \mathbf{e}_1) + \lambda_2 I\left(i = 0, k = 2\right) P(\mathbf{n} - 2\mathbf{e}_3) + \\
&+ \lambda_2 \left(1-\pi\right) I\left(j > 0, k \neq 0\right) P(\mathbf{n} - \mathbf{e}_2) + \mu_1 I\left(i, k \in \{0\}\right) P(\mathbf{n} + \mathbf{e}_3) + \\
&+ \mu_1 I\left(k = 1\right) P(\mathbf{n} + \mathbf{e}_1) + \mu_2 I\left(i, k \in \{0\}\right) P(\mathbf{n} + 2\mathbf{e}_3) + \\
&+ (j+1)\,\sigma I\left(i = 0, k = 2\right) P(\mathbf{n} + \mathbf{e}_2 - 2\mathbf{e}_3) + (j+1)\sigma\pi I\left(k \neq 0\right) P(\mathbf{n} + \mathbf{e}_2) + \\
&+ \lambda_1 I\left(i = 0, j > 0, k = 1\right) P(\mathbf{n} - \mathbf{e}_2 + \mathbf{e}_3), \quad \text{(2a)}
\end{aligned}$$

$$\begin{aligned}
&\big[\lambda_1 + \lambda_2 I\left(i, k \in \{0\}\right) + \lambda_2 \left(1-\pi\right) I\left(k \neq 0\right) + \mu_k I\left(k \neq 0\right) + \\
&+ j\sigma I\left(i, k \in \{0\}\right) + j\sigma\pi I\left(k \neq 0\right)\big] Q(\mathbf{n}) = \lambda_1 I\left(i = 0, k = 1\right) Q(\mathbf{n} - \mathbf{e}_3) + \\
&+ \lambda_1 I\left(i > 0, k = 1\right) Q(\mathbf{n} - \mathbf{e}_1) + \lambda_2 I\left(i = 0, k = 2\right) Q(\mathbf{n} - 2\mathbf{e}_3) + \\
&+ \lambda_2 \left(1-\pi\right) I\left(j > 0, k \neq 0\right) Q(\mathbf{n} - \mathbf{e}_2) + \mu_1 I\left(i, k \in \{0\}\right) Q(\mathbf{n} + \mathbf{e}_3) + \\
&+ \mu_1 I\left(k \in \{1, 2\}\right) Q(\mathbf{n} + \mathbf{e}_1) + \mu_2 I\left(i, k \in \{0\}\right) Q(\mathbf{n} + 2\mathbf{e}_3) + \\
&+ (j+1)\,\sigma I\left(i = 0, k = 2\right) Q(\mathbf{n} + \mathbf{e}_2 - 2\mathbf{e}_3) + (j+1)\sigma\pi I\left(k \neq 0\right) Q(\mathbf{n} + \mathbf{e}_2) + \\
&+ \mu_2 I\left(i = 0, k = 1\right) Q(\mathbf{n} + \mathbf{e}_1 + \mathbf{e}_3), \quad \text{(2b)}
\end{aligned}$$

where $P(\mathbf{n})_{\mathbf{n}\in\mathcal{X}}$ and $Q(\mathbf{n})_{\mathbf{n}\in\mathcal{Y}}$ are the stationary probability distributions under `preemptive` and `non-preemptive scheduling` algorithms respectively; $\mathbf{e}_{s\in\{1,2,3\}}$ — the s-th row of identity matrix of size 3×3; and $I\left(\cdot\right)$ — the function indicator equaling value "1" when condition is met, and value "0" otherwise.

3. Stationary probability distribution

Due to the "infinite" sizes of buffer and orbit, the stationary probability distributions $\mathbf{P} = \left(P(\mathbf{n})\right)_{\mathbf{n}\in\mathcal{X}}$ and $\mathbf{Q} = \left(Q(\mathbf{n})\right)_{\mathbf{n}\in\mathcal{Y}}$ should be computed through `generating function`-based approaches [25], [27], [29]. However, one can compute them using `iteration` methods [31], [32] by simply adding limitations to the storage sizes, setting these to random maximum values. Thus, we set buffer's maximum size to $i_{\max}$ and orbit's to $j_{\max}$. Therefore, we obtain the "finite" state spaces $\widetilde{\mathcal{X}}$ and $\widetilde{\mathcal{Y}}$ under `preemptive` and `non-preemptive scheduling` algorithms respectively:

$$\widetilde{\mathcal{X}} = \left\{\mathbf{n} \in \mathcal{X} : i \leqslant i_{\max} \wedge j \leqslant j_{\max}\right\}, \quad \widetilde{\mathcal{Y}} = \left\{\mathbf{n} \in \mathcal{Y} : i \leqslant i_{\max} \wedge j \leqslant j_{\max}\right\}.$$

The process describing considered system is not a reversible Markov process whether under `preemptive` or `non-preemptive scheduling` algorithm.

Therefore, one can compute either stationary probability distribution $\mathbf{P}$ or $\mathbf{Q}$ using `iteration` method on respective equilibrium's equations system, i.e.

$$\mathbf{P} \cdot \mathbf{A}_{\left[|\widetilde{\mathcal{X}}|\times|\widetilde{\mathcal{X}}|\right]} = \mathbf{0}_{\left[1\times|\widetilde{\mathcal{X}}|\right]}, \quad \mathbf{Q} \cdot \mathbf{B}_{\left[|\widetilde{\mathcal{Y}}|\times|\widetilde{\mathcal{Y}}|\right]} = \mathbf{0}_{\left[1\times|\widetilde{\mathcal{Y}}|\right]},$$

where $\mathbf{A}$ and $\mathbf{B}$ are the infinitesimal generators of Markov process under `preemptive` and `non-preemptive scheduling` algorithms respectively.

The elements $A_{\mathbf{n},\hat{\mathbf{n}}}$ of the infinitesimal generator $\mathbf{A}$ are computed using (3a). Equation (3b) calculates the elements $B_{\mathbf{n},\hat{\mathbf{n}}}$ of the infinitesimal generator $\mathbf{B}$.

$$A_{\mathbf{n},\hat{\mathbf{n}}} = \begin{cases} \lambda_1, \text{ if } \hat{\mathbf{n}} = \mathbf{n} + \mathbf{e}_3, \text{ s.t. } i,k \in \{0\}, \\ \text{ or } \hat{\mathbf{n}} = \mathbf{n} + \mathbf{e}_1, \text{ s.t. } i < i_{\max} \wedge k = 1, \\ \text{ or } \hat{\mathbf{n}} = \mathbf{n} + \mathbf{e}_2 - \mathbf{e}_3, \text{ s.t. } i = 0 \wedge j < j_{\max} \wedge k = 2, \\ \lambda_2, \text{ if } \hat{\mathbf{n}} = \mathbf{n} + 2\mathbf{e}_3, \text{ s.t. } i,k \in \{0\}, \\ \lambda_2\,(1-\pi)\,, \text{ if } \hat{\mathbf{n}} = \mathbf{n} + \mathbf{e}_2, \text{ s.t. } j < j_{\max} \wedge k \in \{1,2\}, \\ \mu_1, \text{ if } \hat{\mathbf{n}} = \mathbf{n} - \mathbf{e}_3, \text{ s.t. } i = 0 \wedge k = 1, \\ \text{ or } \hat{\mathbf{n}} = \mathbf{n} - \mathbf{e}_1, \text{ s.t. } i > 0 \wedge k = 1, \\ \mu_2, \text{ if } \hat{\mathbf{n}} = \mathbf{n} - 2\mathbf{e}_3, \text{ s.t. } i = 0 \wedge k = 2, \\ j\sigma, \text{ if } \hat{\mathbf{n}} = \mathbf{n} + 2\mathbf{e}_3 - \mathbf{e}_2, \text{ s.t. } j > 0 \wedge i,k \in \{0\}, \\ j\sigma\pi, \text{ if } \hat{\mathbf{n}} = \mathbf{n} - \mathbf{e}_2, \text{ s.t. } j > 0 \wedge k \in \{1,2\}, \\ 0, \text{ otherwise}, \end{cases} \tag{3a}$$

with $\mathbf{n} \in \widetilde{\mathcal{X}}$, and $A_{\mathbf{n},\mathbf{n}} = -\sum\limits_{\hat{\mathbf{n}} \in \widetilde{\mathcal{X}}\{\mathbf{n}\}} A_{\mathbf{n},\hat{\mathbf{n}}}$.

$$B_{\mathbf{n},\hat{\mathbf{n}}} = \begin{cases} \lambda_1, \text{ if } \hat{\mathbf{n}} = \mathbf{n} + \mathbf{e}_3, \text{ s.t. } i,k \in \{0\}, \\ \text{ or } \hat{\mathbf{n}} = \mathbf{n} + \mathbf{e}_1, \text{ s.t. } i < i_{\max} \wedge k \in \{1,2\}, \\ \lambda_2, \text{ if } \hat{\mathbf{n}} = \mathbf{n} + 2\mathbf{e}_3, \text{ s.t. } i,k \in \{0\}, \\ \lambda_2\,(1-\pi)\,, \text{ if } \hat{\mathbf{n}} = \mathbf{n} + \mathbf{e}_2, \text{ s.t. } j < j_{\max} \wedge k \in \{1,2\}, \\ \mu_1, \text{ if } \hat{\mathbf{n}} = \mathbf{n} - \mathbf{e}_3, \text{ s.t. } i = 0 \wedge k = 1, \\ \text{ or } \hat{\mathbf{n}} = \mathbf{n} - \mathbf{e}_1, \text{ s.t. } i > 0 \wedge k = 1, \\ \mu_2, \text{ if } \hat{\mathbf{n}} = \mathbf{n} - 2\mathbf{e}_3, \text{ s.t. } i = 0 \wedge k = 2, \\ \text{ or } \hat{\mathbf{n}} = \mathbf{n} - \mathbf{e}_1 - \mathbf{e}_3, \text{ s.t. } i > 0 \wedge k = 2, \\ j\sigma, \text{ if } \hat{\mathbf{n}} = \mathbf{n} + 2\mathbf{e}_3 - \mathbf{e}_2, \text{ s.t. } j > 0 \wedge i,k \in \{0\}, \\ j\sigma\pi, \text{ if } \hat{\mathbf{n}} = \mathbf{n} - \mathbf{e}_2, \text{ s.t. } j > 0 \wedge k \in \{1,2\}, \\ 0, \text{ otherwise}, \end{cases} \tag{3b}$$

with $\mathbf{n} \in \widetilde{\mathcal{Y}}$, and $B_{\mathbf{n},\mathbf{n}} = -\sum\limits_{\hat{\mathbf{n}} \in \widetilde{\mathcal{Y}}\{\mathbf{n}\}} B_{\mathbf{n},\hat{\mathbf{n}}}$.

4. Performance measures

After computing the stationary probability distributions **P** and **Q** one can calculate system's performance measures under `preemptive` and `non-preemptive scheduling` algorithms respectively. Let us consider following main performance measures:

1. The mean number of *first* type requests in buffer

$$\sum_{\mathbf{n}\in\widetilde{\mathcal{X}}} i \cdot P(\mathbf{n}), \quad \sum_{\mathbf{n}\in\widetilde{\mathcal{Y}}} i \cdot Q(\mathbf{n}), \tag{4}$$

2. The mean number of *second* type requests in orbit

$$\sum_{\mathbf{n}\in\widetilde{\mathcal{X}}} j \cdot P(\mathbf{n}), \quad \sum_{\mathbf{n}\in\widetilde{\mathcal{Y}}} j \cdot Q(\mathbf{n}), \tag{5}$$

3. The server's vacancy probability

$$\sum_{\mathbf{n}\in\widetilde{\mathcal{X}}:k=0} P(\mathbf{n}), \quad \sum_{\mathbf{n}\in\widetilde{\mathcal{Y}}:k=0} Q(\mathbf{n}), \tag{6}$$

4. The server's occupancy probability by one *first* type request

$$\sum_{\mathbf{n}\in\widetilde{\mathcal{X}}:k=1} P(\mathbf{n}), \quad \sum_{\mathbf{n}\in\widetilde{\mathcal{Y}}:k=1} Q(\mathbf{n}), \tag{7}$$

5. The server's occupancy probability by one *second* type request

$$\sum_{\mathbf{n}\in\widetilde{\mathcal{X}}:k=2} P(\mathbf{n}), \quad \sum_{\mathbf{n}\in\widetilde{\mathcal{Y}}:k=2} Q(\mathbf{n}). \tag{8}$$

Since limitations were applied to storage sizes, i.e. buffer and orbit, one may find it necessary to also compute following performance measures:

1. The buffer's saturation probability

$$\sum_{\mathbf{n}\in\widetilde{\mathcal{X}}:i=i_{\max}} P(\mathbf{n}), \quad \sum_{\mathbf{n}\in\widetilde{\mathcal{Y}}:i=i_{\max}} Q(\mathbf{n}), \tag{9}$$

2. The orbit's saturation probability

$$\sum_{\mathbf{n}\in\widetilde{\mathcal{X}}:j=j_{\max}} P(\mathbf{n}), \quad \sum_{\mathbf{n}\in\widetilde{\mathcal{Y}}:j=j_{\max}} Q(\mathbf{n}). \tag{10}$$

5. Numerical example

Let us illustrate the behavior of performance measures, computed in previous section 4, depending on various system's parameters. To implement `iteration` method one must set the `error tolerance` ε and, for ergonomic

features, limit the `number of iterations` $MaxIters$. Since *second* type requests are apparently more affected by implemented `priority scheduling` algorithms, one may build the example around performance measures "directly" related to them:

— the mean number of *second* type requests in orbit, i.e. equations (5);
— the server's vacancy probability, i.e. equations (6);
— the server's occupancy probability by one *second* type request, i.e. equations (8);
— the orbit's saturation probability, i.e. equations (10).

Summaries of the numerical examples results are provided in tables 1 to 4.

Table 1

Mean number of *second* type requests in orbit depending on triplet $(j_{\max}, \lambda_1, \lambda_2)$ with $i_{\max} = 10$, $\mu_1 = \mu_2 = 2$, $\pi = 0.001$, $\sigma = 1$, $\varepsilon = 10^{-12}$ and $MaxIters = 1000$

-	-	`Preemptive scheduling`			`Non-preemptive scheduling`		
$j_{\max}$	λ_1 \ λ_2	1	2	3	1	2	3
5	1	2.5438	3.3625	3.8375	2.4659	3.4162	3.9503
	2	3.9805	4.1998	4.3897	4.0846	4.3046	4.4961
	3	4.5566	4.6908	4.7835	4.6314	4.7437	4.8230
10	1	4.9052	7.2944	8.3800	4.7192	7.3611	8.5276
	2	8.5649	8.9173	9.2121	8.7040	9.0528	9.3429
	3	9.4234	9.5984	9.7193	9.5149	9.6616	9.7651
15	1	6.9305	11.4591	13.1148	6.6439	11.5360	13.2783
	2	13.3191	13.7555	14.1114	13.4738	13.9025	14.2497
	3	14.3427	14.5381	14.6738	14.4387	14.6034	14.7205

Table 1 shows that when the arrival rate λ_1 of *first* type requests or λ_2 of *second* type requests increases, the mean number of *second* type requests in orbit also increases. That performance measure is greater under `non-preemptive scheduling` algorithm. This may be explained by the fact that, we have more *second* type requests in system, and consequently, the orbit tends to saturation. This situation is also illustrated by table 2 showing the increase of orbit's saturation probability under the same circumstances.

Table 3 shows that when the arrival rate λ_1 of *first* type requests or λ_2 of *second* type requests increases, the server's vacancy probability decreases. As one can see from that table, and according to table 1, that performance measure is less under `non-preemptive scheduling` algorithm. This may be explained by the fact that the more requests we have in system, the less server will be "vacant".

Table 4 shows that when fixing arrival rate λ_1 of *first* type requests to value "1" and increasing arrival rate λ_2 of *second* type requests, the server's occupancy probability increases.

Table 2

Saturation probability of orbit depending on triplet $(j_{\max}, \lambda_1, \lambda_2)$ with $i_{\max} = 10$, $\mu_1 = \mu_2 = 2$, $\pi = 0.001$, $\sigma = 1$, $\varepsilon = 10^{-12}$ and $MaxIters = 1000$

-	-	Preemptive scheduling			Non-preemptive scheduling		
$j_{\max}$	λ_1 \ λ_2	1	2	3	1	2	3
5	1	0.2229	0.3647	0.4686	0.2256	0.3990	0.5262
	2	0.5322	0.6105	0.6796	0.5862	0.6654	0.7372
	3	0.7602	0.8236	0.8687	0.8015	0.8537	0.8919
10	1	0.1197	0.2889	0.4174	0.1223	0.3216	0.4750
	2	0.4801	0.5653	0.6425	0.5346	0.6210	0.7007
	3	0.7247	0.7913	0.8401	0.7664	0.8215	0.8633
15	1	0.0690	0.2473	0.3889	0.0702	0.2766	0.4436
	2	0.4490	0.5363	0.6171	0.5007	0.5893	0.6729
	3	0.6978	0.7649	0.8154	0.7375	0.7936	0.8374

Table 3

Vacancy probability of server depending on triplet $(j_{\max}, \lambda_1, \lambda_2)$ with $i_{\max} = 10$, $\mu_1 = \mu_2 = 2$, $\pi = 0.001$, $\sigma = 1$, $\varepsilon = 10^{-12}$ and $MaxIters = 1000$

-	-	Preemptive scheduling			Non-preemptive scheduling		
$j_{\max}$	λ_1 \ λ_2	1	2	3	1	2	3
5	1	0.1394	0.0803	0.0556	0.1242	0.0630	0.0395
	2	0.0465	0.0361	0.0285	0.0310	0.0223	0.0162
	3	0.0198	0.0137	0.0098	0.0107	0.0071	0.0048
10	1	0.0923	0.0351	0.0220	0.0847	0.0269	0.0148
	2	0.0183	0.0143	0.0118	0.0114	0.0083	0.0063
	3	0.0082	0.0058	0.0043	0.0042	0.0028	0.0020
15	1	0.0735	0.0197	0.0128	0.0685	0.0146	0.0084
	2	0.0106	0.0086	0.0073	0.0064	0.0048	0.0039
	3	0.0051	0.0037	0.0027	0.0026	0.0018	0.0013

But, when fixing λ_1 to values "2" or "3" that probability decreases. That performance measure is less under `non-preemptive scheduling` algorithm. This may be explained by the fact that the more *first* type requests we have in system, the less server will be occupied by one *second* type request, since `RAC` mechanism suggests that priority is always given to *first* type requests

once server is "vacant". Furthermore, when fixing λ_2 and increasing λ_1 the server's occupancy probability decreases generally except under `preemptive scheduling` algorithm for one case, where orbit's maximum size $j_{\max}$ equals value "5" and λ_2 equals value "1". In that case, that probability increases to a maximum value and then decreases.

Table 4

Occupancy probability of server by one *second* type request depending on triplet $(j_{\max}, \lambda_1, \lambda_2)$ with $i_{\max} = 10$, $\mu_1 = \mu_2 = 2$, $\pi = 0.001$, $\sigma = 1$, $\varepsilon = 10^{-12}$ and $MaxIters = 1000$

-	-	`Preemptive scheduling`			`Non-preemptive scheduling`		
$j_{\max}$	λ_1 \ λ_2	1	2	3	1	2	3
5	1	0.3779	0.4655	0.5232	0.3760	0.4372	0.4608
	2	0.3973	0.3372	0.3070	0.3461	0.2836	0.2446
	3	0.2056	0.1463	0.1112	0.1639	0.1155	0.0857
10	1	0.4163	0.4992	0.5457	0.4156	0.4734	0.4854
	2	0.4157	0.3503	0.3156	0.3657	0.2977	0.2546
	3	0.2113	0.1498	0.1132	0.1706	0.1199	0.0887
15	1	0.4312	0.5087	0.5487	0.4317	0.4856	0.4919
	2	0.4178	0.3509	0.3150	0.3707	0.3012	0.2571
	3	0.2107	0.1491	0.1124	0.1723	0.1211	0.0895

6. Conclusion

One considered a possible model for implementing `slicing` technology with `priority scheduling` algorithms. A comparative analysis of computed main performance measures — mean number of *first* type requests in buffer, mean number of *second* type requests in orbit, server's vacancy probability, server's occupancy probability by one *first* type request, server's occupancy probability by one *second* type request, buffer's saturation probability and orbit's saturation probability — was provided. That analysis showed that system load is higher under `non-preemptive scheduling` algorithm with very low probability of leaving system after an *unsuccessful* attempt to occupy server.

Acknowledgments

This paper has been supported by the RUDN University Strategic Academic Leadership Program (recipient Adou Y.). The reported study was funded by RFBR, project number 20-07-01052 (recipient Markova E. V.)

References

[1] W. Lehr, F. Queder, and J. Haucap, "5G: A new future for Mobile Network Operators, or not?" *Telecommunications Policy*, vol. 45, no. 3, p. 102 086, Jan. 2021. DOI: 10.1016/j.telpol.2020.102086.

[2] Z. Ofir. "What will be the impact of 5g on network operators?" (Nov. 2021), [Online]. Available: https://www.forbes.com/sites/forbestechcouncil/2020/11/24/what-will-be-the-impact-of-5g-on-network-operators/.

[3] "Cloud computing services drive companies' digital transformation." (Jan. 2022), [Online]. Available: https://www.telefonica.com/en/communication-room/blog/cloud-computing-services-drive-companies-digital-transformation/.

[4] K. Budka. "AI + Augmented: Pushing the Limits of What Machines Can Do." (Sep. 2021), [Online]. Available: https://www.industryweek.com/technology-and-iiot/emerging-technologies/article/21174112/ai-augmented-pushes-the-limits-of-what-machines-can-do.

[5] C. Johnson. "What Companies And Governments Really Want From Industry 4.0." (Nov. 2021), [Online]. Available: https://www.forbes.com/sites/nokia-industry-40/2021/11/18/what-companies-and-governments-really-want-from-industry-40/.

[6] Nokia. "How Supply Chain 4.0 delivers the goods other approaches can't." (Dec. 2021), [Online]. Available: http://www.ft.com/partnercontent/nokia/how-supply-chain-4-0-delivers-the-goods-other-approaches-cant.html.

[7] A. Sultan and M. Pope, "Feasibility study on new services and markets technology enablers for network operation; Stage 1," 3rd Generation Partnership Project (3GPP), Technical report (TR) 22.864, Sep. 2016, Version 15.0.0.

[8] J. M. Meredith, F. Firmin, and M. Pope, "Release 16 Description; Summary of Rel-16 Work Items," 3rd Generation Partnership Project (3GPP), Technical report (TR) 21.916, Jan. 2022, Version 16.1.0.

[9] J. M. Meredith, M. C. Soveri, and M. Pope, "Management and orchestration; 5G end to end Key Performance Indicators (KPI)," 3rd Generation Partnership Project (3GPP), Technical specification (TS) 28.554, Dec. 2021, Version 17.5.0.

[10] "5G industry campus network deployment guideline," GSM Association (GSMA), Official Document NG.123, Oct. 2021, Version 2.0.

[11] I. Markopoulos *et al.*, "Service performance measurement methods over 5G experimental networks," 5G PPP, white paper ICT-19, Mar. 2021, Version 1.0. DOI: 10.5281/zenodo.4748482.

[12] L. Nielsen *et al.*, "Basic Testing Guide — A Starter Kit for Basic 5G KPIs Verification," 5G PPP, white paper, Nov. 2021, Version 1.0. DOI: 10.5281/zenodo.5704519.

[13] O. Ohlsson, P. Wallentin, and C.-G. Persson. "Reducing mobility interruption time in 5G networks." (Apr. 2020), [Online]. Available: https://www.ericsson.com/en/blog/2020/4/reducing-mobility-interruption-time-5g-networks.

[14] G. Sevilla. "2022 predictions: Internet and network outages will continue to get worse before they get better." (Dec. 2021), [Online]. Available: https://www.emarketer.com/content/2022-predictions-internet-network-outages-will-continue-worse-before-they-better.

[15] H. Zhu, G. Zhang, D. Hong, S. Zhang, and S. Huang, "Data Access Control Method of Power Terminal Based on 5G Technology," in *Advanced Hybrid Information Processing*, S. Liu and X. Ma, Eds., Cham: Springer International Publishing, 2022, pp. 26–39. DOI: 10.1007/978-3-030-94554-1_3.

[16] D. Alotaibi, V. Thayananthan, and J. Yazdani, "The 5G network slicing using SDN based technology for managing network traffic," *Procedia Computer Science*, vol. 194, pp. 114–121, Dec. 2021, 18th International Learning & Technology Conference 2021. DOI: 10.1016/j.procs.2021.10.064.

[17] R. Moreira, P. F. Rosa, R. L. A. Aguiar, and F. de Oliveira Silva, "NASOR: A network slicing approach for multiple Autonomous Systems," *Computer Communications*, vol. 179, pp. 131–144, Jul. 2021. DOI: 10.1016/j.comcom.2021.07.028.

[18] P. Zhu, J. Zhang, Y. Xiao, J. Cui, L. Bai, and Y. Ji, "Deep reinforcement learning-based radio function deployment for secure and resource-efficient NG-RAN slicing," *Engineering Applications of Artificial Intelligence*, vol. 106, p. 104 490, 2021. DOI: 10.1016/j.engappai.2021.104490.

[19] H. Yang, T. So, and Y. Xu, "Chapter 12 — 5G network slicing," in *5G NR and Enhancements*, J. Shen, Z. Du, Z. Zhang, N. Yang, and H. Tang, Eds., Elsevier, 2022, pp. 621–639. DOI: 10.1016/B978-0-323-91060-6.00012-X.

[20] N. Suganthi and S. Meenakshi, "An efficient scheduling algorithm using queuing system to minimize starvation of non-real-time secondary users in Cognitive Radio Network," *Cluster Computing*, vol. 25, no. 1, pp. 1–11, Jan. 2022. DOI: 10.1007/s10586-017-1595-8.

[21] A. Fathalla, K. Li, and A. Salah, "Best-KFF: a multi-objective preemptive resource allocation policy for cloud computing systems," *Cluster Computing*, vol. 25, no. 1, pp. 321–336, Feb. 2022. DOI: 10.1007/s10586-021-03407-z.

[22] S. J. Ahmad *et al.*, "A Dynamic Priority Based Scheduling Scheme for Multimedia Streaming Over MANETs to Improve QoS," in *Distributed Computing and Internet Technology*, Cham: Springer International Publishing, 2016, pp. 122–126. DOI: 10.1007/978-3-319-28034-9_15.

[23] A. Belgacem and K. Beghdad-Bey, "Multi-objective workflow scheduling in cloud computing: trade-off between makespan and cost," *Cluster Computing*, vol. 25, no. 1, pp. 579–595, Feb. 2022. DOI: 10.1007/s10586-021-03432-y.

[24] J. R. Artalejo and A. Gómez-Corral, *Retrial Queueing Systems*. Springer, Berlin, Heidelberg, Jan. 2008. DOI: 10.1007/978-3-540-78725-9.

[25] P. P. Bocharov, C. D'Apice, and A. V. Pechinkin, *Queueing Theory*. De Gruyter, 2011. DOI: 10.1515/9783110936025.

[26] G. P. Basharin, Y. V. Gaidamaka, and K. E. Samouylov, "Mathematical Theory of Teletraffic and its Application to the Analysis of Multiservice Communication of Next Generation Networks," *Automatic Control and Computer Sciences*, vol. 47, no. 2, pp. 62–69, 2013. DOI: 10.3103/S0146411613020028.

[27] K. Y. Adou and E. V. Markova, "Methods for Analyzing Slicing Technology in 5G Wireless Network Described as Queueing System with Unlimited Buffer and Retrial Group," in *Information Technologies and Mathematical Modelling. Queueing Theory and Applications*, Cham: Springer International Publishing, Mar. 2021, pp. 264–278. DOI: 10.1007/978-3-030-72247-0_20.

[28] E. Markova, Y. Adou, D. Ivanova, A. Golskaia, and K. Samouylov, "Queue with Retrial Group for Modeling Best Effort Traffic with Minimum Bit Rate Guarantee Transmission Under Network Slicing," in *Distributed Computer and Communication Networks*, Cham: Springer International Publishing, 2019, pp. 432–442. DOI: 978-3-030-36614-8_33.

[29] M. Korenevskaya, O. Zayats, A. Ilyashenko, and V. Muliukha, "Retrial Queuing System with Randomized Push-Out Mechanism and Non-Preemptive Priority," *Procedia Computer Science*, vol. 150, pp. 716–725, 2019, Proceedings of the 13th International Symposium "Intelligent Systems 2018" (INTELS'18), 22-24 October, 2018, St. Petersburg, Russia. DOI: 10.1016/j.procs.2019.02.016.

[30] A. M. Yadav, K. N. Tripathi, and S. C. Sharma, "An enhanced multi-objective fireworks algorithm for task scheduling in fog computing environment," *Cluster Computing*, Nov. 2021. DOI: 10.1007/s10586-021-03481-3.

[31] S. N. Stepanov, *Fundamentals of Multiservice Networks [Osnovy teletraffika multiservisnykh setei]*. Moscow: Eqo-Trends, 2010, p. 392, in Russian.

[32] S. N. Stepanov, *Theory of Teletraffic: Concepts, Models, Applications [Teoriya teletraffika: kontseptsii, modeli, prilozheniya]*. Moscow: Goryachaya Liniya-Telekom, 2015, p. 868, in Russian.

For citation:

K. Y. Adou, E. V. Markova, E. A. Zhbankova, Performance analysis of queueing system model under priority scheduling algorithms within 5G networks slicing framework, Discrete and Continuous Models and Applied Computational Science 30 (1) (2022) 5–20. DOI: 10.22363/2658-4670-2022-30-1-5-20.

Information about the authors:

Adou, Kpangny Yves Berenger — PhD Student at the Department of Applied Probability and Informatics, Faculty of Science, Peoples' Friendship University of Russia (RUDN University) (e-mail: 1042205051@rudn.ru, ORCID: https://orcid.org/0000−0003−4669−0898)

Markova, Ekaterina Viktorovna — Candidate of Physical and Mathematical Sciences, Associate Professor at the Department of Applied Probability and Informatics, Faculty of Science, Peoples' Friendship University of Russia (RUDN University) (e-mail: markova-ev@rudn.ru, ORCID: https://orcid.org/0000−0002−7876−2801)

Zhbankova, Elena Aleksandrovna — MSc student at the Department of Applied Probability and Informatics, Faculty of Science, Peoples' Friendship University of Russia (RUDN University) (e-mail: 1032202159@rudn.ru, ORCID: https://orcid.org/0000-0003-2482-4488)

УДК 519.872:519.217
PACS 07.05.Tp, 02.60.Pn, 02.70.Bf
DOI: 10.22363/2658-4670-2022-30-1-5-20

К анализу системы массового обслуживания для сети 5G с технологией NS и приоритетным управлением доступом к радиоресурсам

К. И. Б. Аду, Е. В. Маркова, Е. А. Жбанкова

Российский университет дружбы народов
ул. Миклухо-Маклая, д. 6, Москва, Россия, 117198

Аннотация. Переход к беспроводным сетям пятого поколения 5G ознаменовал новый этап развития информационных и коммуникационных технологий. Сети пятого поколения должны решить такие проблемы, как негибкость «традиционных» сетей и нехватка частотных радиоресурсов для качественного предоставления услуг. Предполагается, что, используя эти сети, мобильные операторы смогут значительно расширить спектр услуг и обеспечить требуемое качество их предоставления. Для удовлетворения требований к качеству обслуживания (*англ.* Quality of Service — QoS) операторам необходимо выполнение «ключевых показателей эффективности» (*англ.* Key Performance Indicators — KPI), описанных в стандартах связи. Для этой цели могут быть использованы алгоритмы приоритетного облуживания. В статье рассмотрена модель беспроводной сети 5G, поддерживающая технологию нарезки сети и реализующая управление доступом к сетевым радиоресурсам при помощи введения приоритетов. Изучена работа модели в рамках двух алгоритмов. Проведён сравнительный анализ основных показателей эффективности модели.

Ключевые слова: сети 5G, нарезка сети NS, QoS, KPI, приоритетное управление доступом, СМО с повторными заявками, итерационный метод

Discrete & Continuous Models
& Applied Computational Science
ISSN 2658-7149 (online), 2658-4670 (print)

2022, 30 (1) 21–38
http://journals.rudn.ru/miph

Research article

UDC 519.872:519.217
PACS 07.05.Tp, 02.60.Pn, 02.70.Bf
DOI: 10.22363/2658-4670-2022-30-1-21-38

Mathematical analysis of a Markovian multi-server feedback queue with a variant of multiple vacations, balking and reneging

Amina Angelika Bouchentouf[1], **Latifa Medjahri**[2], **Mohamed Boualem**[3], **Amit Kumar**[4]

[1] *Djillali Liabes University of Sidi Bel Abbes, 22000, Algeria*
[2] *University of Tlemcen, B.P. 119, 13000, Algeria*
[3] *University of Bejaia, 06000, Algeria*
[4] *Chandigarh University, Mohali (Punjab), Pin No-140413, India*

(received: November 26, 2021; revised: December 20, 2021; accepted: February 18, 2022)

Abstract. In this paper, we analyze a multi-server queue with customers' impatience and Bernoulli feedback under a variant of multiple vacations. On arrival, a customer decides whether to join or balk the system, based on the observation of the system size as well as the status of the servers. It is supposed that customer impatience can arise both during busy and vacation period because of the long wait already experienced in the system. The latter can be retained via certain mechanism used by the system. The feedback occurs as returning a part of serviced customers to get a new service. The queue under consideration can be used to model the processes of information transmission in telecommunication networks. We develop the Chapman–Kolmogorov equations for the steady-state probabilities and solve the differential equations by using the probability generating function method. In addition, we obtain explicit expressions of some important system characteristics. Different queueing indices are derived such as the probabilities when the servers are in different states, the mean number of customers served per unit of time, and the average rates of balking and reneging.

Key words and phrases: Markovian multi-server queue, probability generating function, impatient phenomena, server vacations, Bernoulli feedback

1. Introduction

Queueing models with server vacation have been efficiently studied by many researchers in the last decades and successfully applied in various practical problems such as telecommunication system design and control, manufacturing industries, and other related systems. There are two basic vacation queueing models namely, multiple vacation, and single vacation. In multiple vacation

queueing models, the server continues to take successive vacations until it finds at least one customer waiting in a queue at a vacation completion epoch [1], [2]. Nevertheless, in single vacation queueing models, the server precisely takes one vacation between two consecutive busy periods. These two types of vacation models were first introduced by Levy and Yechiali [3]. Eminent literature on the subject is found in [4]–[8] and others.

Over the past few years, queueing models with Bernoulli feedback have increasingly attracted the attention of many researchers [9]–[14]. Taking into account the feedback effect makes it possible to bring the considered models closer to a real situation, where the claims once serviced may require repeat service for different reasons. For example, in communication networks erroneously transmitted, a data is retransmitted.

In recent years, a growing body of literature has emerged on the analysis of queueing systems with impatient customers [15]. This is due to their potential applications in many related areas, see for instance [16], [17]. Balking is one form of impatience, which is the reluctance of a customer to join a queue upon arrival [18], [19]. The other forms are reneging, the reluctance to remain in line after joining and waiting, and jockeying between lines when each of a number of parallel lines has its own queue [20], [21]. When the impatience becomes sufficiently strong, the manager of the firm concerned has to take some measures to diminish the congestion to levels that customers can tolerate.

In most queueing situations, customers seem to get discouraged from receiving service when the server is absent and tend to leave the system without receiving service. This phenomenon is very precisely observed when the server is on vacation. This results in a potential loss of customers and customer goodwill for a service provider. For a comprehensive overview of the subject, authors may refer to [22]–[29]. Most of the literature mentioned here studies reneging during the vacation state of the server. However, in many real-life situations, the abandonment may occur even when the system is in the busy state. For instance, incoming customers can not have any information about the state of the server, or when they are not satisfied with the service time (in particular, when they find that the server takes too much time to serve the customers). This paper contributes in this sense. In fact, only a few research papers have been done treating this case [9]–[12], [30].

In this paper, we provide the analysis of a multi-server feedback queue with a variant multiple vacation policy, balking and server's states-dependent reneging. When all the customers present in the system have been served, the servers immediately leave for a vacation. If they return from a vacation to find an empty queue, they leave for another vacation; otherwise, the servers, synchronously, return to serve the queue. These latter are permitted to take a finite number, say K, of sequential vacations. It is assumed that an arriving customer who finds the system (all the servers) on vacation period (respectively, on busy period) activates an impatience timer T_{Vac} (respectively, T_{Busy}). If the customer's service has not been completed before the customer's impatience timer expires, the customer abandons the queue. The latter can be convinced to stay in the system (retained) using certain strategy. In addition, if the customer is unhappy with the service, he can rejoin the end of the queue for another one with some probability. That's what we call a feedback customer. To the best of the researchers' knowledge, the

model under consideration has so far not treated in the literature of queues. Moreover, our model can be considered as a generalized version of existing queueing model given by Yue et al. [27] and [20] equipped with many features and associated with many practical situations.

The rest of the paper is arranged as follows. In Section 2, we introduce the mathematical description of the model and we give a practical application. In Section 4, we develop the differential equations for the probability generating functions of the steady-state probabilities. In Section 5, we give the solution of the differential equations. In Section 6, we give the probabilities when the servers are in different states. Some essential system performance measures of this model are obtained in Section 7. Finally, we conclude the paper in Section 8.

2. The mathematical description of the model

We consider a multi-server feedback queueing system with K-variant vacation, balking and server's states-dependent reneging. The following assumptions and notations are taken into account to structure the proposed queueing system:

1. The suggested queueing system consists of c servers. Customers arrive into the system according to a Poisson process with rate $\lambda > 0$, they are served according to First-Come-First-Served (FCFS) discipline. The service times are assumed to be exponentially distributed with rate μ.
2. A multiple synchronous vacation policy is considered; once all the customers present in the system are served, the servers, all together, leave for a vacation. At the end of the vacation period, if the queue is still empty, they immediately leave for another vacation; otherwise, they return to serve the queue. The servers are allowed to take all together K vacations sequentially. When the K consecutive vacations are complete, the servers switch to a busy period and, depending on the arrival of new customers, they stay idle or busy. The vacation period is assumed to be exponentially distributed with rate ϕ.
3. Whenever a customer arrives at the system and finds the servers on vacation period (resp. busy period), it activates an impatience timer T_{Vac} (resp. T_{Busy}), which is exponentially distributed with parameter ξ_0 (resp. ξ_1). If the customer's service has not been completed before the customer's timer expires, this later may leave the system. We suppose that the customers timers are independent and identically distributed random variables and independent of the number of waiting customers.
4. It is supposed that a system employs a certain mechanism in order to keep impatient customers in the system, that is, with some probability α', a customer may be retained in the system, and with a complementary probability α it may decide to leave to never return.
5. If, after completion of service, a customer is not happy with the quality of the service, he can return to the system with some probability β' for another service, or decide to leave the system with probability $\beta = 1 - \beta'$.
6. A customer who on arrival finds at least one customer (resp. c customers) in the system, when the servers are on vacation period (resp. busy

period) either decides to enter the queue with probability θ or balk with probability $\overline{\theta} = 1 - \theta$.

All random variables presented above are mutually independent of each other.

3. Practical application of the model

The operation mode of a call center with vacation and impatience provides an initial motivation for our study; a central office is used for receiving or transmitting a large volume of enquiries. A private branch exchange (PBX) is a private telephone network used within a company or organizations that offers various features such as transfer calls, voicemail, call recording, interactive voice menus (IVR), and call queues. It helps in making an organization's communication simpler and more robust.

The incoming calls are routed to an available customer support manager drawn from the group of agents. Assume that the service facility consists in a group of c channels (servers) available to meet the demands of the requests. If an arriving call finds some servers free it immediately occupies the channel and leaves the system after service. However, the behavior of a call may vary depending on the waiting expectations provided by the call center and the personal preferences of each specific customer. Therefore, each call may decide either to balk or to wait for a while.

The servers commute between busy and vacation periods in groups. When there is no demands to be handled, the latter, all together, go synchronously on vacation and come back as one station to the busy period, once the idle period ends. If there are some waiting calls at the end of the vacation period, they will be immediately served. Alternatively, they quit for another vacation period.

The calls have no information on the queue length nor the state of the servers, then, an increase in the mean waiting time of a customer in the system can anticipate an increase in the average rate of reneging. Thus, to avoid losing potential customers, the system should employ some strategies by choosing the system parameter to further encourage customers to stay in the system. In the case that the service is not successful, the customer can repeat its request again and again until the service succeeds.

4. Governing equations

At an arbitrary time, the system state is defined by a continuous time Markov chain $\{(L(t);\ J(t));\ t \geqslant 0\}$ on the state space $\Omega = \{(n; j) : n \geqslant 0;\ j = \overline{0, K}\}$, where $L(t)$ is the number of customers in the system and $J(t)$ is the state of the servers, i.e.,

$$J(t) = \begin{cases} j, & \text{if the servers are taking the } (j+1)^{\text{th}} \text{ vacation at time } t, \\ & j = \overline{0, K-1}, \\ K, & \text{if the servers are idle or busy at time } t. \end{cases}$$

Let $P_{n,j} = \lim\limits_{t\to\infty} \mathbb{P}(L(t) = n;\ J(t) = j)$, $n \geqslant 0;\ j = \overline{0,K}$, denote the steady-state probabilities of the process $\{(L(t);\ J(t));\ t \geqslant 0\}$. The state-transition diagram is illustrated in Figure 1.

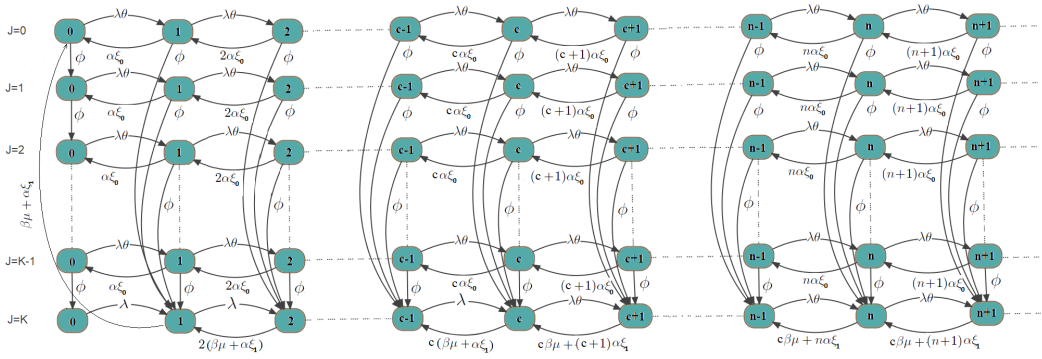

Figure 1. Transition plot

Using Chapman–Kolmogorov equations, we can formulate the balance equations for the suggested queueing model as:

$$(\lambda+\phi)P_{0,0} = \alpha\xi_0 P_{1,0} + (\beta\mu+\alpha\xi_1)P_{1,K}, \quad n = 0, \tag{1}$$

$$(\theta\lambda+\phi+\alpha\xi_0)P_{1,0} = \lambda P_{0,0} + 2\alpha\xi_0 P_{2,0}, \quad n = 1, \tag{2}$$

$$(\theta\lambda+\phi+n\alpha\xi_0)P_{n,0} = \theta\lambda P_{n-1,0} + (n+1)\alpha\xi_0 P_{n+1,0}, \quad n \geqslant 2, \tag{3}$$

$$(\lambda+\phi)P_{0,j} = \alpha\xi_0 P_{1,j} + \phi P_{0,j-1}, \quad j = \overline{1,K-1}, \quad n = 0, \tag{4}$$

$$(\theta\lambda+\phi+\alpha\xi_0)P_{1,j} = \lambda P_{0,j} + 2\alpha\xi_0 P_{2,j}, \quad j = \overline{1,K-1}, \quad n = 1, \tag{5}$$

$$(\theta\lambda+\phi+n\alpha\xi_0)P_{n,j} = \theta\lambda P_{n-1,j} + (n+1)\alpha\xi_0 P_{n+1,j},\ j = \overline{1,K-1},\ n \geqslant 2, \tag{6}$$

$$\lambda P_{0,K} = \phi P_{0,K-1}, \quad n = 0, \tag{7}$$

$$(\lambda+\beta\mu+\alpha\xi_1)P_{1,K} = \lambda P_{0,K} + 2(\beta\mu+\alpha\xi_1)P_{2,K} + \phi\sum_{j=0}^{K-1} P_{1,j}, \quad n = 1, \tag{8}$$

$$(\lambda+n(\beta\mu+\alpha\xi_1))P_{n,K} =$$
$$= \lambda P_{n-1,K} + (n+1)(\beta\mu+\alpha\xi_1)P_{n+1,K} + \phi\sum_{j=0}^{K-1} P_{n,j}, \quad 2 \leqslant n \leqslant c-1, \tag{9}$$

$$(\theta\lambda+c\beta\mu+n\alpha\xi_1)P_{n,K} =$$
$$= \lambda P_{n-1,K} + (c\beta\mu+(n+1)\alpha\xi_1)P_{n+1,K} + \phi\sum_{j=0}^{K-1} P_{n,j}, \quad n = c, \tag{10}$$

$$(\theta\lambda + c\beta\mu + n\alpha\xi_1)P_{n,K} =$$
$$= \theta\lambda P_{n-1,K} + (c\beta\mu + (n+1)\alpha\xi_1)P_{n+1,K} + \phi\sum_{j=0}^{K-1} P_{n,j}, \quad n > c. \quad (11)$$

Consider the probability generating functions (PGFs) as:

$$G_j(z) = \sum_{n=0}^{\infty} z^n P_{n,j},$$

and define

$$G_j'(z) = \frac{d}{dz}G_j(z), \quad j = \overline{0,K}.$$

The normalizing condition is defined as

$$\sum_{n=0}^{\infty}\sum_{j=0}^{K} P_{n,j} = 1.$$

Multiplying Equation (3) by z^n, summing all possible values of n, and using Equations (1) and (2), we get

$$\alpha\xi_0(1-z)G_0^{'}(z) - (\theta\lambda(1-z)+\phi)G_0(z) = -(\beta\mu+\alpha\xi_1)P_{1,K} + \overline{\theta}\lambda(1-z)P_{0,0}. \quad (12)$$

In the same manner, from Equations (4)–(6) and (7)–(11) respectively, we obtain

$$\alpha\xi_0(1-z)G_j'(z) - [\theta\lambda(1-z)+\phi]G_j(z) =$$
$$= \overline{\theta}\lambda(1-z)P_{0,j} - \phi P_{0,j-1}, \quad j = \overline{1,K-1}, \quad (13)$$

and

$$\alpha\xi_1 z(1-z)G_K^{'}(z) - (1-z)(\theta\lambda z - c\beta\mu)G_K(z) =$$
$$= c\beta\mu(1-z)P_{0,K} + z(\beta\mu+\alpha\xi_1)P_{1,K} - \phi z\sum_{j=0}^{K-1} G_j(z) +$$
$$+ \phi z\sum_{j=0}^{K-2} P_{0,j} + \lambda\overline{\theta}z(1-z)\Gamma_1(z) - \beta\mu(1-z)\Gamma_2(z), \quad (14)$$

where

$$\Gamma_1(z) = \sum_{n=0}^{c-1} z^n P_{n,K} \quad \text{and} \quad \Gamma_2(z) = \sum_{n=1}^{c-1}(n-c)z^n P_{n,K}.$$

5. Solution of the differential equations

For $z \neq 1$, Equation (12) can be written as follows:

$$G_0'(z) - \left[\frac{\theta\lambda}{\alpha\xi_0} + \frac{\phi}{\alpha\xi_0(1-z)}\right] G_0(z) = -\frac{\beta\mu + \alpha\xi_1}{\alpha\xi_0(1-z)} P_{1,K} + \frac{\overline{\theta}\lambda}{\alpha\xi_0} P_{0,0}. \quad (15)$$

Multiply both sides of Equation (15) by $e^{-\frac{\theta\lambda}{\alpha\xi_0}z}(1-z)^{\frac{\phi}{\alpha\xi_0}}$, we get

$$\frac{d}{dz}\left(e^{-\frac{\theta\lambda}{\alpha\xi_0}z}(1-z)^{\frac{\phi}{\alpha\xi_0}} G_0(z)\right) = \\ = e^{-\frac{\theta\lambda}{\alpha\xi_0}z}(1-z)^{\frac{\phi}{\alpha\xi_0}} \left(\frac{\overline{\theta}\lambda}{\alpha\xi_0} P_{0,0} - \frac{(\beta\mu + \alpha\xi_1)}{\alpha\xi_0(1-z)} P_{1,K}\right).$$

Next, integrating the above equation from 0 to z, we obtain

$$G_0(z) = e^{\frac{\theta\lambda}{\alpha\xi_0}z}(1-z)^{-\frac{\phi}{\alpha\xi_0}} \times \\ \times \left\{G_0(0) + \frac{\overline{\theta}\lambda}{\alpha\xi_0} P_{0,0} C_1(z) - \frac{\beta\mu + \alpha\xi_1}{\alpha\xi_0} P_{1,K} C_2(z)\right\}, \quad (16)$$

with

$$C_1(z) = \int_0^z e^{-\frac{\theta\lambda}{\alpha\xi_0}s}(1-s)^{\frac{\phi}{\alpha\xi_0}} ds \quad \text{and} \quad C_2(z) = \int_0^z e^{-\frac{\theta\lambda}{\alpha\xi_0}s}(1-s)^{\frac{\phi}{\alpha\xi_0}-1} ds.$$

Since $G_0(1) = \sum_{n=0}^{\infty} P_{n,0} > 0$ and $z = 1$ is the root of denominator of the right hand side of Equation (16), we have that $z = 1$ must be the root of the numerator of the right hand side of Equation (16). So, we obtain

$$G_0(0) = \frac{(\beta\mu + \alpha\xi_1) P_{1,K}}{\alpha\xi_0} C_2(1) - \frac{\overline{\theta}\lambda P_{0,0}}{\alpha\xi_0} C_1(1), \quad (17)$$

where

$$C_1(1) = \int_0^1 e^{-\frac{\theta\lambda}{\alpha\xi_0}s}(1-s)^{\frac{\phi}{\alpha\xi_0}} ds \quad \text{and} \quad C_2(1) = \int_0^1 e^{-\frac{\theta\lambda}{\alpha\xi_0}s}(1-s)^{\frac{\phi}{\alpha\xi_0}-1} ds.$$

Noting $G_0(0) = P_{0,0}$. Then, Equation (17) implies

$$P_{1,K} = \frac{\alpha\xi_0}{(\beta\mu + \alpha\xi_1) C_2(1)} B P_{0,0} = \varpi_1 P_{0,0}, \quad (18)$$

with

$$B = 1 + \frac{\lambda}{\alpha\xi_0}\overline{\theta} C_1(1) \quad \text{and} \quad \varpi_1 = \frac{\alpha\xi_0}{(\beta\mu + \alpha\xi_1) C_2(1)} B.$$

Substituting Equation (18) into Equation (16), we obtain

$$G_0(z) = e^{\frac{\theta\lambda}{\alpha\xi_0}z}(1-z)^{-\frac{\phi}{\alpha\xi_0}}\left\{1+\frac{\overline{\theta}\lambda}{\alpha\xi_0}C_1(z)-\frac{B}{C_2(1)}C_2(z)\right\}P_{0,0}. \tag{19}$$

Next, Equation (13) can be written as

$$G_j'(z)-\left[\frac{\theta\lambda}{\alpha\xi_0}+\frac{\phi}{\alpha\xi_0(1-z)}\right]G_j(z)=\frac{\overline{\theta}\lambda}{\alpha\xi_0}P_{0,j}-\frac{\phi}{\alpha\xi_0(1-z)}P_{0,j-1}. \tag{20}$$

Similarly, as for Equation (15), we multiply both sides of Equation (20) by $e^{-\frac{\theta\lambda}{\alpha\xi_0}z}(1-z)^{\frac{\phi}{\alpha\xi_0}}$. Then, we find

$$\begin{aligned} G_j(z) &= e^{\frac{\theta\lambda}{\alpha\xi_0}z}(1-z)^{-\frac{\phi}{\alpha\xi_0}}\times \\ &\times\left\{G_j(0)+\frac{\lambda\overline{\theta}}{\alpha\xi_0}C_1(z)P_{0,j}-\frac{\phi}{\alpha\xi_0}C_2(z)P_{0,j-1}\right\}, \quad j=\overline{1,K-1}. \end{aligned} \tag{21}$$

Since $G_j(1)=\sum\limits_{n=0}^{\infty}P_{n,j}>0$ ($G_j(1)=P_{\bullet,j}$ represents the probability that the servers are taking the $(j+1)^{\text{th}}$ vacation) and $z=1$ is the root of denominator of the right hand side of Equation (21), we have that $z=1$ must be the root of the numerator of the right hand side of Equation (21). So, we obtain

$$G_j(0)=P_{0,j}=AP_{0,j-1}, \quad j=\overline{1,K-1}, \tag{22}$$

where $A=\dfrac{\phi C_2(1)}{\alpha\xi_0 B}$. Using Equation (22) repeatedly, we get

$$P_{0,j}=A^jP_{0,0}, \quad j=\overline{1,K-1}. \tag{23}$$

Now, by substituting Equation (23) into Equation (21), we find

$$\begin{aligned} G_j(z) &= e^{\frac{\theta\lambda}{\alpha\xi_0}z}(1-z)^{-\frac{\phi}{\alpha\xi_0}}A^j\times \\ &\times\left\{1+\frac{\lambda\overline{\theta}}{\alpha\xi_0}C_1(z)-\frac{B}{C_2(1)}C_2(z)\right\}P_{0,0}, \quad j=\overline{1,K-1}. \end{aligned} \tag{24}$$

To find $P_{0,K}$; the probability that the servers are idle during the busy period, we use Equations (7) and (23). Thus

$$P_{0,K}=\varpi_0P_{0,0}, \tag{25}$$

where $\varpi_0=\dfrac{\phi}{\lambda}A^{K-1}$.

Remark 1. It is easy to see that $0<\phi C_2(1)<\alpha\xi_0$, and $\overline{\theta}\lambda C_1(1)>0$. Thus, $0<\phi C_2(1)<\alpha\xi_0+\overline{\theta}\lambda C_1(1)$. Consequently, we have $0<A<1$.

Next, Equation (14) can be written as:

$$G'_K(z)-\left(\frac{\theta\lambda}{\alpha\xi_1}-\frac{c\beta\mu}{\alpha\xi_1 z}\right)G_K(z)=\frac{\beta\mu+\alpha\xi_1}{\alpha\xi_1(1-z)}P_{1,K}+\frac{c\beta\mu}{\alpha\xi_1 z}P_{0,K}+\frac{\lambda\overline{\theta}}{\alpha\xi_1}\Gamma_1(z)-$$
$$-\frac{\beta\mu}{\alpha\xi_1 z}\Gamma_2(z)+\frac{\phi}{\alpha\xi_1(1-z)}\left(\sum_{j=0}^{K-2}P_{0,j}-\sum_{j=0}^{K-1}G_j(z)\right). \quad (26)$$

In the same way, by multiplying Equation (13) by $\Upsilon(z)=e^{-\frac{\theta\lambda}{\alpha\xi_1}z}z^{\frac{c\beta\mu}{\alpha\xi_1}}$, we get

$$\frac{d}{dz}\left(\Upsilon(z)G_K(z)\right)=\Upsilon(z)\left\{\frac{\beta\mu+\alpha\xi_1}{\alpha\xi_1(1-z)}P_{1,K}+\frac{c\beta\mu}{\alpha\xi_1 z}P_{0,K}+\frac{\lambda\overline{\theta}}{\alpha\xi_1}\Gamma_1(z)-\right.$$
$$\left.-\frac{\beta\mu}{\alpha\xi_1 z}\Gamma_2(z)+\frac{\phi}{\alpha\xi_1(1-z)}\left(\sum_{j=0}^{K-2}P_{0,j}-\sum_{j=0}^{K-1}G_j(z)\right)\right\}. \quad (27)$$

Then, integrating from 0 to z and using Equations (18) and (23)–(25), we obtain

$$G_K(z)=e^{\frac{\theta\lambda}{\alpha\xi_1}z}z^{-\frac{c\beta\mu}{\alpha\xi_1}}\left\{\left((\beta\mu+\alpha\xi_1)\varpi_1+\phi\left(\frac{1-A^{K-1}}{1-A}\right)\right)H_1(z)+\right.$$
$$+\frac{c\beta\mu\phi}{\lambda}A^{K-1}H_2(z)-\phi\left(\frac{1-A^K}{1-A}\right)H_3(z)+\frac{1}{\alpha\xi_1}\times$$
$$\left.\times\left(\lambda\overline{\theta}\int_0^z s^{\frac{c\beta\mu}{\alpha\xi_1}}e^{-\frac{\theta\lambda}{\alpha\xi_1}s}\Gamma_1(s)ds-\beta\mu\int_0^z s^{\frac{c\beta\mu}{\alpha\xi_1}-1}e^{-\frac{\theta\lambda}{\alpha\xi_1}s}\Gamma_2(s)ds\right)\right\}P_{0,0}, \quad (28)$$

where

$$H_1(z)=\frac{1}{\alpha\xi_1}\int_0^z s^{\frac{c\beta\mu}{\alpha\xi_1}}e^{-\frac{\theta\lambda}{\alpha\xi_1}s}(1-s)^{-1}ds,$$

$$H_2(z)=\frac{1}{\alpha\xi_1}\int_0^z s^{\frac{c\beta\mu}{\alpha\xi_1}-1}e^{-\frac{\theta\lambda}{\alpha\xi_1}s}ds,$$

$$H_3(z)=\frac{1}{\alpha\xi_1}\int_0^z s^{\frac{c\beta\mu}{\alpha\xi_1}}e^{-\frac{\theta\lambda}{\alpha\xi_1}s}\Psi(s)(1-s)^{-1}ds,$$

$$\Psi(s)=e^{\frac{\theta\lambda}{\alpha\xi_0}s}(1-s)^{-\frac{\phi}{\alpha\xi_0}}\left\{1+\frac{\lambda\overline{\theta}}{\alpha\xi_0}C_1(s)-\frac{B}{C_2(1)}C_2(s)\right\}.$$

6. Evaluation of probabilities $P_{\bullet,K}$, $P_{\bullet,j}$ and $P_{0,0}$

From Equations (18) and (25), we have $P_{1,K} = \varpi_1 P_{0,0}$ and $P_{0,K} = \varpi_0 P_{0,0}$. Making use of Equations (4)–(6), we recursively get

$$\sum_{j=0}^{K-1} P_{n,j} = \delta_n P_{0,0},$$

where

$$\delta_n = \frac{1}{n\alpha\xi_0}\left\{[\theta\lambda + \phi + (n-1)\alpha\xi_0]\delta_{n-1} - \theta\lambda\delta_{n-2}\right\}.$$

Similarly, from Equations (8), (9), we recursively obtain $P_{n,K} = \varpi_n P_{0,0}$, where

$$\varpi_n = \frac{1}{n(\beta\mu + \alpha\xi_1)}\left\{[\lambda + (n-1)(\beta\mu + \alpha\xi_1)]\varpi_{n-1} - \lambda\varpi_{n-2} - \phi\delta_{n-1}\right\}.$$

Thus, Equation (28) can be written as

$$\begin{aligned} G_K(z) = \\ = e^{\frac{\theta\lambda}{\alpha\xi_1}z} z^{-\frac{c\beta\mu}{\alpha\xi_1}} \left\{\left[\frac{\alpha\xi_0 B}{C_2(1)} + \phi\left(\frac{1-A^{K-1}}{1-A}\right)\right] H_1(z) + \frac{c\beta\mu\phi}{\lambda} A^{K-1} H_2(z) - \right. \\ \left. - \phi\left(\frac{1-A^K}{1-A}\right) H_3(z) + \lambda\bar{\theta} H_4(z) - \beta\mu H_5(z)\right\} P_{0,0}, \quad (29) \end{aligned}$$

with

$$H_4(z) = \frac{1}{\alpha\xi_1}\int_0^z s^{\frac{c\beta\mu}{\alpha\xi_1}} e^{-\frac{\theta\lambda}{\alpha\xi_1}s}\Theta_1(s)ds, \quad H_5(z) = \frac{1}{\alpha\xi_1}\int_0^z s^{\frac{c\beta\mu}{\alpha\xi_1}-1} e^{-\frac{\theta\lambda}{\alpha\xi_1}s}\Theta_2(s)ds,$$

$$\Theta_1(z) = \sum_{n=0}^{c-1} z^n\varpi_n, \quad \text{and} \quad \Theta_2(z) = \sum_{n=1}^{c-1}(n-c)z^n\varpi_n.$$

Thus, for $z = 1$ (noting that $G_K(1) = P_{\bullet,K}$ represents the probability that the servers are busy or idle), we get

$$G_K(1) = P_{\bullet,K} = \Phi(1)P_{0,0}, \quad (30)$$

where

$$\begin{aligned} \Phi(1) = e^{\frac{\theta\lambda}{\alpha\xi_1}} \left\{\left((\beta\mu + \alpha\xi_1)\varpi_1 + \phi\left(\frac{1-A^{K-1}}{1-A}\right)\right) H_1(1) + + \right. \\ \left. + \frac{c\beta\mu\phi}{\lambda} A^{K-1} H_2(1) - \phi\left(\frac{1-A^K}{1-A}\right) H_3(1) + \lambda\bar{\theta} H_4(1) - \beta\mu H_5(1)\right\}, \end{aligned}$$

with

$$H_1(1) = \frac{1}{\alpha\xi_1}\int_0^1 s^{\frac{c\beta\mu}{\alpha\xi_1}} e^{-\frac{\theta\lambda}{\alpha\xi_1}s}(1-s)^{-1}ds,$$

$$H_2(1) = \frac{1}{\alpha\xi_1}\int_0^1 s^{\frac{c\beta\mu}{\alpha\xi_1}-1} e^{-\frac{\theta\lambda}{\alpha\xi_1}s}ds,$$

$$H_3(1) = \frac{1}{\alpha\xi_1}\int_0^1 s^{\frac{c\beta\mu}{\alpha\xi_1}} e^{-\frac{\theta\lambda}{\alpha\xi_1}s}\Psi(s)(1-s)^{-1}ds,$$

$$H_4(1) = \frac{1}{\alpha\xi_1}\int_0^1 s^{\frac{c\beta\mu}{\alpha\xi_1}} e^{-\frac{\theta\lambda}{\alpha\xi_1}s}\Theta_1(s)ds,$$

$$H_5(1) = \frac{1}{\alpha\xi_1}\int_0^1 s^{\frac{c\beta\mu}{\alpha\xi_1}-1} e^{-\frac{\theta\lambda}{\alpha\xi_1}s}\Theta_2(s)ds.$$

Now, from Equations (12) and (13), for $z = 1$, we have

$$P_{\bullet,j} = G_j(1) = A^{j-1}P_{0,0}, \quad j = \overline{0, K-1}. \tag{31}$$

By the definition of $P_{\bullet,j}$, using the normalizing condition, we get

$$\sum_{j=0}^{K} P_{\bullet,j} = 1.$$

Finally, from Equations (30) and (31), we get

$$P_{0,0} = \left(\frac{1-A^K}{A(1-A)} + \Phi(1)\right)^{-1}. \tag{32}$$

7. Performance measures

The prime aim of determining probabilities in previous section is to formulate different metrics in order to examine the performance of the concerned system.

7.1. Mean system sizes

Systematic observations of the system state is very important to enhance the performance and to improve the decision-making.

Let L_j be the system size when the servers are in the state j ($j = \overline{0, K}$). Thus, $\mathbb{E}(L_j)$ is the mean system size when the servers are in the state j,

defined by

$$\mathbb{E}(L_j) = G_j'(1) = \sum_{n=1}^{\infty} nP_{n,j}, \quad j = \overline{0,K},$$

that is, for $j = \overline{0,K-1}$, $\mathbb{E}(L_j)$ represents the mean system size when the servers are taking the $(j+1)^{\text{th}}$ vacation, and $\mathbb{E}(L_K)$ represents the mean system size when the servers are busy. We first derive $\mathbb{E}(L_j)$ for $j = \overline{0,K-1}$.

From Equation (15), using the Hospital rule, we get

$$\mathbb{E}(L_0) = G_0^{'}(1) = \\ = \lim_{z\to 1} \frac{-\theta\lambda G_0(z) + [\theta\lambda(1-z)+\phi]G_0^{'}(z) - \lambda\overline{\theta}P_{0,0}}{-\alpha\xi_0} = \\ = \frac{\theta\lambda G_0(1) - \phi G_0^{'}(1) + \overline{\theta}\lambda P_{0,0}}{\alpha\xi_0}.$$

Thus, we get

$$G_0'(1) = \frac{\theta\lambda G_0(1) + \lambda\overline{\theta}P_{0,0}}{\alpha\xi_0 + \phi}. \tag{33}$$

Similarly, from Equation (13), we find

$$(\alpha\xi_0 + \phi)G_j'(1) = \theta\lambda G_j(1) + \lambda\overline{\theta}P_{0,j}, \quad j = \overline{1,K-1}. \tag{34}$$

Then, from Equations (33) and (34), we have

$$\mathbb{E}(L_j) = G_j'(1) = \frac{\lambda[\theta G_j(1) + \overline{\theta}P_{0,j}]}{\alpha\xi_0 + \phi}, \quad j = \overline{0,K-1}. \tag{35}$$

By substituting Equation (31) and (35), we get

$$\mathbb{E}(L_j) = \frac{\lambda}{\alpha\xi_0 + \phi}\left[\frac{\theta + \overline{\theta}A}{A}\right]A^jP_{0,0}, \quad j = \overline{0,K-1}.$$

Thus, the mean system size when the servers are on vacation is obtained as

$$\mathbb{E}(L_V) = \sum_{j=0}^{K-1}\mathbb{E}(L_j) = \mathbb{E}(L_0) + \sum_{j=1}^{K-1}\mathbb{E}(L_j) = \\ = \frac{\lambda(\theta A^{-1} + \overline{\theta})}{(\alpha\xi_0 + \phi)}P_{0,0} + \frac{\lambda}{(\alpha\xi_0 + \phi)}\left[\frac{\theta + \overline{\theta}A}{A}\right]\sum_{j=1}^{K-1}A^jP_{0,0} = \\ = \left(\frac{\lambda(\theta + \overline{\theta}A)}{\alpha\xi_0 + \phi}\right)\left\{\frac{2 - (A + A^{K-1})}{A(1-A)}\right\}P_{0,0}.$$

Next, from Equation (26) and by using the Hospital rule, we get

$$\mathbb{E}(L_K) = \lim_{z\to 1} G_K^{'}(z) =$$
$$= \frac{1}{\alpha\xi_1}\left\{(\theta\lambda - c\beta\mu)\Phi(1) + c\beta\mu\frac{\phi}{\lambda}A^{K-1} + \frac{\lambda\phi(\theta+\overline{\theta}A)}{\alpha\xi_0+\phi}\left(\frac{1-A^K}{A(1-A)}\right)\right\}P_{0,0} +$$
$$+ \frac{1}{\alpha\xi_1}\left\{\overline{\theta}\lambda\Theta_1(1) - \beta\mu\Theta_2(1)\right\}P_{0,0},$$

where $\Theta_1(1) = \sum_{n=0}^{c-1}\varpi_n$ and $\Theta_2(1) = \sum_{n=1}^{c-1}(n-c)\varpi_n$.

7.2. Queueing model indices

The expressions for the mean queue length, the mean number of customers served and the average rates of impatient customers are established as follows:

— The mean size of the queue is calculated as

$$\mathbb{E}(L_q) = \sum_{j=0}^{K-1}\sum_{n=1}^{\infty} nP_{n,j} + \sum_{n=c}^{\infty}(n-c)P_{n,K} =$$
$$= \mathbb{E}(L) - c + \left\{c\left[\frac{1-A^K}{A(1-A)} + \frac{\phi}{\lambda}A^{K-1}\right] - \Theta_2(1)\right\}P_{0,0}.$$

— The mean number of customers served per unit of time is given as

$$E_{\rm cs} = \beta\mu\sum_{n=1}^{c-1} nP_{n,K} + c\beta\mu\sum_{n=c}^{\infty}P_{n,K} =$$
$$= \beta\mu\left\{c + \left[\Theta_2(1) - c\left(\frac{\phi}{\lambda}A^{K-1} + \frac{1-A^K}{A(1-A)}\right)\right]P_{0,0}\right\}.$$

— The average rate of balking when the servers are in the state $j = \overline{0,K}$ is calculated as

$$B_{\rm r} = \overline{\theta}\lambda\left(\sum_{j=0}^{K-1}\sum_{n=1}^{\infty}P_{n,j} + \sum_{n=c}^{\infty}P_{n,K}\right) =$$
$$= \overline{\theta}\lambda\left\{1 - \left[\frac{2-A-A^{K-1}+(1-A)\Theta_1(1)}{(1-A)}\right]P_{0,0}\right\}.$$

— The average rate of abandonment of a customer due to reneging is as follows

$$R_{\rm ren} = \sum_{j=0}^{K-1}\sum_{n=1}^{\infty} n\alpha\xi_0 P_{n,j} + \sum_{n=1}^{\infty} n\alpha\xi_1 P_{n,K} = \alpha\xi_0\mathbb{E}(L_V) + \alpha\xi_1\mathbb{E}(L_K).$$

8. Conclusion

In this paper, we studied an $M/M/c$ feedback queue under synchronous K-variant vacations, balking, server's states-dependent reneging and retention of reneged customers. We developed the Chapman–Kolmogorov equations for the steady-state probabilities and solved the differential equations by using the probability generating function method. Based on these results, we obtained the probability generating function of the number of customers in the system when the system is on vacation period (resp. on busy period). In addition, we derived explicit expressions of some useful performance measures for the system. Furthermore, we presented closed-form expressions of some important other queueing indices such as the probabilities when the servers are in different states, the proportion of customers served per unit of time, and the average rates of balking and reneging.

It would be interesting to investigate a similar model with two-phase services and multiple vacation policy, server breakdown and repair, and customers' impatience. Further, one can evaluate the optimality of service and repair rates to minimize the waiting time of the customers in the system.

Acknowledgments

The authors thank the anonymous referees for giving great interest to this article.

References

[1] M. Boualem, N. Djellab, and D. Aissani, "Stochastic Inequalities for an $M/G/1$ retrial queues with vacations and constant retrial policy," *Mathematical and Computer Modelling*, vol. 50, no. 1–2, pp. 207–212, 2009. DOI: 10.1016/j.mcm.2009.03.009.

[2] R. Arumuganathan and K. S. Ramaswami, "Analysis of a bulk queue with fast and slow service rates and multiple vacations," *Asia-Pacific Journal of Operational Research*, vol. 22, no. 2, pp. 239–260, 2005. DOI: 10.1142/S0217595905000534.

[3] Y. Levy and U. Yechiali, "An M/M/s Queue With Servers' Vacations," *INFOR: Information Systems and Operational Research*, vol. 14, no. 2, pp. 153–163, 1976. DOI: 10.1080/03155986.1976.11731635.

[4] B. T. Doshi, "Queueing systems with vacations-a survey," *Queueing Systems*, vol. 1, no. 1, pp. 29–66, 1986. DOI: 10.1007/BF01149327.

[5] S. M. Gupta, "Machine interference problem with warm spares, server vacations and exhaustive service," *Performance Evaluation*, vol. 29, no. 3, pp. 195–211, 1997. DOI: 10.1016/S0166-5316(96)00046-6.

[6] N. Tian and Z. G. Zhang, *Vacation queueing models: Theory and applications*. New York, USA: Springer, 2006.

[7] Z. G. Zhang and N. Tian, "Analysis on queueing systems with synchronous vacations of partial servers," *Performance Evaluation*, vol. 52, no. 4, pp. 269–282, 2003. DOI: 10.1016/S0166-5316(02)00192-X.

[8] Z. G. Zhang and N. Tian, "Analysis of Queueing Systems with Synchronous Single Vacation for Some Servers," *Queueing Systems*, vol. 45, pp. 161–175, 2003. DOI: 10.1023/A:1026097723093.

[9] A. A. Bouchentouf, M. Cherfaoui, and M. Boualem, "Performance and economic analysis of a single server feedback queueing model with vacation and impatient customers," *OPSEARCH*, vol. 56, pp. 300–323, 2019. DOI: 10.1007/s12597-019-00357-4.

[10] A. A. Bouchentouf, M. Cherfaoui, and M. Boualem, "Analysis and performance evaluation of Markovian feedback multi-server queueing model with vacation and impatience," *American Journal of Mathematical and Management Sciences*, vol. 40, no. 3, pp. 375–391, 2020. DOI: 10.1080/01966324.2020.1842271.

[11] A. A. Bouchentouf and A. Guendouzi, "Sensitivity analysis of feedback multiple vacation queueing system with differentiated vacations, vacation interruptions and impatient customers," *International journal of applied mathematics & statistics*, vol. 57, no. 6, pp. 104–121, 2018.

[12] A. A. Bouchentouf and A. Guendouzi, "The $M^X/M/c$ Bernoulli feedback queue with variant multiple working vacations and impatient customers: performance and economic analysis," *Arabian Journal of Mathematics*, vol. 9, pp. 309–327, 2020. DOI: 10.1007/s40065-019-0260-x.

[13] M. Boualem, M. Cherfaoui, N. Djellab, and D. Aissani, "Analyse des performances du système $M/G/1$ avec rappels et Bernoulli feedback," French, *Journal Européen des Systèmes Automatisés*, vol. 47, no. 1–3, pp. 181–193, 2013. DOI: 10.3166/jesa.47.181-193.

[14] A. Z. Melikov, S. H. Aliyeva, and M. O. Shahmaliyev, "Methods for computing a system with instantaneous feedback and variable input stream intensity," *Automation and Remote Control*, vol. 81, no. 9, pp. 1647–1658, 2020. DOI: 10.1134/S0005117920090052.

[15] A. A. Bouchentouf, M. Cherfaoui, and M. Boualem, "Modeling and simulation of Bernoulli feedback queue with general customers' impatience under variant vacation policy," *International Journal of Operational Research*, vol. 1, 2020. DOI: 10.1504/IJOR.2020.10034866.

[16] S. Benjaafar, J.-P. Gayon, and S. Tepe, "Optimal control of a production-inventory system with customer impatience," *Operations Research Letters*, vol. 38, no. 4, pp. 267–272, 2010. DOI: 10.1016/j.orl.2010.03.008.

[17] N. Gans, G. Koole, and A. Mandelbaum, "Telephone call centers: tutorial, review, and research prospects," *Manufacturing and Service Operations Management*, vol. 5, no. 2, pp. 79–141, 2003. DOI: 10.1287/msom.5.2.79.16071.

[18] F. Afroun, D. Aïssani, D. Hamadouche, and M. Boualem, "Q-matrix method for the analysis and performance evaluation of unreliable $M/M/1/N$ queueing model," *Mathematical Methods in the Applied Sciences*, vol. 41, no. 18, pp. 9152–9163, 2018. DOI: 10.1002/mma.5119.

[19] M. Boualem, "Stochastic analysis of a single server unreliable queue with balking and general retrial time," *Discrete and Continuous Models and Applied Computational Science*, vol. 28, no. 4, pp. 319–326, 2020. DOI: 10.22363/2658-4670-2020-28-4-319-326.

[20] A. A. Bouchentouf, M. Cherfaoui, M. Boualem, and L. Medjahri, "Variant vacation queueing system with Bernoulli feedback, balking and server's states-dependent reneging," *Yugoslav Journal of Operations Research*, vol. 31, no. 4, pp. 1–19, 2021. DOI: 10.2298/YJOR200418003B.

[21] M. Manoharan and J. K. Jose, "Markovian queueing system with random balking," *OPSEARCH*, vol. 48, no. 3, pp. 236–246, 2011. DOI: 10.1007/s12597-011-0054-1.

[22] E. Altman and U. Yechiali, "Analysis of customer's impatience in queues with server vacations," *Queueing Systems*, vol. 52, no. 4, pp. 261–279, 2006. DOI: 10.1007/s11134-006-6134-x.

[23] E. Altman and U. Yechiali, "Infinite-server queues with systems additional task and impatient customers," *Probability in the Engineering and Informational Sciences*, vol. 22, no. 4, pp. 477–493, 2008. DOI: 10.1017/S0269964808000296.

[24] A. Economou, A. Gómez-Corral, and S. Kanta, "Optimal balking strategies in single-server queues with general service and vacation times," *Performance Evaluation*, vol. 68, no. 10, pp. 967–982, 2011. DOI: 10.1016/j.peva.2011.07.001.

[25] A. A. Bouchentouf and A. Guendouzi, "Cost optimization analysis for an $M^X/M/c$ vacation queueing system with waiting servers and impatient customers," *SeMA Journal*, vol. 76, pp. 309–341, 2019. DOI: 10.1007/s40324-018-0180-2.

[26] W. Sun, S. Li, and E. Cheng-Guo, "Equilibrium and optimal balking strategies of customers in Markovian queues with multiple vacations and N-policy," *Applied Mathematical Modelling*, vol. 40, no. 1, pp. 284–301, 2016. DOI: 10.1016/j.apm.2015.04.045.

[27] D. Yue, W. Yue, Z. Saffer, and X. Chen, "Analysis of an $M/M/1$ queueing system with impatient customers and a variant of multiple vacation policy," *Journal of Industrial and Management Optimization*, vol. 10, no. 1, pp. 89–112, 2014. DOI: 10.3934/jimo.2014.10.89.

[28] D. Yue, W. Yue, and G. Zhao, "Analysis of an $M/M/c$ queueing system with impatient customers and synchronous vacations," *Journal of Applied Mathematics*, vol. 2014, 2014. DOI: 10.1155/2014/893094.

[29] D. Yue, Y. Zhang, and W. Yue, "Optimal performance analysis of an $M/M/1/N$ queue system with balking, reneging and server vacation," *International Journal of Pure and Applied Mathematics*, vol. 28, no. 1, pp. 101–115, 2006.

[30] D. Yue, W. Yue, and G. Zhao, "Analysis of an $M/M/1$ queue with vacations and impatience timers which depend on the server's states," *Journal of Industrial and Management Optimization*, vol. 12, no. 2, pp. 653–666, 2016. DOI: 10.3934/jimo.2016.12.653.

For citation:

A. A. Bouchentouf, L. Medjahri, M. Boualem, A. Kumar, Mathematical analysis of a Markovian multi-server feedback queue with a variant of multiple vacations, balking and reneging, Discrete and Continuous Models and Applied Computational Science 30 (1) (2022) 21–38. DOI: 10.22363/2658-4670-2022-30-1-21-38.

Information about the authors:

Bouchentouf, Amina Angelika — Full Professor, Professor of Mathematics at Djillali Liabes University of Sidi Bel Abbes, Algeria. Permanent researcher at Mathematics Laboratory of Sidi Bel Abbes (e-mail: bouchentouf_amina@yahoo.fr, ORCID: https://orcid.org/0000-0001-8972-4221, ResearcherID: AAI-9425-2021, Scopus Author ID: 56682879900)

Medjahri, Latifa — Faculty Member at Abou Bekr Belkaid University of Tlemcen, Algeria (e-mail: l.medjahri@yahoo.fr)

Boualem, Mohamed — Full Professor, Professor of Applied Mathematics at the Department of Technology at the University of Bejaia, Algeria. Permanent Researcher at the Research Unit LaMOS (Modeling and Optimization of Systems) (e-mail: robertt15dz@yahoo.fr, phone: +21334813708, ORCID: https://orcid.org/0000-0001-9414-714X, ResearcherID: A-3176-2019, Scopus Author ID: 26633399700)

Kumar, Amit — Assistant Professor at the Department of Mathematics at the University of Chandigarh, Mohali (Punjab), Pin No-140413, India (e-mail: amitk251@gmail.com, ORCID: https://orcid.org/0000-0001-5347-1808)

УДК 519.872:519.217
PACS 07.05.Tp, 02.60.Pn, 02.70.Bf
DOI: 10.22363/2658-4670-2022-30-1-21-38

Математический анализ марковской многолинейной системы массового обслуживания с обратной связью, прогулками приборов и нетерпеливыми заявками

Амина Анжелика Бушентуф[1], **Латифа Меджахри**[2], **Мохамед Буалем**[3], **Амит Кумар**[4]

[1] *Университет Джиллали Лябеса в Сиди-Бель-Аббес, 22000, Алжир*
[2] *Университет Тлемсан, 13000, Алжир*
[3] *Университет Беджайя, 06000, Алжир*
[4] *Университет Чандигар, Мохали (Пенджаб), 140413, Индия*

Аннотация. В работе исследуется система массового обслуживания с нетерпеливыми заявками, бернуллиевской обратной связью и прогулками приборов. В момент перед поступлением заявки в систему клиент, анализируя занятость системы и состояние приборов, принимает решение о принятии заявки или её уходе из системы. Предполагается, что нетерпение клиента может возникнуть как в период занятости, так и в период отдыха (прогулки) приборов из-за имевшихся ранее случаев длительного ожидания начала обслуживания в системе, информация о которых предоставляется с помощью определённого механизма. Обратная связь состоит в том, что часть ранее обслуженных клиентов может вернуться в систему для повторного обслуживания. Исследуемая система может применяться для анализа передачи данных в телекоммуникационных системах. Для стационарного распределения вероятностей записаны и решены с помощью производящих функций уравнения Колмогорова–Чепмена. Кроме того, получены аналитические выражения для ряда ключевых характеристик системы, например таких, как вероятности занятости или прогулки прибора, среднее число обслуженных заявок в единицу времени, средние интенсивности отказов от поступления и отказов от ожидания начала обслуживания.

Ключевые слова: марковская многолинейная система массового обслуживания, производящая функция, нетерпеливые заявки, прогулка прибора, обратная связь

Discrete & Continuous Models
& Applied Computational Science
ISSN 2658-7149 (online), 2658-4670 (print)

2022, 30 (1) 39–51
http://journals.rudn.ru/miph

Research article

UDC 519.711.3
DOI: 10.22363/2658-4670-2022-30-1-39-51

The quantization of the classical two-dimensional Hamiltonian systems

Irina N. Belyaeva

Belgorod State National Research University
85, Pobedy St., Belgorod, 308015, Russian Federation

(received: December 26, 2021; revised: January 18, 2022; accepted: February 18, 2022)

Abstract. The paper considers the class of Hamiltonian systems with two degrees of freedom. Based on the classical normal form, according to the rules of Born–Jordan and Weyl–MacCoy, its quantum analogs are constructed for which the eigenvalue problem is solved and approximate formulas for the energy spectrum are found. For particular values of the parameters of quantum normal forms using these formulas, numerical calculations of the lower energy levels were performed, and the obtained results were compared with the known data of other authors. It was found that the best and good agreement with the known results is obtained using the Weyl–MacCoy quantization rule. The procedure for normalizing the classical Hamilton function is an extremely time-consuming task, since it involves hundreds and even thousands of polynomials for the necessary transformations. Therefore, in the work, normalization is performed using the REDUCE computer algebra system. It is shown that the use of the Weyl–MacCoy and Born–Jordan correspondence rules leads to almost the same values for the energy spectrum, while their proximity increases for large quantities of quantum numbers, that is, for highly excited states. The canonical transformation is used in the work, the quantum analog of which allows us to construct eigenfunctions for the quantum normal form and thus obtain analytical formulas for the energy spectra of different Hamiltonian systems. So, it is shown that quantization of classical Hamiltonian systems, including those admitting the classical mode of motion, using the method of normal forms gives a very accurate prediction of energy levels.

Key words and phrases: Hamilton function, normal form, Weyl–MacCoy rules, Born–Jordan rule, quantum normal form, computer modeling, energy spectra

Introduction

Representation of the original classical Hamilton function in normal form as the sum of homogeneous polynomials in canonically conjugate coordinates and momenta [1] allows us to carry out its quantum-mechanical description.

The main provisions of the new quantum mechanics were discovered by W. Heisenberg in 1925 [2]. In the same year, the paper was published by

M. Born and P. Jordan [3], in which the commutation relation for the quantum-mechanical operators of coordinate $\hat{q}$ and momentum $\hat{p}$ was obtained for the first time in the form

$$\hat{p}\hat{q} - \hat{q}\hat{p} = h/2\pi i, \tag{1}$$

as well as the rule of matching to the classical monom of the form $q^m p^n$, $(m, n = 1, 2, 3, ...)$ of its quantum analog, which we present as

$$\mathrm{BJ}\{q^m p^n = p^n q^m\} = \frac{1}{n+1}\sum_{k=0}^{n} \hat{p}^{n-k}\hat{q}^m\hat{p}^k. \tag{2}$$

The results obtained by P.A.M. Dirac [4] should be added to this. In this paper P.A.M. Dirac wrote: "In a recent work [2], Heisenberg put forward a new theory, which suggests that not the equations of classical mechanics are erroneous in any way, but that mathematical operations, by which physical results are derived from these equations, need modification. Thus, all the information provided by the classical theory can be used in the new theory... We make the basic assumption that the difference of the Heisenberg products of two quantum quantities is equal to the Poisson bracket of these quantities multiplied by $ih/2\pi$":

$$\{q, p\} \to \frac{1}{i\hbar}[\hat{q}, \hat{p}] = \frac{1}{i\hbar}(\hat{q}\hat{p} - \hat{p}\hat{q}) = 1, \tag{3}$$

here $\{q; p\}$ is the Poisson bracket, $[\hat{q}, \hat{p}]$ is the commutator for the operators, $\hat{q}, \hat{p}$, $\hbar$ is Planck's constant.

In 1927, G. Weyl published a paper [5], (see also [6]), in which the author, on the basis of group-theoretic ideas, proposed the following rule of correspondence between classical quantities and their quantum analogs in integral form. Let the classical function $f(q, p)$ be determined by the following Fourier integral

$$f(q, p) = \iint \exp(i\sigma p + i\tau q)\zeta(\sigma, \tau)d\sigma d\tau,$$

then the corresponding function $F(\hat{q}, \hat{p})$ in quantum mechanics is given by

$$F(\hat{q}, \hat{p}) = \iint \exp(i\sigma\hat{p} + i\tau\hat{q})\zeta(\sigma, \tau)d\sigma d\tau,$$

and the operators $\hat{q}, \hat{p}$ satisfy the commutation relation (1). Based on these assumptions for functions of polynomial form $f(q, p) = q^m p^n$, a number of different relations were obtained [7], one of which can be written as

$$\mathrm{WMc}\{q^m p^n \ = p^n \ q^m\} = \frac{1}{2^n}\sum_{k=0}^{n} \frac{n!}{k!(n-k)!}\hat{p}^{n-k}\hat{q}^m\hat{p}^k, \tag{4}$$

which we will call the Weyl–MacCoy quantization rule.

In [8], the correspondence rule was obtained in the following form

$$f(q)p^n \ \to \frac{1}{2^n}\sum_{k=0}^{n}\frac{n!}{k!(n-k)!}\hat{p}^k f(\hat{q})\hat{p}^{n-k},$$

which is represented by repeating anti-commutators $[\hat{a},\hat{b}]_+ = \hat{a}\hat{b} + \hat{b}\hat{a}$ as follows:

$$f(q)p^n \ \to [[...[f(\hat{q}),\hat{p}]_+,\hat{p}]_+,...]_+.$$

In addition to the main works mentioned above, there are publications in which the problem of the correspondence of classical quantities and their quantum analogs is discussed from different perspectives (see, for example, [9]–[14]).

A critical review of various quantization rules for classical Hamilton functions was carried out in [15].

In this paper, for the Hamiltonian, in general, non-integrable system with two degrees of freedom, we have received the classical normal Birkhoff–Gustavson form for which the corresponding quantum analogs are obtained by the Born–Jordan and Weyl–MacCoy quantization rules. For these quantum analogs, i.e., Schrödinger operators, approximate formulas for energy spectra are found. According to these formulas, for some specific numerical values of the parameters, the energy spectra were calculated and compared with the literature results obtained by direct numerical calculations.

1. A quantum analog of the classical normal form

The paper considers a classical system with two degrees of freedom, whose Hamilton function is

$$\begin{gathered} H = \frac{1}{2}\left(p_1^2 + p_2^2\right) + V(q_1,q_2), \\ V(q_1,q_2) = \frac{1}{2}\left(q_1^2+q_2^2\right) + b\left(q_1^2 q_2 + \frac{1}{3}q_2^3\right) + cq_1^2q_2^2 + d\left(q_1^2+q_2^2\right)^2, \end{gathered} \tag{5}$$

where the coordinates q_1, q_2 and momenta p_1, p_2 are canonically conjugate variables, b, c, d are dimensionless parameters.

Since system (5) is resonant with a frequency ratio of 1:1, when we bring it to normal form for the initial Hamilton function, we apply the canonical transformation with a valence equal to an imaginary unit [16]:

$$\begin{gathered} q_1 = \frac{1}{2i}(-Q_1 + Q_2 + P_1 - P_2), \quad q_2 = \frac{1}{2}(Q_1 + Q_2 + P_1 + P_2), \\ p_1 = \frac{1}{2}(Q_1 - Q_2 + P_1 - P_2), \quad p_2 = \frac{1}{2i}(Q_1 + Q_2 - P_1 - P_2), \end{gathered} \tag{6}$$

and its inverse transformation is written in the form

$$\begin{aligned} Q_1 &= \frac{1}{2}(q_2 - ip_2) + \frac{i}{2}(q_1 - ip_1), \quad Q_2 = \frac{1}{2}(q_2 - ip_2) - \frac{i}{2}(q_1 - ip_1), \\ P_1 &= \frac{1}{2}(q_2 + ip_2) - \frac{i}{2}(q_1 + ip_1), \quad P_2 = \frac{1}{2}(q_2 + ip_2) + \frac{i}{2}(q_1 + ip_1). \end{aligned} \tag{7}$$

It directly follows from expressions (7) that the variables Q_1, Q_2 are complex conjugate to the variables P_1, P_2 respectively.

Canonical transformations (7) using standard substitution

$$p_\nu \to \hat{p}_\nu = -i\frac{\partial}{\partial q_\nu}, \quad q_\nu \to \hat{q}_\nu = q_\nu, \quad \nu = 1, 2$$

with a known commutation rule (Planck constant $\hbar = 1$)

$$[\hat{p}_\nu, \hat{q}_\nu] = i\delta_{\mu\nu}, \quad \mu, \nu = 1, 2 \tag{8}$$

($\delta_{\mu\nu}$ — Kronecker symbol) will be presented by us in the operator form

$$\hat{Q}_1 = \hat{a}_2^+ + i\hat{a}_1^+, \quad \hat{Q}_2 = \hat{a}_2^+ - i\hat{a}_1^+, \quad \hat{P}_1 = \hat{a}_2 - i\hat{a}_1, \quad \hat{P}_2 = \hat{a}_2 + i\hat{a}_1, \tag{9}$$

where

$$\begin{aligned} \hat{a}_1^+ &= \frac{1}{2}(\hat{q}_1 - i\hat{p}_1), \quad \hat{a}_2^+ = \frac{1}{2}(\hat{q}_2 - i\hat{p}_2), \\ \hat{a}_1 &= \frac{1}{2}(\hat{q}_1 + i\hat{p}_1), \quad \hat{a}_2 = \frac{1}{2}(\hat{q}_2 + i\hat{p}_2), \end{aligned} \tag{10}$$

where the upper "+" symbol denotes Hermitian conjugation. Taking into account expressions (8), it is easy to verify that the operators (10) commute by the rule

$$[\hat{a}_\mu, \hat{a}_\nu^+] = \frac{i}{2}\delta_{\mu\nu},$$

and the operators (9) obey the rule

$$[\hat{P}_\mu, \hat{Q}_\nu^+] = \delta_{\mu\nu}. \tag{11}$$

However, the commutation (11) can be directly obtained from the Dirac quantization condition (3), given that the classical canonical transformation (6) has a valence equal to an imaginary unit.

From the expressions (9), (10) it follows that the operators $\hat{P}_\nu$ and $\hat{Q}_\nu$, ($\nu = 1, 2$) are the annihilation and birth operators, respectively.

Using the quantization rules (2) and (4), we obtain two expressions of its quantum analogs $\hat{K}_6^{\mathrm{BJ}}$ and $\hat{K}_6^{\mathrm{WMc}}$, respectively, and each expression can be represented as the sum of the diagonal and nondiagonal parts

$$\hat{K}_6^{\mathrm{BJ}} = \hat{K}_{\mathrm{diag}}^{\mathrm{BJ}} + \hat{K}_{\mathrm{nondiag}}^{\mathrm{BJ}}.$$

$$\hat{K}_6^{\mathrm{WMc}} = \hat{K}_{\mathrm{diag}}^{\mathrm{WMc}} + \hat{K}_{\mathrm{nondiag}}^{\mathrm{WMc}}.$$

Below we present the diagonal parts only:

$$\hat{K}^{\mathrm{BJ}}_{\mathrm{diag}} = \hat{Q}_1\hat{P}_1 + \hat{Q}_2\hat{P}_2 + 1 + K_{41}\left[(\hat{Q}_1\hat{P}_1 + \hat{Q}_2\hat{P}_2 + 1)^2 + \frac{5}{2}\right] +$$
$$+ K_{42}\left(\hat{Q}_1\hat{P}_1 + \hat{Q}_2\hat{P}_2 + 2\hat{Q}_1\hat{P}_1\hat{Q}_2\hat{P}_2 + \frac{1}{2}\right) + K_{43}\left[(\hat{Q}_1\hat{P}_1 - \hat{Q}_2\hat{P}_2)^2 + \frac{5}{2}\right] +$$
$$+ K_{61}\left[(\hat{Q}_1\hat{P}_1 + \hat{Q}_2\hat{P}_2 + 1)^3 + \frac{1}{4}(\hat{Q}_1\hat{P}_1)^2 + \right.$$
$$\left. + \frac{1}{4}(\hat{Q}_2\hat{P}_2)^2 + \frac{27}{4}(\hat{Q}_1\hat{P}_1 + \hat{Q}_2\hat{P}_2) + \frac{13}{2}\right] -$$
$$- K_{64}\left[(\hat{Q}_1\hat{P}_1 + \hat{Q}_2\hat{P}_2 + 1)(\hat{Q}_1\hat{P}_1 + \hat{Q}_2\hat{P}_2 + 2\hat{Q}_1\hat{P}_1\hat{Q}_2\hat{P}_2 + 3)\right] +$$
$$+ K_{66}\left[(\hat{Q}_1\hat{P}_1 + \hat{Q}_2\hat{P}_2 + 1)\left((\hat{Q}_1\hat{P}_1 - \hat{Q}_2\hat{P}_2)^2 + \frac{1}{4}(\hat{Q}_1\hat{P}_1 + \hat{Q}_2\hat{P}_2)\right) - \right.$$
$$\left. - \frac{1}{2}\hat{Q}_1\hat{P}_1\hat{Q}_2\hat{P}_2\right]. \quad (12)$$

$$\hat{K}^{\mathrm{WMc}}_{\mathrm{diag}} = \hat{Q}_1\hat{P}_1 + \hat{Q}_2\hat{P}_2 + 1 + K_{41}\left[(\hat{Q}_1\hat{P}_1 + \hat{Q}_2\hat{P}_2 + 1)^2 + \frac{1}{2}\right] +$$
$$+ K_{42}\left(\hat{Q}_1\hat{P}_1 + \hat{Q}_2\hat{P}_2 + 2\hat{Q}_1\hat{P}_1\hat{Q}_2\hat{P}_2 + \frac{1}{2}\right) + K_{43}\left[(\hat{Q}_1\hat{P}_1 - \hat{Q}_2\hat{P}_2)^2 + \frac{1}{2}\right] +$$
$$+ K_{61}\left[(\hat{Q}_1\hat{P}_1 + \hat{Q}_2\hat{P}_2 + 1)^3 + 2(\hat{Q}_1\hat{P}_1 + \hat{Q}_2\hat{P}_2 + 1)\right] -$$
$$- K_{64}\left[(\hat{Q}_1\hat{P}_1 + \hat{Q}_2\hat{P}_2 + 1)(\hat{Q}_1\hat{P}_1 + \hat{Q}_2\hat{P}_2 + 2\hat{Q}_1\hat{P}_1\hat{Q}_2\hat{P}_2 + 1)\right] +$$
$$+ K_{66}\left[(\hat{Q}_1\hat{P}_1 + \hat{Q}_2\hat{P}_2 + 1)\left((\hat{Q}_1\hat{P}_1)^2 + (\hat{Q}_2\hat{P}_2)^2 - 2\hat{Q}_1\hat{P}_1\hat{Q}_2\hat{P}_2 + 1\right)\right]. \quad (13)$$

We note that the quantum state vectors [2]

$$|N, L\rangle = \left[\left(\frac{N+L}{2}\right)!\left(\frac{N-L}{2}\right)!\right]^{-1/2} \hat{Q}_2^{(\frac{N-L}{2})}\hat{Q}_1^{(\frac{N+L}{2})}|0,0\rangle, \quad (14)$$
$$\hat{P}_1|0,0\rangle = \hat{P}_2|0,0\rangle = 0,$$

where N is the main quantum number, $N = 0, 1, 2, 3, ...$, and L is the orbital quantum number, which for a given value N takes the following values: $L = \pm N$, $\pm(N-2)$, $\pm(N-4)$, ..., $\pm 1(0)$, are eigenvectors for the diagonal parts of quantum analogs (12) and (13). The presence of nondiagonal terms in quantum analogs (12) and (13) is due to the fact that in the original classical Hamiltonian system (5) there is a 1:1 resonance ratio between frequencies.

2. The energy spectra of quantum normal forms

Since vectors (14) represent an orthonormal basis, the energy spectra of quantum normal forms (12) and (13) are determined by the following expressions:

$$E_{\mathrm{BJ}}^{NL} = \langle N, L|\hat{K}_{\mathrm{diag}}^{\mathrm{BJ}}|N, L\rangle + \sum_{N',L'} \langle N', L'|\hat{K}_{\mathrm{nondiag}}^{\mathrm{BJ}}|N, L\rangle, \tag{15}$$

$$E_{\mathrm{WMc}}^{NL} = \langle N, L|\hat{K}_{\mathrm{diag}}^{\mathrm{WMc}}|N, L\rangle + \sum_{N',L'} \langle N', L'|\hat{K}_{\mathrm{nondiag}}^{\mathrm{WMc}}|N, L\rangle. \tag{16}$$

Using the relations

$$\hat{Q}_1\hat{P}_1|N, L\rangle = \left(\frac{N+L}{2}\right)|N, L\rangle, \quad \hat{Q}_2\hat{P}_2|N, L\rangle = \left(\frac{N-L}{2}\right)|N, L\rangle,$$

from expressions (15) and (16) without taking into account the nondiagonal terms, we obtain the formulas for the energy spectra

$$\begin{aligned} E_{NL}^{\mathrm{BJ}} = N + 1 + \frac{1}{2}K_{41}(2N^2 + 4N + 7) + \frac{1}{2}K_{42}(N^2 + 2N - L^2 + 1) + \\ \frac{1}{2}K_{43}(2L^2 + 5) + \frac{1}{8}K_{61}(8N^3 + 25N^2 + 78N + L^2 + 60) - \\ \frac{1}{2}K_{64}(N^3 + 3N^2 + 8N - NL^2 - L^2 + 3) + \\ + \frac{1}{8}K_{66}(N^2 + 14N + 8NL^2 + 9L^2 + 12), \end{aligned} \tag{17}$$

$$\begin{aligned} E_{NL}^{\mathrm{WMc}} = N + 1 + \frac{1}{2}K_{41}(2N^2 + 4N + 3) + \frac{1}{2}K_{42}(N^2 + 2N - L^2 + 1) + \\ + \frac{1}{2}K_{43}(2L^2 + 1) + K_{61}(N^3 + 3N^2 + 5N + 3) - \\ - \frac{1}{2}K_{64}(N^3 + 3N^2 + 2N - NL^2 - L^2 + 1) + \\ + K_{66}(N + NL^2 + L^2 + 1). \end{aligned} \tag{18}$$

As it can be seen, the energy spectrum in both cases of quantization is degenerate by sign of the orbital quantum moment L. Besides, taking into account the contributions of nondiagonal terms can lead to a shift of energy levels, which differ in the value of the orbital quantum number by four and six units. Therefore, it is expected that approximate formulas (17), (18) with satisfactory accuracy describe the energy spectrum of the lowest states in the vicinity of a stationary point located at the origin.

From the comparison of formulas (17), (18) for energy spectra, a general conclusion can be drawn that the quantization rules of Born–Jordan and Weyl–MacCoy predict different values for the ground state energy, which are determined by the numerical values of the parameters b, c and d.

More specific conclusions can be obtained by comparing the results of numerical calculations using formulas (17), (18) with exact energy levels calculated for any particular values of the parameters of the Hamiltonian, which will be performed in the next section. In cases where the classical

system (5) is integrable, approximate formulas (17), (18), expressed directly through the parameters b, c and d have the following form.

1. If there is a relationship $c = 4d$, and the parameter b is not equal to or is equal to zero, then the energy spectra are calculated by the formulas:

$$E_{NL}^{\mathrm{BJ}} = N + 1 + d\left(\frac{9}{4}N^2 + \frac{9}{2}N - \frac{3}{4}L^2 + 6\right) - d^2\left(\frac{85}{8}N^3 + \frac{1037}{32}N^2 + \frac{1479}{16}N - \frac{187}{32}L^2 - \frac{51}{8}NL^2 + \frac{561}{8}\right) - b^2\left(\frac{5}{8}N^2 + \frac{5}{4}N - \frac{5}{24}L^2 + \frac{5}{3}\right) + db^2\left(\frac{125}{8}N^3 + \frac{1525}{32}N^2 + \frac{2175}{16}N - \frac{275}{32}L^2 - \frac{75}{8}NL^2 + \frac{825}{8}\right) - b^4\left(\frac{1175}{864}N^3 + \frac{14335}{3456}N^2 + \frac{6815}{576}N - \frac{2585}{3456}L^2 - \frac{235}{288}NL^2 + \frac{2585}{288}\right), \quad (19)$$

$$E_{NL}^{\mathrm{WMc}} = N + 1 + d\left(\frac{9}{4}N^2 + \frac{9}{2}N - \frac{3}{4}L^2 + 3\right) + d^2\left(\frac{17}{8}N^3 + \frac{51}{8}N^2 + \frac{17}{4}N - \frac{51}{8}L^2 - \frac{51}{8}NL^2\right) - b^2\left(\frac{5}{8}N^2 + \frac{5}{4}N - \frac{5}{24}L^2 + \frac{5}{6}\right) - db^2\left(\frac{25}{8}N^3 + \frac{75}{8}N^2 + \frac{25}{4}N - \frac{75}{8}L^2 - \frac{75}{8}NL^2\right) + b^4\left(\frac{235}{864}N^3 + \frac{235}{288}N^2 + \frac{235}{432}N - \frac{235}{288}L^2 - \frac{235}{288}NL^2\right). \quad (20)$$

2. If the parameters $b = c = 0$, but the parameter $d > 0$, then the formulas have the form:

$$E_{NL}^{\mathrm{BJ}} = N + 1 + d\left(\frac{3}{2}N^2 + 3N - \frac{1}{2}L^2 + 4\right) - d^2\left(\frac{17}{4}N^3 + 13N^2 + \frac{75}{2}N - 2L^2 - \frac{9}{4}NL^2 + \frac{57}{2}\right), \quad (21)$$

$$E_{NL}^{\mathrm{WMc}} = N + 1 + d\left(\frac{3}{2}N^2 + 3N - \frac{1}{2}L^2 + 2\right) - d^2\left(\frac{17}{4}N^3 + \frac{51}{4}N^2 + 19N - \frac{9}{4}L^2 - \frac{9}{4}NL^2 + \frac{21}{2}\right). \quad (22)$$

3. If the parameters $b = 0$, $c = -2d$, $d \neq 0$, then we obtain the formulas:

$$E_{NL}^{\mathrm{BJ}} = N + 1 + d\left(\frac{9}{8}N^2 + \frac{9}{4}N - \frac{3}{8}L^2 + 3\right) -$$

$$- d^2 \left(\frac{85}{32} N^3 + \frac{1037}{128} N^2 + \frac{1479}{64} N - \frac{187}{128} L^2 - \frac{51}{32} N L^2 + \frac{561}{32} \right), \quad (23)$$

$$E_{NL}^{\mathrm{WMc}} = N + 1 + d \left(\frac{9}{8} N^2 + \frac{9}{4} N - \frac{3}{8} L^2 + \frac{3}{2} \right) - \\ - d^2 \left(\frac{187}{32} N^3 + \frac{561}{32} N^2 + \frac{391}{16} N - \frac{153}{32} L^2 - \frac{153}{32} N L^2 + \frac{51}{4} \right). \quad (24)$$

3. The comparison of energy spectra

Unfortunately, the exact spectrum obtained, for example, by direct numerical calculations of the Schrödinger equation with its quantum analog of the original Hamilton function (5), in which a well-known replacement is to be made $p_1 \to \hat{p}_1 = -i\dfrac{\partial}{\partial q_1}$, $p_2 \to \hat{p}_2 = -i\dfrac{\partial}{\partial q_2}$, $q_1 \to \hat{q}_1 = q_1$, $q_2 \to \hat{q}_2 = q_2$ for arbitrary values of its parameters, is not available in the literature.

Also, direct numerical calculations using modern computer technologies face the difficulty of solving eigenvalue problems, for example, even with the help of carefully developed software packages based on the diagonalization method, which is also the task of integrating the Schrödinger equation for two or more independent variables.

Below we present the results of numerical calculations of energy spectra for specific numerical values of the parameters b, c, d in cases where the classical system (5) is integrable.

Table 1 shows the values of the lowest energy levels calculated by the approximate formulas (19) and (20) in the first case of integrability, i.e., under the condition $c = 4d$ and $b = 0$.

Table 1
The comparison of energy levels at parameter values $b = 0$, $c = 0.02$, $d = 0.005$, $(c = 4d)$

No	$E_{N,L}$	E_{NL}^{BJ}	E_{NL}^{WMc}	$E_{NL}^{\mathrm{BJ}} - E_{NL}^{\mathrm{WMc}}$	$E_{n+1}^{\mathrm{WMc}} - E_{n}^{\mathrm{WMc}}$	$E_{n+1}^{\mathrm{BJ}} - E_{n}^{\mathrm{BJ}}$
1.	$E_{0,0}$	1.028247	1.015000	0.013247	-	-
2.	$E_{1,\pm1}$	2.055166	2.045000	0.010166	1.030000	1.026919
3.	$E_{2,\pm2}$	3.095512	3.089363	0.006149	1.044363	1.039953
4.	$E_{2,0}$	3.108259	3.106275	0.001984	0.016913	0.013141
5.	$E_{3,\pm3}$	4.147469	4.147450	0.000019	1.041175	1.039209
6.	$E_{3,\pm1}$	4.172475	4.182550	−0.010075	0.035100	0.025006
7.	$E_{4,\pm4}$	5.211578	5.218625	−0.007047	1.036075	1.039103
8.	$E_{4,\pm2}$	5.247175	5.273188	−0.026013	0.054563	0.035597
9.	$E_{4,0}$	5.259041	5.291375	−0.032334	0.018188	0.011866

From the table 1, it follows that the Weyl–MacCoy quantization rule leads to a lower energy level for the ground state and a greater decomposition of the levels with respect to the orbital moment at a given value of the principal quantum number N. In the classically integrable case under consideration, there are no exact (analytical or numerical) values of the energy spectrum in the current literature. However, the spectrum is known [17] in the second classical case of integrability, when the parameters of the quantum analog of the Hamilton function (5) are equal $b = 0$, $c = 0$, $d \neq 0$.

Besides, the values of the energy spectrum of a one-dimensional anharmonic oscillator are known and also with great accuracy, in particular, with a fourth degree in potential energy. Knowing this spectrum, it is possible to construct an approximate spectrum of a quantum analog of the original Hamilton function (5), but already a two-dimensional Hamiltonian given the values of parameters $b = 0$, $c = -2d$, $d \neq 0$, for which system (5) is integrable in the classical case.

We will compare below these well-known and very reliable numerical results for the energy spectra with our results, which are calculated by formulas (23), (24) according to the Born–Jordan and Weil–McCoy quantization rules.

For parameter values $b = 0$, $c = 0$ and $d \neq 0$ the Schrödinger equation corresponding to the classical Hamilton function (5) allows separation of variables in polar coordinates, and the energy spectrum is characterized by a radial quantum number n and orbital momentum l. In [17] a method for numerical solving the radial Schrödinger equation was developed and energy levels were calculated for the values of quantum numbers equal $n, l = 0, 1, 2$ for a parameter value $d = 0.000005$. Quantum numbers n, l are connected with our numbers N, L by the following relations: $N = 2n + l$, $|L| = l$.

Table 2 shows the energy levels obtained in [17], as well as their values calculated for the same value of the parameter using formulas (21) and (22) based on quantization of the classical normal form, according to the Born–Jordan and Weil–McCoy rules, respectively.

Table 2 shows that a very good approximation to the exact spectrum is given by the application of the Weyl–MacCoy quantization rule. In particular, the ground state energy obtained using the Weyl–MacCoy quantization rule differs from the result of [17] by $0.5 \cdot 10^{-7}\%$, and when quantized by the Born–Jordan rule, by 0.001%. At the same time, for energy of level 14, these errors are equal, respectively, $0.4 \cdot 10^{-8}\%$ and 0.0001%, i.e., the prediction according to the Born–Jordan rule improves.

In the third case ($b = 0$, $c = -2d$, $d \neq 0$) of integrability of the classical system (5), with its quantum-mechanical description, it is necessary to solve the following two-dimensional Schrödinger equation

$$(\hat{H}_1 + \hat{H}_2)\Psi = 2E\Psi, \quad \hat{H}_i = -\frac{d^2}{dq_i^2} + q_i^2 + 2dq_i^4, \quad i = 1, 2, \qquad (25)$$

where the variables are separated. Therefore, its solving is reduced to solving two identical one-dimensional equations for the anharmonic oscillator, and the energy spectrum is found in the form of the following sum $2E = 2E_1 + 2E_2$.

The quantum numbers of an isotropic two-dimensional oscillator (N, L) are connected with the quantum numbers $(n1, n2)$ of one-dimensional oscillators

by the following relations: $N = n1 + n2$ and $L = n1 - n2$. We note that the ordering of the values of the energy spectrum levels by the value of quantum numbers (N, L) as compared to another numbering of states has the advantage that the values of the energy spectrum levels, numbered by quantum numbers (N, L), grow with an increase of the main quantum number.

Table 2

The comparison of energy levels E_{NL}^{BJ} and E_{NL}^{WMc} with their values from [17] for $d = 0.000005$

No.	$2E_{N,L}$	E_{NL}^{BJ}	E_{NL}^{WMc}	Results [17]
1.	$2E_{0,0}$	2.0000399985	2.0000199995	2.0000199995
2.	$2E_{1,\pm1}$	4.0000799961	4.0000599979	4.0000599981
3.	$2E_{2,\pm2}$	6.0001399918	6.0001199946	6.0001199949
4.	$2E_{2,0}$	6.0001599905	6.0001399933	6.0001399936
5.	$2E_{3,\pm3}$	8.0002199853	8.0001999892	8.0001999892
6.	$2E_{3,\pm1}$	8.0002599818	8.0002399856	8.0002399859
7.	$2E_{4,\pm4}$	10.000319975	10.000299981	10.000299981
8.	$2E_{4,\pm2}$	10.000379969	10.000359974	10.000359975
9.	$2E_{4,0}$	10.000399967	10.000379971	10.000379972
10.	$2E_{5,\pm5}$	12.000439962	12.000419969	12.000419969
11.	$2E_{5,\pm3}$	12.000519952	12.000499958	12.000499958
12.	$2E_{5,\pm1}$	12.000559947	12.000539953	12.000539953
13.	$2E_{6,\pm6}$	14.000579946	14.000559953	14.000559953
14.	$2E_{6,\pm4}$	14.000679930	14.000659937	14.000659937
15.	$2E_{6,\pm2}$	14.000739921	14.000719928	14.000719929
16.	$2E_{6,0}$	14.000759918	14.000739925	14.000739925

Conclusions

In this paper for a classical system with two degrees of freedom with the Hamilton function (5), a classical normal form is obtained in the Birkhoff-Gustavson approach, for which its quantum analogs are constructed according to the Born–Jordan and Weyl–MacCoy heuristic quantization rules. For these quantum analogs, which are nothing but approximate differential expressions for the exact Schrödinger operator, the eigenvalue problem is solved and the formulas of energy spectra are found.

Using these formulas, in two special cases with specific numerical values of the parameters, the lower energy levels were calculated and the results obtained were compared with the data available in the works published by other authors. It was found that the best and good agreement with the known results of calculating the energy spectrum is obtained using the Weyl–MacCoy quantization rule in comparison with the Born–Jordan rule.

Both the Weyl–MacCoy and Born–Jordan quantization rules are derived from the fundamental, but different postulates of classical and quantum mechanics. For the system under consideration, particular numerical results for the energy spectrum reveal the advantage of the Weyl–MacCoy quantization rule, however, it is probably premature to extend this conclusion to other systems.

References

[1] N. N. Chekanova, I. K. Kirichenko, V. E. Bogachev, and N. A. Chekanov, "The classical and quantum approach in the study of a nonlinear Hamiltonian system," *Bulletin of the Tambov State University. Series "Natural and Technical Sciences"*, vol. 20, no. 1, pp. 120–137, 2015.

[2] W. Heisenberg, "Über quanten theoretische Umdeutung kinematischer und mechanischer Beziehungen," *Zeitschrift für Physik*, vol. 33, pp. 879–893, 1925. DOI: 10.1007/BF01328377.

[3] M. Born and P. Jordan, "Zur quanten mechanik," *Zeitschrift für Physik*, vol. 34, pp. 858–888, 1925. DOI: 10.1007/BF01328531.

[4] P. Digas, "Fundamental Equations of Quantum Mechanics," *Proc. Roy Soc. (Lnd.).*, pp. 642–653, 1925. DOI: 10.3367/UFNr.0122.197708e.0611.

[5] H. Weyl, "Quanten Mechanik und Gruppen Theorie," *Zeitschrift für Physik*, vol. 46, pp. 1–46, 1927. DOI: 10.1063/1.1664478.

[6] G. Weil, *The theory of groups and quantum mechanics*. Martino Fine Books, 2014.

[7] N. H. McCoy, "On the function in quantum mechanics which corresponds to a given function in classical mechanics," *Proceedings of the National Academy of Sciences (PNAS)*, vol. 18, pp. 674–676, 1932. DOI: 10.1073/pnas.18.11.674.

[8] S. R. De Groot and L. G. Suttorp, *Foundations of Electrodynamics*. Amsterdam: North-Holland publishing company, 1972. DOI: 10.12691/amp-2-3-6.

[9] A. N. Argyers, "The Bohr-Sommerfeld quantization rule and the Weyl correspondence," *Physics*, vol. 2, p. 131, 1965. DOI: 10.1103/PhysicsPhysiqueFizika.2.131.

[10] L. Castellani, "Quantization rules and Dirac's correspondence," *Il Nuovo Cimento A*, vol. 48, pp. 359–368, 1978. DOI: 10.1007/BF02781602.

[11] P. Crehan, "The parametrisation of quantization rules equivalent to operator orderings and the effect of different rules on the physical spectrum," *Journal of Physics A: Mathematical and General*, vol. 22, no. 7, pp. 811–822, 1989. DOI: 10.1088/0305-4470/22/7/013.

[12] P. Crehan, "The proper quantum analogue of the Birkhoff–Gustavson method of normal forms," *Journal of Physics A: Mathematical and General*, vol. 23, no. 24, pp. 5815–5828, 1990. DOI: 10.1088/0305-4470/23/24/022.

[13] W. A. Fedak and J. J. Prentis, "The 1925 Born and Jordan paper "On quantum mechanics"," *American Journal of Physics*, vol. 77, pp. 128–139, 2009. DOI: 10.1119/1.3009634.

[14] M. A. Gosson, "Born–Jordan quantization and the uncertainty principle," *Journal of Physics A: Mathematical and Theoretical*, vol. 46, pp. 445–462, 2013. DOI: 10.1088/1751-8113/46/44/445301.

[15] M. Razavy, *Heisenberg's quantum mechanics*. Singapore: World Scientific Publishing Co. Pte. Ltd., 2011. DOI: 10.1080/00107514.2011.603435.

[16] N. A. Chekanov, "Quantization of the normal form of Birkhoff–Gustavson [Kvantovaniye normal'noy formy Birkgofa–Gustavsona]," *Nuclear Physics*, vol. 50, no. 8, pp. 344–346, 1989, in Russian.

[17] H. Taseli, "On the Exact Solution of the Schroedinger Equation with a Quartic Anharmonicity," *International Journal of Quantum Chemistry*, vol. 57, no. 1, pp. 63–71, 1996. DOI: 10.1002/(SICI)1097-461X(1996)57:1<63::AID-QUA7>3.0.CO;2-X.

For citation:

I. N. Belyaeva, The quantization of the classical two-dimensional Hamiltonian systems, Discrete and Continuous Models and Applied Computational Science 30 (1) (2022) 39–51. DOI: 10.22363/2658-4670-2022-30-1-39-51.

Information about the authors:

Belyaeva, Irina N. — Candidate of Physical and Mathematical Sciences, Associate Professor of Belgorod State National Research University (e-mail: ibelyaeva@bsu.edu.ru, ORCID: https://orcid.org/0000-0002-1368)

УДК 519.711.3
DOI: 10.22363/2658-4670-2022-30-1-39-51

Квантование классических двумерных гамильтоновых систем

И. Н. Беляева

Белгородский государственный исследовательский университет
ул. Победы, д. 85, Белгород, 308015, Россия

Аннотация. В статье рассматривается класс гамильтоновых систем с двумя степенями свободы. На основе классической нормальной формы, согласно правилам Борна–Йордана и Вейля–Маккоя, построены её квантовые аналоги, для которых решена задача на собственные значения и найдены приближённые формулы для энергетического спектра. Для конкретных значений параметров квантовых нормальных форм с использованием этих формул были проведены численные расчёты нижних энергетических уровней, полученные результаты были сопоставлены с известными данными других авторов. Обнаружено, что наилучшее согласие с известными результатами достигается с использованием правила квантования Вейля–Маккоя. Процедура нормализации классической функции Гамильтона является крайне трудоёмкой задачей, так как вовлекает сотни и даже тысячи многочленов для необходимых преобразований. Поэтому в работе нормализация выполняется с помощью системы компьютерной алгебры REDUCE. Показано, что использование правил соответствия Борна–Йордана и Вейля–Маккоя приводит практически к одним и тем же значениям для энергетического спектра, при этом их близость увеличивается для больших величин квантовых чисел, то есть для высоковозбуждённых состояний. В работе использовано каноническое преобразование, квантовый аналог которого позволяет построить собственные функции для квантовой нормальной формы и получить таким образом аналитические формулы для энергетических спектров разных гамильтоновых систем. Итак, показано, что квантование классических гамильтоновых систем, в том числе допускающих классический режим движения, с применением метода нормальных форм даёт очень точное предсказание уровней энергии.

Ключевые слова: функция Гамильтона, нормальная форма, правило Вейля–Маккоя, правило Борна–Йордана, квантовая нормальная форма, компьютерное моделирование, энергетические спектры

Discrete & Continuous Models
& Applied Computational Science
ISSN 2658-7149 (online), 2658-4670 (print)

2022, 30 (1) 52–61
http://journals.rudn.ru/miph

Research article

UDC 517.938:531.32
PACS 07.05.Tp, 02.60.Pn, 02.70.Bf
DOI: 10.22363/2658-4670-2022-30-1-52-61

On the many-body problem with short-range interaction

Mark M. Gambaryan[1], **Mikhail D. Malykh**[1, 2]

[1] *Peoples' Friendship University of Russia (RUDN University)*
6, Miklukho-Maklaya St., Moscow, 117198, Russian Federation
[2] *Meshcheryakov Laboratory of Information Technologies*
Joint Institute for Nuclear Research
6, Joliot-Curie St., Dubna, Moscow Region, 141980, Russian Federation

(received: January 21, 2022; revised: January 30, 2022; accepted: February 18, 2022)

Abstract. The classical problem of the interaction of charged particles is considered in the framework of the concept of short-range interaction. Difficulties in the mathematical description of short-range interaction are discussed, for which it is necessary to combine two models, a nonlinear dynamic system describing the motion of particles in a field, and a boundary value problem for a hyperbolic equation or Maxwell's equations describing the field. Attention is paid to the averaging procedure, that is, the transition from the positions of particles and their velocities to the charge and current densities. The problem is shown to contain several parameters; when they tend to zero in a strictly defined order, the model turns into the classical many-body problem. According to the Galerkin method, the problem is reduced to a dynamic system in which the equations describing the dynamics of particles, are added to the equations describing the oscillations of a field in a box. This problem is a simplification, different from that leading to classical mechanics. It is proposed to be considered as the simplest mathematical model describing the many-body problem with short-range interaction. This model consists of the equations of motion for particles, supplemented with equations that describe the natural oscillations of the field in the box. The results of the first computer experiments with this short-range interaction model are presented. It is shown that this model is rich in conservation laws.

Key words and phrases: many-body problem, Galerkin method, short-range interaction

1. Interaction

Studying the motion of a beam of charged particles in an external electromagnetic field with the interaction of particles taken into account is one of the most important and popular problems in plasma electronics. In the framework of the generally accepted approach to its study [1, § 2.3], the time interval is divided into discrete steps of length Δt. At each step, based on the

current positions of the charges and their velocities that define the currents, the induced field is calculated as a solution of Maxwell's equations. Then this 'induced' field is added to the external field and the new positions and velocities of the particles are calculated, which they acquire in this field under the action of the Lorentz force.

The described scheme allows for many variations [1]–[3]. However, these details do not at all remove the division into processes: for one time step, first, the charges and their velocities generate a field, and then the field acts on the bodies through the Lorentz force.

It is quite obvious that what has been said gives a description of a numerical method for studying a certain mathematical model of the many-body problem with short-range interaction. The latter is explicitly taken into account in the model: at each step, the field is calculated and the interaction between particles is carried out through this field, which is described using the Maxwell's equations, that is, hyperbolic equations that describe the propagation of signals with the speed of light c. However, the model itself remains undescribed; moreover, the issue of the convergence of the described numerical method, i.e., the study of the limit at $\Delta t \to 0$, is usually avoided.

From a mathematical point of view, it is necessary to combine two models into one system: a nonlinear dynamic system that describes the motion of charges based on the Lorentz law, and a linear system of Maxwell's equations that describes the dynamics of the electromagnetic field. Separately, these models are well studied. Dynamical systems with analytic right-hand sides are solved in analytic functions, and the convergence of the finite-difference method is proved in the C norm [4]. Maxwell's equations, as well as linear partial differential equations in general, are naturally solved in Sobolev spaces, and an approximate solution is also sought in one or another integral norm, for example, in L^2 over the space [5]. However, when combining these models, we must consider dynamical systems, the right-hand sides of which are elements of Sobolev spaces, and Maxwell's equations, in which currents and charges are combinations of δ-functions. We do not have a theorem on the existence of a solution for such problems.

A detailed description of the model, separated from the numerical method of its study, is very useful, firstly, in order to be able to assess the quality of the study in terms of closeness to the exact solution, and not in terms of closeness to the expectations of the experimenters. Secondly, good mathematical models always have a large number of symmetries, which correspond to conservation laws. Checking their performance provides another important criterion for assessing the quality of the numerical method. Finally, it cannot be ruled out that less obvious, but more effective numerical methods for studying this model can be found.

Thus, for example, by means of computer experiments it was found that the Boris difference scheme for solving the equations of motion corresponds to the expectations of experimenters more than others [1]. To explain this effect, Hong Qin et al. [6] showed that this scheme is the phase volume when integrating the equations of motion of one particle in an external electromagnetic field. The question of whether the Boris scheme inherits the properties of the original system in the many-many problem, which, we note, is not Hamiltonian, was not raised.

In this paper, we consider the simplest formulation of the many-body problem with short-range interaction described by the wave equation. To add

boundary conditions to the wave equation, we consider the problem in a finite domain. The question of setting the radiation conditions in such a problem does not seem trivial to us, although to simplify the problem it is usually assumed that the field in the far zone should be equal to zero.

2. Short-range interaction mathematical model

Let there be N identical bodies of mass m, under the assumption of short-range interaction between them, they produce a field with potential u and move in it in accordance with the second Newton's law. The simplest formulation can be written as follows: the dynamics of particles is described by the set of equations

$$m\ddot{\vec{r}}_n = -\nabla u\big|_{\vec{r}=\vec{r}_n}, \quad n = 1, 2, \dots, N, \tag{1}$$

and the field dynamics is described by a wave equation

$$\frac{1}{c^2}\frac{\partial^2 u}{\partial t^2} = \Delta u + \rho, \tag{2}$$

where ρ is the density of mass distribution:

$$\rho = \gamma \sum_{n=1}^{N} \delta_s(\vec{r} - \vec{r}_n). \tag{3}$$

Here it is reasonable to consider δ as a smoothed prototype of Dirac delta function that tends to the delta function in the limit $s \to 0$.

By virtue of the Poisson formula [7] and regardless of the boundary conditions imposed on the field, this problem becomes classical if we first proceed to the limit $c \to \infty$, and then to the limit $s \to 0$.

Theorem 1. *Let there be a family of solutions to the system* (1)–(2)*, parameterized by two parameters* $c \geqslant 0$ *and* $s > 0$*, and let it satisfy the condition*

$$u, u_t \in L^2(\mathbb{R}^3)$$

at $t = 0$*. If we first proceed to the limit* $c \to \infty$*, and then to the limit* $s \to 0$*, then this solution becomes the solution of the classical many-body problem.*

Proof. According to the Poisson formula

$$u(\vec{r}, t) = \frac{1}{4\pi} \iiint\limits_{|\vec{r}|<ct} \frac{\rho(\vec{r}', t - |\vec{r} - \vec{r}'|/c)}{|\vec{r} - \vec{r}'|} dv' + \\ + \frac{1}{4\pi c}\frac{\partial}{\partial t} \iint\limits_{|\vec{r}|=ct} \frac{u(\vec{r}', 0)}{|\vec{r} - \vec{r}'|} ds' + \frac{1}{4\pi c} \iint\limits_{|\vec{r}|=ct} \frac{u_t(\vec{r}', 0)}{|\vec{r} - \vec{r}'|} ds'. \tag{4}$$

Under the assumptions made about the initial conditions, the last two terms tend to zero as $c \to \infty$ and we get

$$u(\vec{r}, t) = \frac{1}{4\pi} \iiint\limits_{\mathbb{R}^3} \frac{\rho(\vec{r}', t)}{|\vec{r} - \vec{r}'|} dv'.$$

Substituting Eq. (3) here yields an expression that, at $s \to 0$, becomes

$$u = \gamma \sum_{n=1}^{N} \frac{1}{|\vec{r} - \vec{r}_n|}.$$

However, we cannot substitute it directly into (1) because this would lead to dividing by zero. However, for $s \neq 0$, the expression for u is a sum of terms of the form $\phi_s(\vec{r} - \vec{r}_n)$, having an extreme at $\vec{r} = \vec{r}_n$. So

$$\nabla \phi_s(\vec{r} - \vec{r}_n)\big|_{\vec{r}=\vec{r}_n} = 0$$

and there is no division by zero:

$$\nabla u\big|_{\vec{r}=\vec{r}_m} = \gamma \sum_{n \neq m} \nabla \phi_s(\vec{r}_m - \vec{r}_n).$$

Now, proceeding to the limit, we get in the right-hand side of equation (1) exactly an expression that should be in the many-body problem

$$m\ddot{\vec{r}}_n = -\gamma \nabla_{\vec{r}_n} \sum_{m \neq n} \frac{1}{|\vec{r}_n - \vec{r}_m|}.$$

The proved theorem allows us to hope that for large c the solutions of the system under consideration resemble the classical many-body problem. However, it is important to emphasize that the order of proceeding to the limit is important.

We are interested in constructing a model of many-body motion, in which short-range interaction is explicitly taken into account, rather than in the classical limit itself. For our purpose, it is necessary to supplement the differential equations with initial and boundary conditions.

Let the bodies occupy fixed positions up to $t < 0$, then for $t < 0$ we know u as a solution to the Poisson equation

$$\Delta u = -\rho.$$

At the moment $t = 0$ the bodies are given initial velocities. Adding the initial condition $u_t = 0$ to the wave equation, we get the classical initial value problem for finding the potential u, if we assume that the density ρ is known.

Let us turn to the boundary conditions. We assume that the bodies do not radiate waves that are noticeable in the far zone. To treat this problem numerically, we place the systems in a Dirichlet box G and set the conditions $u\big|_{\partial G} = 0$ on its boundary. This box will replace the boundary conditions at infinity.

The complete problem is formulated as follows. Given initial positions $\vec{r}_n^{(0)}$ and initial velocities $\vec{v}_n^{(0)}$ of the bodies, the solution is calculated to the boundary value problem

$$\begin{cases} \Delta u_0 = -\gamma \sum\limits_{n=1}^{N} \delta_s(\vec{r} - \vec{r}_n^{(0)}), \\ u\big|_{\partial G} = 0. \end{cases} \tag{5}$$

It is required to find the functions $\vec{r}_n(t)$ and $u(x, y, z, t)$ satisfying the initial and boundary value problem:

$$\begin{cases} m\ddot{\vec{r}}_n = -\nabla u\big|_{\vec{r}=\vec{r}_n}, \quad n = 1, 2, \ldots, N, \\ \dfrac{1}{c^2}\dfrac{\partial^2 u}{\partial t^2} = \Delta u + \gamma \sum\limits_{n=1}^{N} \delta_s(\vec{r} - \vec{r}_n), \end{cases} \tag{6}$$

with the initial conditions

$$\vec{r}_n = \vec{r}_n^{(0)}, \quad \dot{\vec{r}}_n = \vec{v}_n^{(0)}, \quad u = u_0, \quad u_t = 0 \quad (t = 0)$$

and the boundary conditions $u\big|_{\partial G} = 0$.

We believe that this problem has a unique solution for small t. However, the proof of this assertion requires a more careful description of the class of functions in which the solution is sought. We confine ourselves to a few computer experiments with this model.

3. Galerkin method

A natural method for solving the oscillation equation in a finite domain is the Galerkin method [8]–[10]. Let ϕ_n be the normalized eigenfunctions of the Laplace operator in G, and let α_n^2 be the corresponding eigenvalues. We seek the solution of the wave equation in the form

$$u(x, y, z, t) = \sum_{j=1}^{\infty} u_j(t)\phi_j(x, y, z), \tag{7}$$

where u_j are coefficients yet unknown. Then

$$\frac{1}{c^2}\frac{d^2 u_j}{dt^2} + \alpha_j^2 u_j = \gamma \sum_{n=1}^{N} \iiint\limits_{G} \delta_s(\vec{r} - \vec{r}_n(t))\phi_j dx dy dz, \quad j = 1, 2, \ldots$$

and

$$m\frac{d^2\vec{r}_n}{dt^2} = -\sum_{j=1}^{\infty} u_j(t)\nabla\phi_j\big|_{\vec{r}=\vec{r}_n}, \quad n = 1, 2, \ldots, N.$$

If we truncate the sum over j to any finite number of terms J, then the system has a unique solution, taking into account the initial conditions.

In the limit $s \to 0$ we get

$$\frac{1}{c^2}\frac{d^2u_j}{dt^2} + \alpha_j^2 u_j = \gamma \sum_{n=1}^{N} \phi_j\big|_{\vec{r}=\vec{r}_n}, \quad j = 1, 2, \dots, J \tag{8}$$

and

$$m\frac{d^2\vec{r}_n}{dt^2} = -\sum_{j=1}^{J} u_j(t)\nabla\phi_j\big|_{\vec{r}=\vec{r}_n}, \quad n = 1, 2, \dots, N. \tag{9}$$

The initial conditions for $\vec{r}_n$ are given and for u_j they are found from equation (5) using the explicit formulae

$$\alpha_j^2 u_j(0) = \gamma \sum_{n=1}^{N} \iiint\limits_G \delta_s(\vec{r} - \vec{r}_n)\phi_j dxdydz$$

or

$$u_j(0) = \frac{\gamma}{\alpha_j^2} \sum_{n=1}^{N} \phi_j\big|_{\vec{r}=\vec{r}_n} \tag{10}$$

and

$$\dot{u}_j(0) = 0. \tag{11}$$

By virtue of the Weyl lemma [11], [12], the eigenfunctions of the Laplace operator are twice continuously differentiable in the domain considered. Therefore, the system of ordinary differential equations (8), (9) falls under the conditions of the classical Cauchy theorem. This means that the initial value problem for equations (8), (9) with initial conditions (10), (11) has a unique solution, at least in the vicinity of the initial data. Moreover, standard numerical methods can be applied to this problem, for example, the Runge-Kutta method [4].

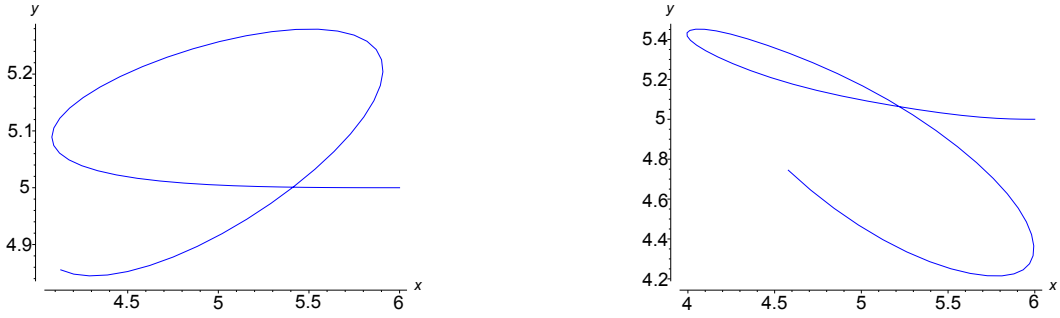

Figure 1. The first body trajectory at $c = 1$ and $c = 10$

Example 1. For example, let us take the box in the form of a cube $[0, L]^3$. Then the eigenfunctions are expressed as

$$\sin\frac{\pi m x}{L}\sin\frac{\pi n y}{L}\sin\frac{\pi k z}{L}, \quad n, m, k \in \mathbb{N},$$

with the corresponding eigenvalues

$$\alpha_{mnk}^2 = \frac{\pi^2}{L^2}(m^2 + n^2 + k^2).$$

Taking the first J functions from this set, the initial positions and velocities of the bodies, we uniquely determine the initial problem (8)–(11), which we will solve by the classical Runge-Kutta method of the 4th order.

Let us take, for example, $c = 1$, $m = 1$, $\gamma = 1$, $L = 10$ and consider the problem of two bodies. We place the first body at the point $(6, 5, 5)$ and the second one at the point $(4, 5, 5)$. Let the first body be at rest, and the second one have an initial velocity $\vec{v}_2 = (0, 1, 0)$ In the classical case, this leads to the rotation of bodies along ellipses around their center of gravity $(5, 5, 5)$, and the motion occurs in the xy plane. Our computer experiment shows that in the case of short-range interaction, the motion also turns out to be planar, but instead of ellipses, more complex non-closed curves are obtained. If we set the velocity in the direction of the Oz axis, the motion still remains flat, only the plane itself changes. Therefore, our system is rich in integrals of motion.

4. Conclusion

The initial value problem (8)–(11) can and should be considered as a mathematical model describing the many-body problem with short-range interaction. Equation (9) has a very simple physical meaning of a mechanical equation of motion (the second Newton law), and equation (8) describes the natural oscillations of the field in the resonator G. The transformation of the box G into a resonator seems quite natural in the framework of the theory of short-range interaction.

A few computer experiments that we have managed to perform demonstrate that this system is rich in conservation laws. However, it is not yet clear to us how to study them analytically. We hope that further experiments with this new problem will clarify the issue.

With respect to the system (1), (2), this problem is a simplification, however, a simplification different from that leading to classical mechanics. By virtue of theorem 1, we will pass to classical mechanics if we first proceed to the limit $c \to \infty$ (long-range interaction), and then to the limit $s \to 0$ (narrowing the charge density to δ-functions). When deriving the system (8)–(11), we restrict the number of oscillations in the box to a finite number of modes (Galerkin method) and immediately proceed to the limit $s \to 0$. In this case, the limit $c \to \infty$ makes the singularity problem perturbed, and, from the point of view of the Tikhonov and Vasilieva theory [13], [14], slow variables correspond to the bodies, and fast variables correspond to the field.

Acknowledgments

This work is supported by the Russian Science Foundation (grant no. 20-11-20257).

References

[1] C. K. Birdsall and L. A. Bruce, *Plasma physics via computer simulation*. Bristol, Philadelphia and New York: Adam Hilger, 1991.

[2] R. W. Hockney and J. W. Eastwood, *Computer simulation using particles*. Bristol, Philadelphia and New York: Adam Hilger, 1988.

[3] V. P. Tarakanov, *User's manual for code KARAT*. Springfield, VA: Berkley Research, 1999.

[4] E. Hairer, G. Wanner, and S. P. Nørsett, *Solving Ordinary Differential Equations*, 3rd ed. New York: Springer, 2008, vol. 1.

[5] G. Duvaut and J. L. Lions, *Inequalities in Mechanics and Physics*. Berlin: Springer-Verlag, 1976.

[6] H. Qin, S. Zhang, J. Xiao, J. Liu, and Y. Sun, "Why is Boris algorithm so good?" *Physics of Plasmas*, vol. 20, p. 084 503, 2013. DOI: 10.1063/1.4818428.

[7] A. G. Sveshnikov, A. N. Bogolyubov, and K. V. V., *Lectures on Mathematical Physics [Lektsii po matematicheskoy fizike]*. Moscow: MGU, 1993, in Russian.

[8] I. I. Vorovich, "On some direct methods in the nonlinear theory of oscillations of shallow shells [O nekotorykh pryamykh metodakh v nelineynoy teorii kolebaniy pologikh obolochek]," *Izvestiya Akademii Nauk USSR, Seriya Matematicheskaya*, vol. 21, no. 6, pp. 747–784, 1957, in Russian.

[9] P. G. Ciarlet, *The finite element method for elliptic problems*. North-Holland, 1978.

[10] N. G. Afendikova, "The history of Galerkin's method and its role in M. V. Keldysh's work [Istoriya metoda Galerkina i yego rol' v tvorchestve M.V.Keldysha]," *Keldysh Institute preprints*, no. 77, 2014, in Russian.

[11] G. Hellwig, *Partial differential equations. An introduction*. Leipzig: Teubner, 1960.

[12] G. Hellwig, *Differential operators of Mathematical Physics*. Reading, MA: Addison-Wesley, 1967.

[13] A. N. Tikhonov, "Systems of differential equations containing small parameters at derivatives [Sistemy differentsial'nykh uravneniy, soderzhashchiye malyye parametry pri proizvodnykh]," *Mat. Sb.*, vol. 31, no. 3, pp. 575–586, 1952, in Russian.

[14] A. B. Vassilieva and V. F. Butuzov, *Asymptotic methods in singular perturbation theory [Asimptoticheskiye metody v teorii singulyarnykh vozmushcheniy]*. Moscow: Vysshaya shkola, 1990, in Russian.

For citation:

M. M. Gambaryan, M. D. Malykh, On the many-body problem with short-range interaction, Discrete and Continuous Models and Applied Computational Science 30 (1) (2022) 52–61. DOI: 10.22363/2658-4670-2022-30-1-52-61.

Information about the authors:

Gambarayan, Mark — PhD student of Department of Applied Probability and Informatics of Peoples' Friendship University of Russia (RUDN University) (e-mail: gamb.mg@gmail.com, ORCID: https://orcid.org/0000-0002-4650-4648)

Malykh, Mikhail D. — Doctor of Physical and Mathematical Sciences, Assistant Professor of Department of Applied Probability and Informatics of Peoples' Friendship University of Russia (RUDN University); Researcher in Meshcheryakov Laboratory of Information Technologies, Joint Institute for Nuclear Research (e-mail: malykh-md@rudn.ru, phone: +7(495)9550927, ORCID: https://orcid.org/0000-0001-6541-6603, ResearcherID: P-8123-2016, Scopus Author ID: 6602318510)

УДК 517.938:531.32
PACS 07.05.Tp, 02.60.Pn, 02.70.Bf
DOI: 10.22363/2658-4670-2022-30-1-52-61

О задаче многих тел с близкодействием

М. М. Гамбарян[1], **М. Д. Малых**[1, 2]

[1] *Российский университет дружбы народов*
ул. Миклухо-Маклая, д. 6, Москва, 117198, Россия
[2] *Лаборатория информационных технологий им. М. Г. Мещерякова*
Объединённый институт ядерных исследований
ул. Жолио-Кюри, д. 6, Дубна, Московская область, 141980, Россия

Аннотация. В статье рассматривается классическая задача о взаимодействии заряженных частиц в рамках представления о близкодействии. Обсуждаются трудности математического описания близкодействия, для чего необходимо объединение двух моделей — нелинейной динамической системы, описывающей движение частиц в поле, и краевой задачи для гиперболического уравнения или уравнений Максвелла, описывающих поле. Уделено внимание процедуре осреднения, то есть перехода от положений частиц и их скоростей к плотностям заряда и тока. Показано, что задача содержит несколько параметров, при стремлении которых к нулю в строго определённом порядке рассматриваемая модель переходит в классическую задачу многих тел. По методу Галёркина эта задача сведена к динамической системе, в которой к уравнениям, описывающим динамику частиц, добавляются уравнения, описывающие колебания поля в ящике. Эта задача представляет собой упрощение, отличное от того, которое ведёт к классической механике. Её предлагается рассматривать как простейшую математическую модель, описывающую задачу многих тел с близкодействием. Эта модель состоит из уравнений движения частиц, к которым добавлены уравнения, описывающие собственные колебания поля в ящике. Представлены результаты первых компьютерных экспериментов с этой моделью близкодействия. Показано, что модель богата законами сохранения.

Ключевые слова: задача многих тел, метод Галёркина, близкодействие

Discrete & Continuous Models & Applied Computational Science
ISSN 2658-7149 (online), 2658-4670 (print)

2022, 30 (1) 62–78
http://journals.rudn.ru/miph

Review article

UDC 535:535.3:681.7
DOI: 10.22363/2658-4670-2022-30-1-62-78

Finite-difference methods for solving 1D Poisson problem

Serge Ndayisenga[1],
Leonid A. Sevastianov[1,2], **Konstantin P. Lovetskiy**[1]

[1] *Peoples' Friendship University of Russia (RUDN University)*
6, Miklukho-Maklaya St., Moscow, 117198, Russian Federation
[2] *Bogoliubov Laboratory of Theoretical Physics*
Joint Institute for Nuclear Research
6, Joliot-Curie St., Dubna, Moscow Region, 141980, Russian Federation

(received: January 21, 2022; revised: February 2, 2022; accepted: February 18, 2022)

Abstract. The paper discusses the formulation and analysis of methods for solving the one-dimensional Poisson equation based on finite-difference approximations — an important and very useful tool for the numerical study of differential equations. In fact, this is a classical approximation method based on the expansion of the solution in a Taylor series, based on which the recent progress of theoretical and practical studies allowed increasing the accuracy, stability, and convergence of methods for solving differential equations. Some of the features of this analysis include interesting extensions to classical numerical analysis of initial and boundary value problems. In the first part, a numerical method for solving the one-dimensional Poisson equation is presented, which reduces to solving a system of linear algebraic equations (SLAE) with a banded symmetric positive definite matrix. The well-known tridiagonal matrix algorithm, also known as the Thomas algorithm, is used to solve the SLAEs. The second part presents a solution method based on an analytical representation of the exact inverse matrix of a discretized version of the Poisson equation. Expressions for inverse matrices essentially depend on the types of boundary conditions in the original setting. Variants of inverse matrices for the Poisson equation with different boundary conditions at the ends of the interval under study are presented — the Dirichlet conditions at both ends of the interval, the Dirichlet conditions at one of the ends and Neumann conditions at the other. In all three cases, the coefficients of the inverse matrices are easily found and the algorithm for solving the problem is practically reduced to multiplying the matrix by the vector of the right-hand side.

Key words and phrases: 1D Poisson equation, finite difference method, tridiagonal matrix inversion, Thomas algorithm, Gaussian elimination

1. Introduction

Applied mathematical models are mainly based on the use of partial differential equations [1]. The solution must satisfy a given equation of mathematical physics and some additional relations, which are, first, boundary

and initial conditions. The most important for applications [2] are second-order equations — elliptic, parabolic, and hyperbolic. Currently for equations of mathematical physics, methods of numerical solution and the appropriate software [3], [4], as well as computer algebra systems (CASs) such as Sage, Mathematica, Maxima and Maple are actively developed to implement these methods. Many features of stationary problems of mathematical physics described by elliptic equations of the second order can be illustrated by considering the simplest boundary value problems for an ordinary differential equation of the second order. Perhaps the simplest second-order elliptic equation is the Poisson equation.

Let us consider some methods for the numerical solution of this equation and compare the investigated methods.

The Poisson equation [1] is a special case of the heat conduction equation describing the dependence of the temperature of a medium on spatial coordinates and time, and the heat capacity and thermal conductivity of the medium (in the general case, inhomogeneous) are considered to be given. We will consider the problem of finding the steady-state distribution of density or temperature (e.g., when the distribution of sources does not depend on time). In this case, terms with time derivatives are eliminated from the non-stationary equation and a stationary heat equation is obtained, which belongs to the class of elliptic equations. A two-point boundary value problem is the problem of finding a solution to an ordinary differential equation or second-order systems in the interval $a \leqslant x \leqslant b$. Additional conditions are imposed on the solution at any two points of the interval, e.g., a and b — the 'boundaries' of the segment (hence the name of the problem).

Consider a second-order differential equation

$$-\frac{d}{dx}\left(k\left(x\right)\frac{du}{dx}\right)+p\left(x\right)u\left(x\right)=f\left(x\right),\quad a\leqslant x\leqslant b. \tag{1}$$

It is called the one-dimensional stationary heat conduction equation and arises in the mathematical modeling of many important processes. For example, this equation describes the steady-state temperature distribution $u\left(x\right)$ in a heat-conducting rod of length $l=b-a$. In this case, $k\left(x\right)$ is the thermal conductivity coefficient; $w\left(x\right)=-k\left(x\right)\dfrac{du}{dx}$ is the heat flux density, $p\left(x\right)$ is the heat transfer coefficient (pu is the heat sink power proportional to the temperature u); $f\left(x\right)$ is the density of heat sources (at $f\leqslant 0$ it is the density of heat sinks).

The boundary value problem is much harder to solve than the Cauchy problem, and various approaches are used for this purpose. The most common are various sampling methods that allow replacing the original problem with a certain discrete analog. The resulting discrete boundary value problem is a system of equations (possibly nonlinear) with a finite number of unknowns and can be numerically solved using special direct or iterative methods. One of the simplest discretization algorithms often used in applied scientific and technical calculations is the method of finite differences [5].

The most commonly used method for solving difference equations arising in the approximation of boundary value problems for equations of mathematical physics is the sweep method [6], [7], or the Thomas method [8].

Below we will show how the difference method is applied to solve the boundary value problem (1), restricting ourselves, for simplicity, to an equation with a constant coefficient $k(x) \equiv 1$. In this case, the boundary value problem with Dirichlet boundary conditions takes the form

$$u''(x) - p(x)\,u(x) = f(x), \quad a < x < b, \tag{2}$$

$$u(a) = \alpha, \quad u(b) = \beta. \tag{3}$$

Introduce on $[a, b]$ a grid $a = x_0 < x_1 < x_2 < ... < x_n = b$, which for simplicity is assumed uniform. Let us approximately express the second derivative of the solution in terms of the values of the future solution at the grid nodes $u_n = u(x_n)$. We use the simplest symmetric difference approximation

$$u''(x_n) \approx \frac{1}{h^2}\left(u_{n-1} - 2u_n + u_{n+1}\right), \quad h = x_{n+1} - x_n = \text{const}. \tag{4}$$

Using such an approximation at each internal grid node x_n, $1 \leqslant n \leqslant N-1$ and substituting it into the differential equation (2), we transform the differential equation (1) into a system of finite-difference equations, i.e., into a system of approximate linear algebraic equations, the solution of which will be an approximate solution $y_n \approx u(x_n)$. Finite-difference equations cannot be written at the boundary nodes $n = 0$, $n = N$, otherwise the indices of the nodes will go beyond the permissible limits [5]. Denoting $p_n = p(x_n)$ and $f_n = f(x_n)$, we get a system of $(N-1)$ linear equations with respect to the approximate values of the solution at grid nodes

$$y_{n-1} - (2 + h^2 p_n)\,y_n + y_{n+1} = h^2 f_n, \quad 1 \leqslant n \leqslant N-1. \tag{5}$$

The number of unknowns y_n, $0 \leqslant n \leqslant N$ equals $(N+1)$, i.e., it is greater than the number of equations (5). The lacking two equations are to be obtained from the boundary conditions (3)

$$y_0 = \alpha, \quad y_N = \beta. \tag{6}$$

Solving the algebraic system (5), (6) we get an approximate solution of the boundary value problem (2), (3).

Further analysis of the described algorithm of solving the boundary value problem is to answer three important questions.

— What are the conditions for the existence of a solution to the system of algebraic equations?
— Does the solution of the system of algebraic equations tend to the exact solution of the boundary value problem upon reducing the grid step?
— Is it possible to develop an algorithm (procedure) for finding the solution with given accuracy by reducing the grid step?

It is known [5, P. 66], that for a rather wide class of the boundary value problem coefficients it is possible to prove the existence of a finite-difference solution and its convergence to the exact solution. The following theorem takes place.

Theorem 1. *Let $p(x)$, $f(x)$ are twice continuously differentiable on $[a, b]$, $p(x) \geqslant m$, where the constant $m \geqslant 0$. Also let the step h be small enough, so that $h \leqslant 2$. Then the finite-difference solution exists, its difference from the exact solution by the norm c being of the order of $O(h^2)$.*

Remark 1. The matrix of the system (5), (6) is tridiagonal. It is not difficult to solve the system by the Gaussian method for a strip matrix or by sweep method. These are direct methods. They allow finding a solution, executing about nine arithmetic operations for each node. By virtue of the conditions of the theorem, the solution of the system of equations by the sweep method exists, is unique and found without accumulating round-off errors.

Remark 2. The conditions of the theorem are sufficient, but not necessary. Even if the conditions are not met, in most cases the finite-difference solution exists and converges to the exact one. Under additional assumptions, it is possible to construct an asymptotically accurate estimate of the error. Then it is possible to apply the grid refinement and Richardson's method to find the posterior estimate of the error and calculations with control of the accuracy.

2. Finite-difference scheme

The problem in matrix form can be represented as

$$\begin{pmatrix} -2+p_1 & 1 & 0 & \cdots & 0 \\ 1 & -2+p_2 & 1 & \cdots & 0 \\ 0 & 1 & -2+p_3 & \cdots & 0 \\ 0 & 0 & 1 & \cdots & 0 \\ \vdots & \vdots & \ddots & \ddots & 0 \\ 0 & 0 & 0 & \ddots & 1 \\ 0 & 0 & 0 & 1 & -2+p_N \end{pmatrix} \begin{pmatrix} u_1 \\ u_2 \\ u_3 \\ u_4 \\ \vdots \\ \vdots \\ u_N \end{pmatrix} = \begin{pmatrix} h^2 f_1 - u_a \\ h^2 f_2 \\ h^2 f_3 \\ h^2 f_4 \\ \vdots \\ \vdots \\ h^2 f_N - u_b \end{pmatrix}. \quad (7)$$

When applying the sweep method to systems of the form (7), during a forward sweep, both the coefficients of the matrix and the elements of the vector on the right-hand side are recalculated. The matrix is thus reduced to two-diagonal form. During the backward sweep, the components of the solution are calculated at the second stage. Tridiagonal matrices, which are inverted using the simple sweep method, often arise when solving differential equations of two independent variables by the finite-difference method, e.g., when solving a linear one-dimensional heat equation.

For such systems, the solution can be obtained in operations instead of required by the Gaussian elimination method. The first sweep of the method calculates the sweep coefficients, based on which the inverse substitution yields the solution. Examples of such matrices usually arise from discretization of the one-dimensional Poisson equation and interpolation by the natural cubic spline.

For the simplest one-dimensional Poisson equation in the case when $p(x) \equiv 0$, the authors of Refs. [9], [10] proposed a solution based on the analytical (exact) representation of the inverse matrix coefficients.

3. The exact formulation of the inverse of the tridiagonal matrix for solving the 1D Poisson equation with the finite difference method

Consider a method for solving the one-dimensional Poisson equation using the finite difference method based on exact formulas for the inverse of the Laplacian tridiagonal matrix. In the method proposed in Ref. [11], formulas for the coefficients of the inverse matrix are directly derived. Thus, the procedure of solving the one-dimensional Poisson equation becomes very accurate and very fast. This method is a very important tool for solving many physical and technical problems, where the Poisson equation often appears when describing (modeling) various physical phenomena.

3.1. The finite difference method for solving the Poisson equation with Dirichlet–Dirichlet boundary conditions

Consider a function $u(x)$, that satisfies the Poisson equation $u''(x) = f(x)$ on the interval $]a, b[$, where $f(x)$ is a given function. We require that the function $u(x)$ satisfy the Dirichlet–Dirichlet boundary conditions: $u(a) = \alpha$, $u(b) = \beta$. On the considered interval $[a, b]$ we specify a one-dimensional grid $x_i = a + i \cdot \Delta x$, $i = 0, \ldots, N+1$, where the uniform step of the grid is calculated as $\Delta x = \dfrac{b-a}{N+1} = h$. We denote by $u_i = u(x_i)$ and $f_i = f(x_i)$, $i = 0, \ldots, N+1$ the values of the approximate solution and the function in the right-hand side.

Replacing the second derivative by symmetric difference expressions, we obtain the following system for internal nodes:

$$u_{i-1} - 2u_i + u_{i+1} = h^2 f_i, \quad i = 1, \ldots, N. \tag{8}$$

In matrix form, the system of linear algebraic equations (8), taking into account the boundary conditions, can be written in the form $Au = F$, where $F = \left(h^2 f_1 - u_a, h^2 f_2, \ldots, h^2 f_{N-1}, h^2 f_N - u_b\right)^T$, or

$$\begin{pmatrix} -2 & 1 & 0 & 0 & 0 & \cdots & \cdots & 0 \\ 1 & -2 & 1 & 0 & 0 & \cdots & \cdots & 0 \\ 0 & 1 & -2 & 1 & 0 & \cdots & \cdots & 0 \\ 0 & 0 & 1 & -2 & 1 & \ddots & \cdots & 0 \\ 0 & 0 & 0 & 1 & -2 & \ddots & \ddots & \vdots \\ \vdots & \vdots & \vdots & \ddots & \ddots & \ddots & \ddots & 0 \\ 0 & 0 & 0 & 0 & \ddots & \ddots & \ddots & 1 \\ 0 & 0 & 0 & 0 & 0 & 0 & 1 & -2 \end{pmatrix} \times \begin{pmatrix} u_1 \\ u_2 \\ u_3 \\ u_4 \\ u_5 \\ \vdots \\ u_{N-1} \\ u_N \end{pmatrix} = \begin{pmatrix} h^2 f_1 - u_a \\ h^2 f_2 \\ h^2 f_3 \\ h^2 f_4 \\ h^2 f_5 \\ \vdots \\ h^2 f_{N-1} \\ h^2 f_N - u_b \end{pmatrix}. \tag{9}$$

Thus, the solution of the one-dimensional Poisson equation is reduced to the inversion of the tridiagonal symmetric negative definite matrix

$$A = \left(a_{ij}\right), \quad i, j = 1, \ldots, N.$$

The inverse matrix which we denote by

$$B = \left(b_{ij}\right), \quad i, j = 1, \ldots, N,$$

is also symmetric.

The elements of matrix A may be briefly written as

$$a_{ij} = \begin{cases} -2, & i = j, \\ 1, & |i-j| = 1, \quad i = 1, \ldots, N \\ 0, & |i-j| > 1, \end{cases} \tag{10}$$

and the elements of matrix B are related by the following formulas:

$$\begin{cases} -2b_{i1} + b_{i2} = \delta_i^1, \\ b_{ij-1} - 2b_{ij} + b_{ij+1} = \delta_i^j, \quad 1 < i, \quad j < N, \\ b_{iN-1} - 2b_{iN} = \delta_i^N, \end{cases} \tag{11}$$

where δ_i^j is the Kronecker symbol.

3.2. Calculating the inverse matrix

Relations (11) allow deriving the following interesting dependencies

$$b_{ij+1} = b_{ij} + b_{i1}, \quad b_{ij} = jb_{i1} + (j-1). \tag{12}$$

From relations (12) it follows that the elements of inverse matrix B are unambiguously determined by the value of the element b_{11}. This coefficient can be determined based on the behavior of matrix B at different dimensionalities N:

$$b_{11} = -N/(N+1). \tag{13}$$

From relations (12) and (13), it is easy to express the elements of the first row and the first column of the inverse matrix

$$\begin{cases} b_{1j} = -(N-(j-1))/(N+1), \\ b_{i1} = -(N-(i-1))/(N+1). \end{cases} \tag{14}$$

These relations allow completing the accurate and full determination of the coefficients of the inverse matrix $B = \left(b_{ij}\right)$, $i, j = 1, \ldots, N$:

$$b_{ij} = \begin{cases} -j(N-(i-1))/(N+1), & i \geqslant j, \\ -i(N-(j-1))/(N+1), & i < j; \end{cases} \tag{15}$$

$$B = -\frac{1}{(N+1)} \times$$
$$\times \begin{pmatrix} N & N-1 & \cdots & N-(j-1) & \cdots & 2 & 1 \\ N-1 & 2(N-1) & \cdots & 2[N-(j-1)] & \cdots & 4 & 2 \\ \vdots & \vdots & \ddots & \vdots & \vdots & \vdots & \vdots \\ N-(i-1) & 2[N-(i-1)] & \cdots & i[N-(j-1)] & \cdots & 2i & i \\ \vdots & \vdots & \vdots & \vdots & \ddots & \vdots & \vdots \\ 2 & 4 & \cdots & 2j & \cdots & 2(N-1) & N-1 \\ 1 & 2 & \cdots & j & \cdots & N-1 & N \end{pmatrix}.$$

With the inverse matrix elements known, it is easy to get the solution of the one-dimensional Poisson equation by mere multiplication of the matrix by the right-hand side vector $u = BF$.

3.3. Classification of media

Taking into account the specific form of the inverse matrix and its persymmetry makes it easy to express the solution u_N at the point x_n

$$u_N = -(N+1)^{-1} \sum_{i=1}^{N} i \cdot F_i. \tag{16}$$

The direct search for the solution u_{N-1} at the point x_{N-1} leads to the expression

$$u_{N-1} = -(N+1)^{-1} \left[\left[\sum_{i=1}^{N-1} 2i \cdot F_i \right] + (N-1) F_N \right]. \tag{17}$$

In a similar way, it is possible to derive the expressions for calculating the rest components of the solution in the form

$$u_{N-k} = -(N+1)^{-1} \times$$
$$\times \left[(k+1) \left[\sum_{i=1}^{N-k} iF_i \right] + (N-k) \left[\sum_{i=N-k+1}^{N} (N-(i-1)) F_i \right] \right], \quad k = 0, 1, \ldots, N-1 \tag{18}$$

or in the form

$$u_k = -(N+1)^{-1} \times$$
$$\times \left[(N-k+1) \left[\sum_{i=1}^{k} iF_i \right] + k \left[\sum_{i=k+1}^{N} (N-(i-1)) F_i \right] \right], \quad k = 1, \ldots, N. \tag{19}$$

From the computational point of view, it is preferable to use Eqs. (15), when programming the procedure of calculating the solution.

Let us consider the numerical solution of the problem of finding a scalar potential given on the interval $[-1, 1]$ and satisfying the Poisson equation $\Delta\Phi(x) = \dfrac{\partial^2\Phi(x)}{\partial x^2} = f(x) = -\cos^2(\pi(x-0.5))$ and the Dirichlet–Dirichlet boundary conditions: $\Phi(-1) = -0.2$, $\Phi(1) = 0.1$.

The exact solution is expressed by the formula

$$\Phi_{\text{exact}} = -\frac{x^2}{4} + \left[\frac{\cos(\pi(x-0.5))}{2\pi}\right]^2 + \frac{x}{4} - 0.1(x+1) + 0.3. \qquad (20)$$

The software implementation of the algorithm consists of several lines, namely, filling the vector on the right-hand side of Eq. (9) and multiplying the inverse matrix B by this vector using Eqs. (14).

Figure 1 illustrates the results of the numerical experiment.

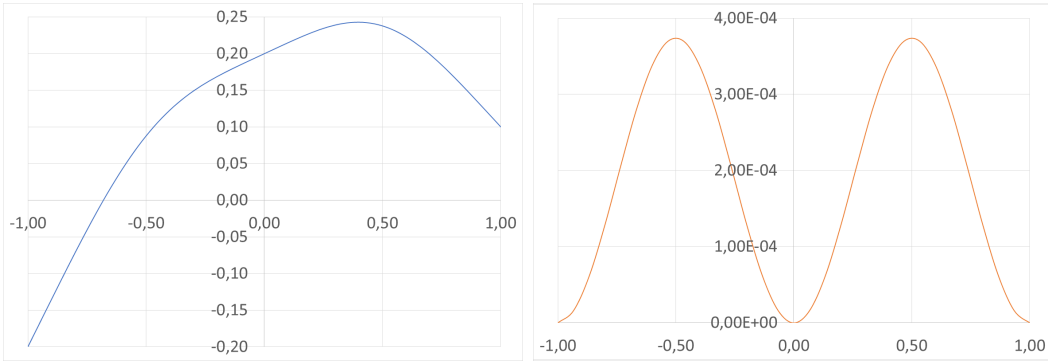

(a) Exact solution

(b) Calculation error

Figure 1. The maximal error at points $x = \pm 0.5$ is 0.36 at $N = 30$ and decreases to 0.036 at $N = 300$

4. Solving the 1D Poisson equation with the Neumann–Dirichlet and Dirichlet–Neumann boundary conditions

The problem is to determine the scalar potential $u(x)$ satisfying the one-dimensional Poisson equation $\Delta u(x) = f(x)$ on the interval $]a, b[$, where $f(x)$ is a given function. It is necessary to find the solution satisfying the Neumann–Dirichlet boundary conditions $u'(a) = u'_a$ and $u(b) = u_b$. Let us consider a special uniform grid for the finite difference method with the step $\Delta x = \dfrac{b-a}{N} = h$, consisting of $N+1$ points. The coordinates of the grid nodes (x_i) are determined by the expression $x_i = a + (i-1)\cdot h$, $i = 0, 1, \ldots N+1$. We denote by u_i the approximate values of the desired solution at point

x_i : $u_i = u(x_i)$, and by f_i the value of the given function in the right-hand side at the same point. In addition, let us denote by $u'_i = u'(x_i)$ and $u''_i = u''(x_i)$ the values of the first and second derivatives of the sought solution at the grid node at the same point. Replacing the derivatives with symmetric finite-difference expressions [12], we arrive at the approximation formulas of the second order of accuracy for the first derivatives

$$u'_i = \frac{u_{i+1} - u_{i-1}}{2h} + O(h^2), \quad i = 1, 2, 3, \dots, N \tag{21}$$

and for the second derivatives

$$u''_i = \frac{u_{i-1} - 2u_i + u_{i+1}}{h^2} + O(h^2), \quad i = 1, 2, \dots, N. \tag{22}$$

The system of linear equations for the internal nodes of the interval looks as

$$u_{i-1} - 2u_i + u_{i+1} = h^2 f_i, \quad i = 1, \dots, N. \tag{23}$$

4.1. The Neumann–Dirichlet boundary conditions

Let us derive equations complementing the system with the boundary conditions at the left and right ends of the interval taken into account. Assuming the use of Eqs. (21) and (23) possible and combining them at $i = 0$, we eliminate u_{-1} from the system of equations.

$$-u_1 + u_2 = h^2 \frac{f_i}{2} + h u'_a, \quad i = 1, \dots, N. \tag{24}$$

Thus, introducing into consideration an additional virtual point $x_0 = a - h$ allows using the central differences with the order of approximation $O(h^2)$ for the sought solution even at the boundary point of the interval.

We introduce the vector F with the components expressed as

$$F_1 = h^2 \frac{f_i}{2} + h u'_a, \quad F_N = h^2 f_N - u_b, \quad F_i = h^2 f_i, \quad i = 2, 3, \dots, N-1. \tag{25}$$

As a result, the system of equations that determines the solution components reduces to the form

$$\begin{pmatrix} -1 & 1 & 0 & 0 & 0 & \cdots & \cdots & 0 \\ 1 & -2 & 1 & 0 & 0 & \cdots & \cdots & 0 \\ 0 & 1 & -2 & 1 & 0 & \cdots & \cdots & 0 \\ 0 & 0 & 1 & -2 & 1 & \ddots & \cdots & 0 \\ 0 & 0 & 0 & 1 & -2 & \ddots & \ddots & \vdots \\ \vdots & \vdots & \vdots & \ddots & \ddots & \ddots & \ddots & 0 \\ 0 & 0 & 0 & 0 & \ddots & \ddots & \ddots & 1 \\ 0 & 0 & 0 & 0 & 0 & 0 & 1 & -2 \end{pmatrix} \times \begin{pmatrix} u_1 \\ u_2 \\ u_3 \\ u_4 \\ u_5 \\ \vdots \\ u_{N-1} \\ u_N \end{pmatrix} = \begin{pmatrix} \frac{h^2}{2} f_1 + h u'_a \\ h^2 f_2 \\ h^2 f_3 \\ h^2 f_4 \\ h^2 f_5 \\ \vdots \\ h^2 f_{N-1} \\ h^2 f_N - u_b \end{pmatrix}, \tag{26}$$

where the matrix $A = \{a_{ij}\}$, $i, j = 1, \dots, N$ of system (8) is symmetric tridiagonal negative definite and possesses the property of diagonal transformation. The presence of diagonal dominance in the coefficient matrix guarantees the stability of the sweep method; however, in this case, there is a way to calculate the elements of the inverse matrix.

4.2. Calculation of the inverse matrix elements

Let us write down the properties of the inverse matrix $B = \{b_{ij}\}$, $i, j = 1, \dots, N$, $B = A^{-1}$, following directly from its definition. It must be symmetrical and its elements must satisfy the following relations:

$$\begin{cases} -b_{1j} + b_{2j} = \delta_j^1, \quad 1 < j < N, \\ b_{i1} - 2b_{i2} + b_{i3} = \delta_i^2, \quad 1 < i < N, \\ b_{i-1j} - 2b_{ij} + b_{i+1j} = \delta_i^j, \quad 1 < i, j < N, \\ b_{iN-1} - 2b_{iN} = \delta_i^N, \quad 1 < i < N, \end{cases} \tag{27}$$

where δ_i^j is the Kronecker symbol.

The elements of the inverse matrix also satisfy the relations

$$b_{ij} = \begin{cases} b_{11} + (j-1), & i \leqslant j, \\ b_{11} + (i-1), & i > j. \end{cases} \tag{28}$$

The analysis of behavior of the system determinant allows deriving the expressions

$$\det(B) = (-1)^N,$$
$$b_{11} = \frac{N \cdot (-1)^{N-1}}{(-1)^N} = -N, \text{ and } b_{NN} = \frac{(-1)^{N-1}}{(-1)^N} = -1 = b_{1N}. \tag{29}$$

Using Eqs. (27)–(29), we can exactly determine the elements of the inverse matrix, which is related to the search for the approximate solution in the case of the Neumann–Dirichlet boundary conditions. Thus, the elements of matrix B are determined by the expressions

$$b_{ij} = \begin{cases} -[N - (j-1)], & i \leqslant j, \\ -[N - (i-1)], & i > j. \end{cases} \tag{30}$$

The elements of the inverse matrix can be alternatively expressed as

$$b_{ij} = -[N - [\max(i, j) - 1]] = -\left[N - \left[\frac{(i+j) + |i-j|}{2} - 1\right]\right]. \tag{31}$$

The expressions (30) and (31) are equivalent. However, for software implementation, the first one is preferable.

As a result of the transformations carried out, explicit expressions for the elements of the inverse matrix are obtained, and the solution of the Poisson

problem with Neumann–Dirichlet boundary conditions can be obtained using a simple multiplication of the inverse matrix by the vector of the right-hand side: $U = BF$, where

$$B = -\begin{pmatrix} N & N-1 & N-2 & \cdots & \cdots & 2 & 1 \\ N-1 & N-1 & N-2 & \cdots & \cdots & 2 & 1 \\ N-2 & N-2 & N-2 & \cdots & \cdots & 2 & 1 \\ \vdots & \vdots & \vdots & \ddots & \vdots & \vdots & \vdots \\ \vdots & \vdots & \vdots & \vdots & \ddots & \vdots & \vdots \\ 2 & 2 & 2 & \cdots & \cdots & 2 & 1 \\ 1 & 1 & 1 & \cdots & \cdots & 1 & 1 \end{pmatrix}.$$

Each solution component can be expressed directly using the formula

$$u_k = -\left[(N-k+1)\left[\sum_{i=1}^{k} F_i\right] + \left[\sum_{i=k+1}^{N} (N-(i-1))\cdot F_i\right]\right], \quad k = 1, 2, \ldots, N. \quad (32)$$

Formula (32) gives a simple analytical expression for the solution of the Poisson equation with Neumann–Dirichlet boundary conditions. It is very easy to program it either directly or based on Eq. (30). One double loop will be enough to compute the entire solution.

4.3. Example

Consider a numerical solution of the problem of finding a scalar potential defined on the interval $[-a, b]$ and satisfying the Poisson equation

$$\Delta\Phi(x) = \frac{\partial^2 \Phi(x)}{\partial x^2} = f(x) = V_0 \cos(kx + \varphi_0),$$

where a, b, V_0, k and φ_0 are given constants, and the Neumann–Dirichlet boundary conditions $\dfrac{d\Phi}{dx}(a) = \Phi'_a$ and $\Phi(b) = \Phi_b$.

The known exact solution is expressed as

$$\Phi_{\text{exact}}(x) = \left[\Phi'_a - \frac{V_0}{k}\sin(ka + \varphi_0)\right](x-b) - \frac{V_0}{k^2}\left[\cos(kx+\varphi_0) - \cos(kb+\varphi_0)\right] + \Phi_b. \quad (33)$$

Let us consider the finite-difference solution at $a = -\dfrac{\pi}{2}$, $b = \dfrac{\pi}{4}$, $V_0 = 1$, $k = \dfrac{\pi}{2}$ and $\varphi_0 = \dfrac{\pi}{4}$.

We define the computational grid with the following parameters:

$$N = 100, \quad \Delta x = h = \frac{b-a}{N}, \quad x_i = (i-1)\,\Delta x, \quad \Phi_i = \Phi\,(x_i)$$

and $f_i = f(x_i) = \cos(kx_i + \varphi_0)$. The solution is assumed to satisfy the Neumann–Dirichlet conditions specified as: $\Phi'_a = 1/4$ and $\Phi_b = -1/2$.

We calculate the solution of the Poisson problem multiplying the inverse matrix with the elements determined by expressions (30) by the right-hand side vector, corrected using Eqs. (26).

The software implementation of the algorithm consists of a few lines: filling the right-hand side vector (26) and multiplying the inverse matrix B by this vector using Eqs. (30).

Figure 2 illustrates the results of the numerical experiment.

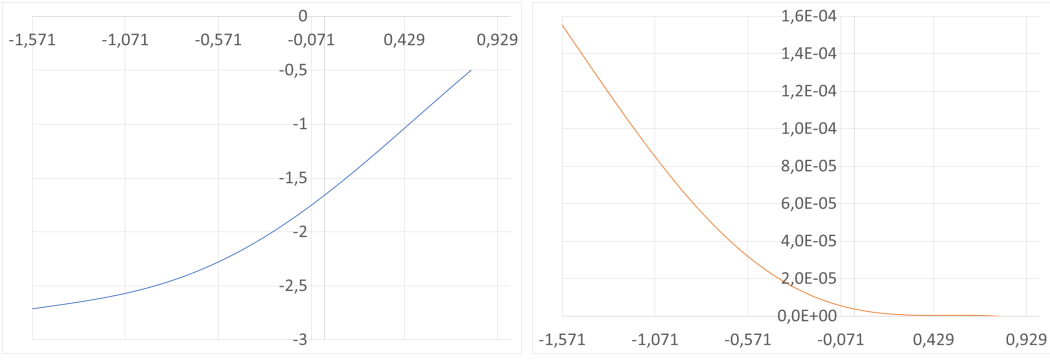

(a) Exact solution (b) Calculation error

Figure 2. The maximal error at $x = -1.571$ is $1.55E-04$ for $N = 100$ and decreases to $1.55E-06$ for $N = 1000$

5. Dirichlet–Neumann boundary conditions

5.1. Discretization and matrix equation

By analogy with the case of the Neumann–Dirichlet boundary conditions, we consider the symmetric case with the Dirichlet–Neumann boundary conditions. Let us first define a suitable sampling grid on the interval $[a, b]$. Grid points $\{x_i,\ i = 0, 1, \ldots, N+1\}$ are specified as $x_i = a + ih$. The boundary conditions u_a and u'_b, complementing the Poisson equation redefine the system of finite-difference equations (23). The solution value u_{N+1} at the 'virtual' point x_{N+1} is expressed using the boundary condition for the derivative, approximating the latter by symmetric central differences. As the last equation of the system, we get

$$u_{N-1} - u_N = h^2 \frac{f_N}{2} - hu'_b. \tag{34}$$

The transformed right-hand side vector F is presented as

$$F_N = h^2 \frac{f_N}{2} - hu'_b, \quad F_1 = h^2 f_1 - u_a, \quad F_i = h^2 f_i, \quad i = 2, \dots, N-1. \quad (35)$$

Like in the previous case of Neumann–Dirichlet boundary conditions, the resulting matrix of the equation

$$\begin{pmatrix} -2 & 1 & 0 & 0 & 0 & \cdots & \cdots & 0 \\ 1 & -2 & 1 & 0 & 0 & \cdots & \cdots & 0 \\ 0 & 1 & -2 & 1 & 0 & \cdots & \cdots & 0 \\ 0 & 0 & 1 & -2 & 1 & \ddots & \cdots & 0 \\ 0 & 0 & 0 & 1 & -2 & \ddots & \ddots & \vdots \\ \vdots & \vdots & \vdots & \ddots & \ddots & \ddots & \ddots & 0 \\ 0 & 0 & 0 & 0 & \ddots & \ddots & \ddots & 1 \\ 0 & 0 & 0 & 0 & 0 & 0 & 1 & -1 \end{pmatrix} \times \begin{pmatrix} u_1 \\ u_2 \\ u_3 \\ u_4 \\ u_5 \\ \vdots \\ u_{N-1} \\ u_N \end{pmatrix} = \begin{pmatrix} h^2 f_1 - u_a \\ h^2 f_2 \\ h^2 f_3 \\ h^2 f_4 \\ h^2 f_5 \\ \vdots \\ h^2 f_{N-1} \\ h^2 \frac{f_N}{2} - hu'_b \end{pmatrix} \quad (36)$$

is symmetric three-diagonal negative definite, with the dominant main diagonal.

With respect to the antidiagonal, this matrix is symmetric to the matrix used in the solution of the Poisson problem with the Neumann–Dirichlet boundary conditions. The system is definite and has a unique solution for any right-hand side.

Using the antidiagonal symmetry with respect to the Neumann–Dirichlet problem, we construct the inverse matrix for the Dirichlet–Neumann case:

$$B = -\begin{pmatrix} 1 & 1 & 1 & 1 & \cdots & 1 & 1 \\ 1 & 2 & 2 & 2 & \cdots & 2 & 2 \\ 1 & 2 & \ddots & \cdots & \cdots & \cdots & \cdots \\ \cdots & \cdots & \cdots & \ddots & \cdots & \cdots & \cdots \\ 1 & 2 & \cdots & \cdots & N-2 & N-2 & N-2 \\ 1 & 2 & \cdots & \cdots & N-2 & N-1 & N-1 \\ 1 & 2 & \cdots & \cdots & N-2 & N-1 & N \end{pmatrix}.$$

Therefore, the exact solution of the system of equations (36) can be written very simply (in a single line)

$$u_k = -\left[\left[\sum_{i=1}^{k} i \cdot F_i\right] + k \cdot \left[\sum_{i=k+1}^{N} F_i\right]\right], \quad k = 1, 2, \dots, N. \quad (37)$$

The software implementation of the method reduces to simple multiplication of the inverse matrix by the right-hand side vector.

Figure 3 illustrates the results of the numerical experiment.

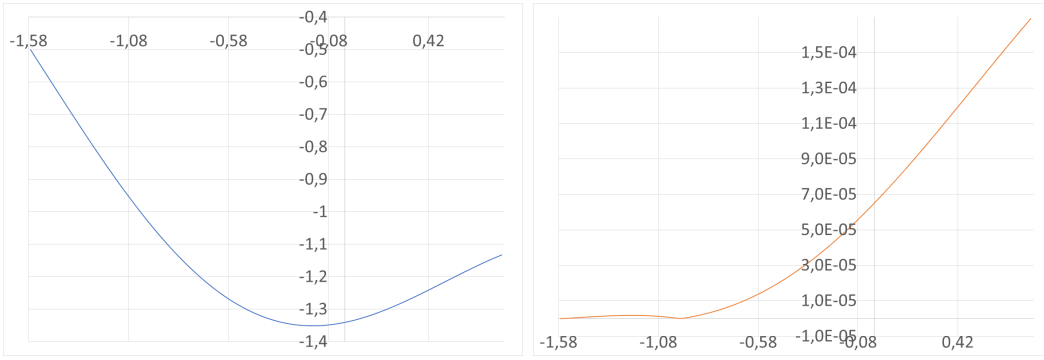

(a) Exact solution

(b) Calculation error

Figure 3. The maximal error in this case at point $x = 0.785$ is $1.69E-04$ for $N = 100$ and reduces to $1.69E-6$ for $N = 1000$

5.2. Example

An example of the previous section is considered, which differs only in that the boundary conditions set earlier at the left end of the interval are transferred to the right and vice versa. The software implementation of the algorithm consists of several lines: filling in the vector of the right-hand side (34) and multiplying the inverse matrix B by this vector using Eq. (37).

6. Conclusion

The paper gives examples of practical problems, in the simulation of which it is necessary to solve second-order elliptic equations with different boundary conditions. The case of the one-dimensional Poisson equation and its finite-difference solution are described in detail. Estimates of the complexity of the sweep algorithm in the case of a uniform grid are given. An approach to solving the one-dimensional Poisson equation using explicitly calculated coefficients of inverse matrices for various types of boundary conditions is also described. The Dirichlet and Neumann boundary conditions in various combinations are considered.

A comparative analysis of the computational complexity of methods for solving the one-dimensional Poisson equation, based on the use of the sweep method and methods using an explicit representation of inverse matrices is presented.

Direct calculation shows that to implement calculations by right-sweep formulas, approximately $8N$ arithmetic operations are required, whereas in the Gauss method for fully filled matrices this number is approximately $(2/3)\,N^3$. It is also important that the tridiagonal structure of the matrix of the system makes it possible to use for its storage only an array of real variables of dimension $3N - 2$.

The assertion of the author of Ref. [4] that the method he proposed using the explicit form of inverse matrices allows solving the Poisson equations with different boundary conditions faster and more accurately is, to put it mildly, incorrect. Provided that the stability conditions of the sweep method are met,

the speed of solving the problem by the sweep (Thomas) method is an order of magnitude higher due to a much smaller number of required operations.

However, unlike the sweep method [13], the practical implementation of the proposed method does not imply the allocation of additional arrays for software implementation, since the elements of the inverse matrix have a very simple form and their calculation within the loop determining the components of the solution is not difficult.

References

[1] A. N. Tikhonov and A. A. Samarskii, *Equations of Mathematical Physics [Uravneniya matematicheskoy fiziki]*, 7th ed. Moscow: Moscow State University, Nauka, 2004, in Russian.

[2] D. A. Yakovlev, V. G. Chigrinov, and H. S. Kwok, *Modeling and optimization of LCD optical performance*. New York: Wiley, 2015. DOI: 10.1002/9781118706749.

[3] L. N. Trefethen, *Approximation theory and approximation practice*. Philadelphia: SIAM – Society for Industrial and Applied Mathematics, 2019.

[4] M. Planitz *et al.*, *Numerical Recipes: The Art of Scientific Computing*, 3rd ed. New York: Cambridge University Press, 2007.

[5] N. N. Kalitkin and P. V. Koryakin, "Numerical methods [Chislennyye metody]," in *Methods of Mathematical Physics*, 1st ed. Moscow: Academia, 2013, vol. 2, in Russian.

[6] A. A. Abramov and V. B. Andreyev, "On the application of the method of successive substitution to the determination of periodic solutions of differential and difference equations," *USSR Computational Mathematics and Mathematical Physics*, vol. 3, no. 2, pp. 498–504, 1963. DOI: 10.1016/0041-5553(63)90034-x.

[7] A. A. Samarskiy and A. V. Gulin, *Numerical Methods of Mathematical Physics [Chislennyye metody matematicheskoy fiziki]*. Moscow: Scientific world, 2003, in Russian.

[8] L. H. Thomas, *Elliptic problems in linear difference equations over a network*. New York: Waston Sci. Comput. Lab. Rept., Columbia University, 1949.

[9] S. B. Gueye, K. Talla, and C. Mbow, "Generalization of the exact solution of 1D Poisson equation with robin boundary conditions, using the finite difference method," *Journal of Electromagnetic Analysis and Applications*, vol. 6, no. 12, pp. 372–381, 2014. DOI: 10.4236/jemaa.2014.612038.

[10] S. B. Gueye, K. Talla, and C. Mbow, "Solution of 1D Poisson equation with Neumann–Dirichlet and Dirichlet–Neumann boundary conditions, using the finite difference method," *Journal of Electromagnetic Analysis and Applications*, vol. 6, no. 10, pp. 309–318, 2014. DOI: 10.4236/jemaa.2014.610031.

[11] S. B. Gueye, "The exact formulation of the inverse of the tridiagonal matrix for solving the 1D Poisson equation with the finite difference method," *Journal of Electromagnetic Analysis and Applications*, vol. 6, no. 10, pp. 303–308, 2014. DOI: 10.4236/jemaa.2014.610031.

[12] N. N. Kalitkin and E. A. Alshina, "Numerical Methods [Chislennyye metody]," in *Numerical analysis*. Moscow: Academia, 2013, vol. 1, in Russian.

[13] A. Amosov, Y. Dubinsky, and N. Kopchenova, *Computational Methods [Vychislitel'nyye metody]*, 4th ed. St. Petersburg: Lan', 2021, in Russian.

For citation:

S. Ndayisenga, L. A. Sevastianov, K. P. Lovetskiy, Finite-difference methods for solving 1D Poisson problem, Discrete and Continuous Models and Applied Computational Science 30 (1) (2022) 62–78. DOI: 10.22363/2658-4670-2022-30-1-62-78.

Information about the authors:

Sevastianov, Leonid A. — Doctor of Physical and Mathematical Sciences, Professor of Department of Applied Probability and Informatics of Peoples' Friendship University of Russia (RUDN University), Leading Researcher of Bogoliubov Laboratory of Theoretical Physics, JINR (e-mail: sevastianov-la@rudn.ru, phone: +7(495)9522572, ORCID: https://orcid.org/0000-0002-1856-4643, ResearcherID: B-8497-2016, Scopus Author ID: 8783969400)

Lovetskiy, Konstantin P. — Candidate of Physical and Mathematical Sciences, Associate Professor of Department of Applied Probability and Informatics of Peoples' Friendship University of Russia (RUDN University) (e-mail: lovetskiy-kp@rudn.ru, phone: +7(495)9522572, ORCID: https://orcid.org/0000-0002-3645-1060 , ResearcherID: A-5725-2017, Scopus Author ID: 18634692900)

Ndayisenga, Serge — Student of Department of Applied Probability and Informatics of Peoples' Friendship University of Russia (RUDN University) (e-mail: 1032195775@rudn.ru, phone: +7(977)9086946, ORCID: https://orcid.org/0000-0002-9297-9839, ResearcherID: AAC-3303-2022)

УДК 535:535.3:681.7
DOI: 10.22363/2658-4670-2022-30-1-62-78

Конечно-разностные методы решения 1D задачи Пуассона

С. Ндайисенга[1], **Л. А. Севастьянов**[1, 2], **К. П. Ловецкий**[1]

[1] *Российский университет дружбы народов*
ул. Миклухо-Маклая, д. 6, Москва, 117198, Россия
[2] *Лаборатория теоретической физики им. Н. Н. Боголюбова*
Объединённый институт ядерных исследований
ул. Жолио-Кюри, д. 6, Дубна, Московская область, 141980, Россия

Аннотация. В статье обсуждается постановка и анализ методов решения одномерного уравнения Пуассона на основе конечно-разностных аппроксимаций — важного и очень полезного инструмента численного исследования дифференциальных уравнений. По сути, это классический метод аппроксимации, основанный на разложении решения в ряд Тейлора. Развитие теоретических и практических результатов на базе этого метода в последние годы позволили повысить точность, стабильность и сходимость методов решения дифференциальных уравнений. Некоторые особенности этого анализа включают интересные расширения классического численного анализа начальных и граничных задач. В первой части излагается численный метод решения одномерного уравнения Пуассона, сводящийся к решению системы линейных алгебраических уравнений (СЛАУ) с ленточной симметричной положительно определённой матрицей. В качестве метода решения СЛАУ используется широко известный метод прогонки (метод Томаса). Во второй части представлен метод решения, основанный на аналитическом представлении точной обратной матрицы дискретизированного варианта уравнения Пуассона. Выражения для обратных матриц существенно зависят от типов граничных условий в исходной постановке. Представлены варианты обратных матриц для уравнения Пуассона с различными граничными условиями на концах исследуемого интервала — условиями Дирихле на обоих концах интервала, условиями Дирихле на одном из концов и Неймана на другом. Во всех трёх случаях коэффициенты обратных матриц легко вычисляются (выписываются) и алгоритм решения задачи практически сводится к умножению матрицы на вектор правой части.

Ключевые слова: 1D уравнение Пуассона, метод конечных разностей, обращение трехдиагональной матрицы, алгоритм Томаса, исключение Гаусса

Discrete & Continuous Models
& Applied Computational Science
ISSN 2658-7149 (online), 2658-4670 (print)

2022, 30 (1) 79–87
http://journals.rudn.ru/miph

Research article

UDC 519.6
PACS 07.05.Tp,
DOI: 10.22363/2658-4670-2022-30-1-79-87

On methods of building the trading strategies in the cryptocurrency markets

Eugeny Yu. Shchetinin

Financial University under the Government of Russian Federation
49, Leningradsky Prospect, Moscow, 125993, Russian Federation

(received: November 26, 2021; revised: January 18, 2022; accepted: February 18, 2022)

Abstract. The paper proposes a trading strategy for investing in the cryptocurrency market that uses instant market entries based on additional sources of information in the form of a developed dataset. The task of predicting the moment of entering the market is formulated as the task of classifying the trend in the value of cryptocurrencies. To solve it, ensemble models and deep neural networks were used in the present paper, which made it possible to obtain a forecast with high accuracy. Computer analysis of various investment strategies has shown a significant advantage of the proposed investment model over traditional machine learning methods.

Key words and phrases: bitcoin, trading strategy, ensemble models, deep learning

1. Introduction

The development of the financial market for cryptocurrencies in 2021 has become one of the key trends in global capital. The COVID-19 pandemic, which began in 2020, only accelerated this process, as it caused a drop in traditional markets, forcing investors to look for alternative tools and products [1]. For many, the financial market for cryptocurrencies has become such a solution. This paper studies the investor's trading strategies in the cryptocurrency market and analyzes their effectiveness in comparison with the classical financial asset market. Their feature is the high volatility of the cryptocurrency market, so it would be natural to apply portfolio formation strategies to change the asset trend. Under these conditions, investors usually use strategies that allow them to open a position at the initial stage of a trend formation. Thus, the main goal of the work is to develop a computer system for detecting the moment of entering the cryptocurrency market and testing its effectiveness using the example of bitcoin.

2. Methods for modeling and forecasting the value of cryptocurrencies

Methods for modeling and forecasting prices for financial assets can be divided into methods of technical and fundamental analysis, which determine the characteristics and form the value of an asset and features of its behavior. The first approach is based on the laws of probability theory and mathematical statistics, which allow solving various problems with different qualitative characteristics using universal methods [2]. As a rule, the first approach assumes a fundamental theory that is well formalized, understandable and logical. However, its working conditions are 'ideal' and its application in practice does not always make it possible to make a reliable prediction. The second approach aims to test complex mathematical methods and tools to solve the first one. At the same time, methods of regression, variance, and correlation analyzes are widely used. They allow understanding the interdependencies between the asset in question and other factors. However, these methods poorly predict asset dynamics.

Since the value of an asset is measured over time, it can be analyzed using econometric time series methods. However, this requires the condition of stationarity and linearity, which are not present in the real asset market. To solve this problem, the change or profitability of the asset is considered rather than its value. The use of various econometric models in trading strategies is justified in the short term, but in the long term, this approach is extremely risky due to high volatility [3], [4]. Recently, machine learning methods have become widely used for trading in financial markets due to their ability to build effective dynamic forecasting models. They solve a wide range of problems: regression, classification, clustering. Moreover, these methods show themselves best in solving such problems.

We will use the following investor strategy to generate revenue in the cryptocurrency market:

$$y_t = \begin{cases} 0, & CSMA_w(t) \leqslant BB_w^{\text{down}}(t) - \text{downward}, \\ 1, & BB_w^{\text{down}}(t) < CSMA_w(t) < BB_w^{\text{up}}(t) - \text{flat}, \\ 2, & CSMA_w(t) \geqslant BB_w^{\text{up}}(t) - \text{upward}, \end{cases} \tag{1}$$

where y_t is the trend label, CSMA is the centered moving average, BB_w is the Bollinger band with the superscript for upper and lower one. The use of CSMA is due to the fact that the characteristics to be used have significant predictive power. In this paper, the dominant cryptocurrency bitcoin was chosen, for which there is also a large amount of information. It is possible to single out the data sources from where the information will be taken [3]:

— market;
— fundamental;
— alternative.

For more accurate forecasts, it was decided to create a complex dataset that consists of all the types of data sources listed above. In the market data, the prices and trading volumes of Bitcoin itself, VIX and gold were selected. VIX is an index of fear, which is calculated based on supply and demand for option contracts, which reflects expectations for such a popular index as the S&P

500 [3]. If the indicator exceeds the 40-point mark, then it is considered that panic begins in the classic markets. It is at times like these that investors try to find alternative investments, which include Bitcoin. Gold is also considered to be an asset that people begin to actively invest in during the crisis. The data was obtained through the yahoo finance API. The information field also greatly influenced the value of bitcoin and cryptocurrencies [2]. The names in the table correspond to the queries. Fundamental factors directly represent the value of an asset. The information was taken from the blockchain.info website using the API. Market indicators that were obtained using the TA-Lib library helped to assess the 'pulse' of the market and understand which trading patterns are applied at the current time. The data were scaled and then their daily increments were calculated, taking into account their balance by class. A general description of the data can be seen in the table 1.

3. Selection of optimal model parameters and forecasting

After solving the problem of creating a dataset, it is necessary to choose a computer model that will allow us to build an optimal forecast for the value of bitcoin. Machine learning provides a large number of classification models. For example, the following ensemble models are especially popular [5]:

— Random forest;
— Ada boost;
— Light GBM;
— XG Boost.

In addition, to classify the trend at the time of entering the market, a recurrent neural network with a long short-term memory (LSTM) cell was used [6]. The described dataset is preliminarily divided into a training set and a test set. Their distribution can be seen in the figure 1.

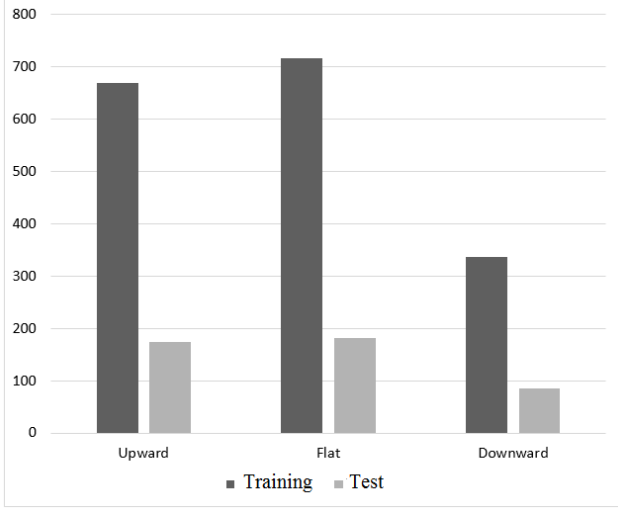

Figure 1. Distribution of the training and test sample over trend labels

Table 1

Description of the dataset and the factors it contains

Market	— btc_vol – bitcoin open — Open – Bitcoin opening price — Vix – VIX index opening — Gold – gold opening price — Gold_vol – gold trading volumes
Alternative	— Bitcoin – Google popularity index for the query 'bitcoin' — bitcoin wallet – Google popularity index for the query 'bitcoin wallet' — buy bitcoin – Google popularity index for the query 'buy bitcoin' — sell bitcoin – Google popularity index for the query 'sell bitcoin' — Blockchain – Google popularity index for the query 'bitcoin wallet'
Fundamental	— tr_per_block – transactions in the block — tr_cost – transaction cost — Miners_rev – miners' revenue — N_unique addresses – number of unique addresses — NVT is a metric calculated by dividing the network value by the total volume of transactions in USD in 24 hours. — NVTS – the same as NVT, the difference in the denominator of which is the moving average over the last 90 days
Market (indicators)	— Willr_sig – Williams indicator signal
Market	— Willr_sig – Stoch_sig – Stochastic indicator signal — Mfi_sig – cash flow indicator signal — Rsi_sig – relative strength indicator signal

After training the models using the training set, predictions were made with the test set. We chose the accuracy indicator as the quality metric of the estimates obtained. As seen from the table 2, the gradient boosting of the Light GBM library turned out to be the best model [5]. The most important features were technical indicators and market data: 6 indicators out of 8 main ones. Fundamentals of NVT and NVTS also contributed. In terms of importance, these two indicators are equated to P/E for the stock market [7].

To further model the behavior of an investor using the strategy described above, we have chosen the Light GBM model.

Table 2

The accuracy of the forecast for the test sample

Model	Accuracy, %
Random forest	68
Ada boost	69
Light GBM	70.4
XG Boost	70.28
LSTM	68

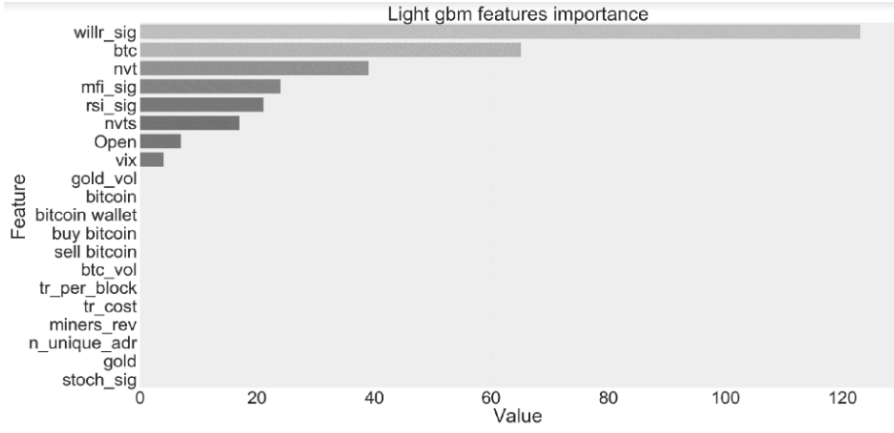

Figure 2. Distribution of data set factors according to the strength of their impact on the forecast

Further, to test the selected Light GBM algorithm and select the optimal values of its parameters, backtesting was performed, i.e., a financial analysis procedure that allows you to tune the model to the current data stream. In the classic version, this is performed on ready-made data, however, existing solutions impose restrictions on the implementation of the project, therefore, a backtest was developed, which made it possible to simulate the dynamics of a portfolio that is built according to the strategy principle. The proposed backtesting algorithm takes into account the cost at which the asset, account, commission, credit when opening a short position and the flag of the possibility of opening a short position will be bought or sold. The following variables are specified in the backtest:

— Investment amount equal to $ 10,000;
— Credit 0.1%;
— Commission 0.09%;
— The purchase price is the closing price.

Actions of buying or selling are presented in the table 3.

Table 3

Actions of the portfolio management strategy

Signal	t_{sig}	$t_{sig} - 1$	Action
Flat (lateral movement)	0	0	keep short
Flat	1	1	we keep funds in foreign currency
Flat	2	2	hold a long position
Upward	2	1	open a long position
Downward	0	1	open a short position
Flat	1	2	close a long position
Downward	0	2	close long, open short
Flat	1	0	close a short position
Upward	2	0	close short, open long

The dynamics of the value of the bitcoin portfolio is shown in the figure 3. The portfolio worked in unstable conditions throughout 1.11.2019–01.01.2021. It can also be noted that a portfolio with short positions wins and loses equally well to a less aggressive portfolio. However, when the price goes out of the sideways, the model starts to be profitable. Forecasts and quotation of the cost of bitcoin for the period 11.2019–01.2020 are shown in the Figure 4.

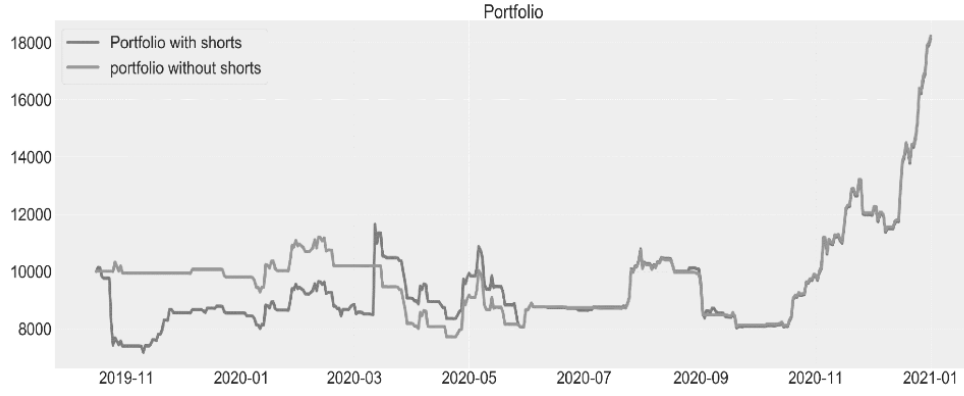

Figure 3. Dynamics of the portfolio value with and without short positions

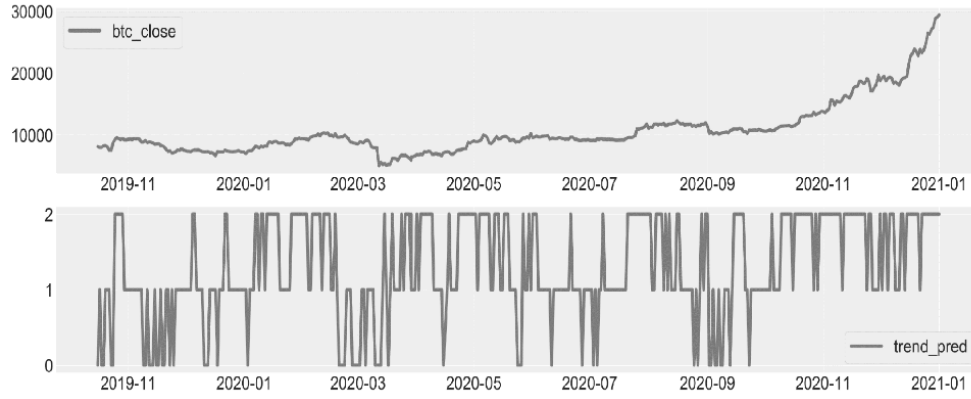

Figure 4. Bitcoin Quote and Forecast Labels

The table 4 shows the results of evaluating the profitability of built portfolios with and without short positions, as well as the S&P 500 index. As seen from the table, an investor using the proposed strategy would have been able to earn 80% of the profit, whereas if he invested in the S&P 500 for the tested period, he would have earned only 24%.

Table 4

Model backtesting results

Portfolio model	Profitability
short portfolio	81.43 %
no short portfolio	82.23 %
S&P 500 index	24.28 %

4. Discussion of results and conclusions

This paper proposes an original trading strategy for investing in cryptocurrencies using the example of bitcoin. Its main properties and advantages are the ability to classify the current state of the trend and form a possible opening or closing a position for an asset or their portfolio. For the computer implementation of the proposed strategy, a machine learning model was developed based on the Light GBM model. To test the effectiveness of the formulated characteristics of the model, a synthetic dataset was developed based on the most important features extracted from market factors. Model testing and comparative analysis of the results obtained with other models showed a high degree of stability and accuracy of the proposed strategy. The proposed approach is universal and, therefore, it can be applied in various financial markets with high volatility.

References

[1] E. Y. Shchetinin, "Study of the impact of the COVID-19 pandemic on international air transportation," *Discrete and Continuous Models and Applied Computational Science*, vol. 29, no. 1, pp. 22–35, 2021. DOI: 10.22363/2658-4670-2021-29-1-22-35.

[2] E. Y. Shchetinin, Y. G. Prudnikov, and P. N. Markov, "Long range memory modeling and estimation for financial time series," *RUDN Journal of Mathematics, Information Sciences and Physics*, no. 1, pp. 98–106, 2011, in Russian.

[3] J. Spörer, "Backtesting of algorithmic cryptocurrency trading strategies," *Available at SSRN*, 2020. DOI: 10.2139/ssrn.3620154.

[4] A. Y. Mikhailov, "Cryptoassets pricing and equity indices correlation," *Finance and Credit*, vol. 24, no. 3, pp. 641–651, 2018, in Russian. DOI: 10.24891/fc.24.3.641.

[5] A. Geron, *Hands-on machine learning with Scikit-Learn, Keras, and TensorFlow: concepts, tools, and techniques to build intelligent systems, 2nd Edition.* O'Reilly Media, Inc., 2019.

[6] G. G. Ognev and E. Y. Shchetinin, "Deep neural networks with LSTM architecture for predicting financial time series," in *Information and Telecommunication Technologies and Mathematical Modeling of High-Tech Systems 2020 (ITTMM 2020)*, in Russian, Moscow, Russia, April 13–17, 2020, pp. 280–283.

[7] A. Arratia and A. X. Lopez-Barrantes, "Do Google trends forecast bitcoins? Stylized facts and statistical evidence," *Journal of Banking and Financial Technology*, vol. 5, no. 1, pp. 45–57, 2021.

For citation:

E. Y. Shchetinin, On methods of building the trading strategies in the cryptocurrency markets, Discrete and Continuous Models and Applied Computational Science 30 (1) (2022) 79–87. DOI: 10.22363/2658-4670-2022-30-1-79-87.

Information about the authors:

Shchetinin, Eugeny Yu. — Doctor of Physical and Mathematical Sciences, Lecturer of Department of Mathematics, Financial University under the Government of Russian Federation (e-mail: riviera-molto@mail.ru, ORCID: https://orcid.org/0000-0003-3651-7629)

УДК 519.6
PACS 07.05.Tp,
DOI: 10.22363/2658-4670-2022-30-1-79-87

О методах построения торговых стратегий на криптовалютных рынках

Е. Ю. Щетинин

Финансовый университет при Правительстве Российской Федерации
Ленинградский проспект, д. 49, Москва, 125993, Россия

Аннотация. В работе предлагается торговая стратегия инвестирования в рынок криптовалют, использующая мгновенные входы на рынок на основе дополнительных источников информации в виде разработанного набора данных. Задача прогнозирования момента входа на рынок формулируется как задача классификации тренда стоимости криптовалют. Для её решения в статье использовались ансамблевые модели и глубокие нейронные сети, что позволило получить прогноз с высокой точностью. Компьютерный анализ различных инвестиционных стратегий показал значительное преимущество предложенной модели инвестирования перед традиционными методами машинного обучения.

Ключевые слова: биткойн, торговая стратегия, ансамблевые модели, глубокое обучение